SIMPLIFIED SHIP COLLISION MODEL

Donghui Chen

Dissertation submitted to the faculty of
Virginia Polytechnic Institute and State University
in partial fulfillment of the requirements for the degree of

MASTER OF SCIENCE
in
Ocean Engineering

Dr. Alan J. Brown, Chairman

Dr. Rakesh K. Kapania

Dr. Owen F. Hughes

January 2000
Blacksburg, Virginia

Keywords: collision, ship, damage

SIMPLIFIED SHIP COLLISION MODEL

Donghui Chen

ABSTRACT

The serious consequence of ship collisions necessitates the development of regulations and requirements for the subdivision and structural design of ships to reduce damage and environmental pollution from collision, and improve safety. The on-going revision of IMO regulations on oil outflow performance and damage stability in grounding and collision is focused on a transition to probabilistic performance-based standards. This thesis addresses one aspect of this problem, a simplified collision model sufficient to predict collision damage, and fast enough to be used in probabilistic analysis requiring thousands of collision simulations.

The simplified collision model (SIMCOL) developed and evaluated in this thesis is based on a time domain simultaneous solution of external dynamics and internal deformation mechanics. The external sub-model uses a three-degree of freedom system for ship dynamics. The internal sub-model determines reacting forces from side and bulkhead structures using mechanisms adapted from Rosenblatt and McDermott, and absorbed energy by decks, bottoms and stringers calculated using the Minorsky correlation as modified by Reardon and Sprung.

SIMCOL is applied to a series of collision scenarios. Results are compared with MIT's DAMAGE, a Danish Technical University (DTU) model and ALPS/SCOL. SIMCOL provides a fast, consistent and reasonable result for ship collision analysis. An actual collision case is used in an initial attempt to validate the model.

This research is sponsored by the Society of Naval Architects and Marine Engineers (SNAME) and the Ship Structure Committee (SSC).

ACKNOWLEDGEMENTS

Without the help of many others, it would be impossible for me to complete this thesis, and many other things, in three semesters. I would like to express my thanks to them, especially the following:

- Ying Chen, Zhiyi Lin, Hao Long and Lei Xie, for their helps from course works, like aerodynamics, to daily life.
- Josh King and Chimi Zacot, for developing ship arrangement and structural data.
- Dr. Jeom Kee Paik and Ick Hung Choe, for providing details and simulation results of ALPS/SCOL.
- Suryanarayana Vakkalanka, for discussions during the model development.
- Jianjun Xia, for helping me handling all the administrative works during the last stage of my thesis and defense preparation.
- Bo Jin, for providing simulation results of test matrices using DAMAGE.
- Marie Lützen, for offering details of the DTU model, and simulation results of test matrices using the DTU model.
- Professor Alan Brown, for guiding me through all this work.

TABLE OF CONTENTS

CHAPTER 1 INTRODUCTION

1.1 MOTIVATION [1,2]

The serious consequence of ship collisions necessitates the development of regulations and requirements for the subdivision and structural design of ships so that damage and environmental pollution is reduced, and safety is improved.

The International Maritime Organization (IMO) is responsible for regulating the design of oil tankers and other ships to provide for ship safety and environmental protection. Their ongoing transition to probabilistic performance-based standards requires the ability to predict the environmental performance and safety of specific ship designs. This is a difficult problem requiring the application of fundamental engineering principles and risk analysis [3,4,5]. This thesis addresses one aspect of this problem, a simplified collision model sufficient to predict collision damage, and fast enough to be used in probabilistic analysis requiring thousands of collision simulations.

IMO's first attempt at this transition for oil tankers was in response to the US Oil Pollution Act of 1990 (OPA 90). In OPA 90 the US requires that all oil tankers entering US waters must have double hulls. IMO responded to this unilateral action by requiring double hulls or their equivalent. Equivalency is determined based on probabilistic oil outflow calculations specified in the "Interim Guidelines for the Approval of Alternative Methods of Design and Construction of Oil Tankers Under Regulation 13F(5) of Annex I of MARPOL 73/78" [6], hereunder referred to as the Interim Guidelines.

The Interim Guidelines are an excellent beginning, but they have a number of significant shortcomings:

- They use a single set of damage extent probability density functions (pdf's) from limited single hull data applied to all ships independent of structural design.
- Damage pdf's consider only damage significant enough to breach the outer hull. This penalizes structures able to resist rupture.

- Damage extents are treated as independent random variables when they are actually dependent variables, and ideally should be described using a joint pdf.

- Damage pdf's are normalized with respect to ship length, breadth and depth when damage may depend to a large extent on local structural features and scantlings vice global ship dimensions.

1.1.1 SNAME/SSC Collision and Grounding Research Project

Research sponsored by the Society of Naval Architects and Marine Engineers (SNAME) and the Ship Structure Committee (SSC) addresses the shortcomings in the Interim Guidelines using a fundamentally-based model to predict probabilistic damage in collision and grounding for a specific design, vice basing damage prediction on a single set of limited data.

SNAME Ad Hoc Panel #6 was established specifically to consider structural design and response in collision and grounding. Ad Hoc Panel #6 objectives include the consideration of structural design or crashworthiness in predicting probabilistic damage response. This panel was formed under the SNAME T&R Steering Committee on May 14, 1998 with support from SNAME and SSC. It has four working groups studying tools for predicting damage in grounding and collision, data, collision and grounding scenarios, and innovative design concepts. Funded research is centered at Virginia Tech and Webb Institute of Naval Architecture. Virginia Tech is specifically tasked with:

- Developing collision and grounding scenarios

- Assessing and developing a simplified collision model sufficient for probabilistic analysis

Figure 1.1 illustrates the process being used at Virginia Tech to predict probabilistic damage as a function of ship structural design. A similar process is required for grounding.

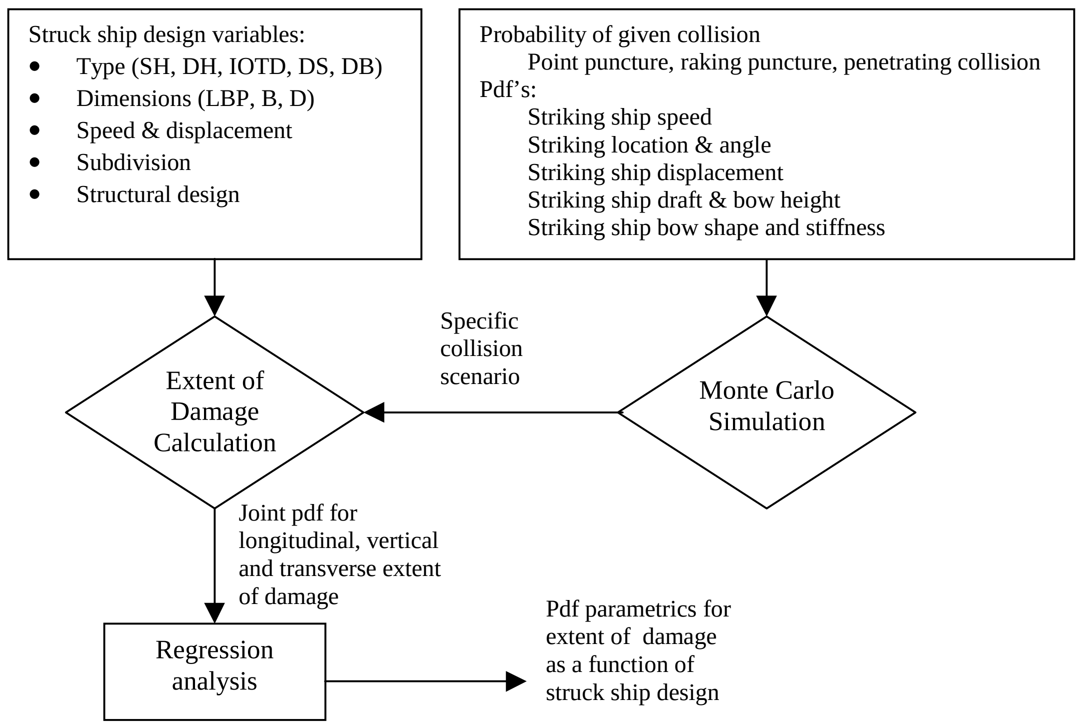

Figure 1.1 Methodology to Predict Probabilistic Damage in Collision [2]

The process begins with a set of probability density functions (pdfs) defining possible collision scenarios. Based on these pdfs, a specific scenario is selected in a Monte Carlo simulation, and combined with a specific ship structural design to predict collision damage. This process is repeated for thousands of scenarios and a range of structural designs until sufficient data is generated to build a set of parametric equations relating probabilistic damage extent to structural design. These parametric equations can then be used in oil outflow or damage stability calculations.

Critical to this process is a simple, but sufficient collision model.

1.1.2 Collision Model for Probabilistic Analysis

The collision problem consists of two sub-problems:

- External problem – includes the principal characteristics of the striking and struck ships and their motion before, during and after collision;

- Internal problem - includes the internal mechanics and structural response of the struck ship and possibly the striking ship bow during collision.

The responses of the colliding structures are highly transient and non-linear, and involve a continuous change in geometry.

Direction from SNAME Ad Hoc Panel #6 is to consider three types of side damage with emphasis on penetrating collision:

- Low energy puncture at point

- Low energy raking puncture

- Penetrating Collision – right angle and oblique sufficient to penetrate outer hull with significant damage extending in at least 2 directions (penetration, horizontal, vertical)

At Virginia Tech, the initial work is focused on the penetrating collision using a simplified collision model for internal damage with three degree-of-freedom external ship motion dynamics. This collision model is based on Crake's model [7].

Crake uses a modified Minorsky method in a probabilistic analysis, where the absorbed kinetic energy is obtained by a linear correlation with the damaged volume of structural steel [8]. The slope of the Minorsky's correlation used in Crake's study is as modified by Reardon and Sprung [9]. Membrane effects of side shell and longitudinal bulkheads, as developed by Jones and Van Mater [10], are considered in defining the minimum energy intercept. Crake's model is the starting point of this thesis and is identified as Version 0.0 of the current work.

Although a good beginning, Crake's model has a number of shortcomings:

- The only structural members considered in Crake's model are shell, deck, inner bottom and longitudinal bulkhead plating.

- The side shell and longitudinal bulkhead membrane-effect model is very simple and does not consider the deformation of transverse web frames.

- The connection of the side shell and inner skin is not addressed.

- The collision simulation procedure does not correctly calculate damaged volume.

This thesis addresses these shortcomings. Geometry calculations are refined. More rigorous analysis models are considered for predicting shell penetration. By combining the modified-Minorsky method and the minor collision model developed by McDermott [11] and Rosenblatt and Son, Inc. [12], all of the major structural members are included in the analysis.

1.2 PLAN AND PROGRESS

In order to develop a proper collision model for probabilistic analysis, it was first necessary to carry out a thorough literature search. The findings of this literature search are given in Chapter 2.

Next, Crake's Matlab code was converted into a Fortran code and errors were corrected. The result is the first version of the Simplified Collision Model (SIMCOL), Version 0.1 developed at Virginia Tech, also under Dr. Brown.

Based on the literature survey and test runs of the first version, improvements are progressively made to the collision model. First the sweeping segment method is developed in Version 1.0. In the sweeping segment method, the wedge-shape striking bow is defined by straight-line segments. The total area swept-out by all segments determines the damaged area of decks and bottoms. The Rosenblatt method is applied in Version 1.1 to improve the calculation of membrane resistance. In Version 2.0, the lateral deformation of web frames is included. Finally, in Version 2.1, the vertical extents of the striking ship bow are considered. The complete description of model mechanisms is presented in Chapter 3. The format of input files, flow charts and complete source code are presented in Appendix A.

In order to verify the model's consistency and sensitivity, the model is tested in a series of collision scenarios with a range of tanker sizes and designs. The baseline tanker design in this analysis is a 150,000 dwt double hull tanker. It is developed to be consistent with the dimensions of the 150,000 dwt reference tanker in the IMO Interim Guidelines. HECSALV and SafeHull are used to develop the details of the design, and to insure that the arrangement satisfies IMO regulations and the structural design satisfies ABS classification requirements. This design is the primary tanker design used in the model verification and comparison, and in the design parameter sensitivity analysis. The striking ship in this study is a 150,000 dwt bulk carrier selected from Pederson's study [13]. In addition, an actual collision described by Kuroiwa [14] is chosen as a model validation case. The struck ship, in this case, is a 100,000 dwt single hull tanker. Its general arrangement and structural details are developed in accordance with Kuroiwa's description and consistent with IMO regulations and ABS Class Rules. The striking ship in this case is a 23,000 dwt container ship. A summary of the design data for the above struck and striking ships is given in Chapter 4. The details are provided in Appendix B. A comparison of test results to other available collision simulation tools is also made. The data from these comparisons are also presented in Chapter 4 with discussion and analysis.

Finally, in Chapter 5, conclusions are made based on the data presented in Chapter 4, and recommendations are provided for future work.

CHAPTER 2 EXISTING ANALYSIS METHODS AND MODELS

Models for analyzing ship collision were initially developed in 1950s for ships transporting radioactive materials, and later on, were applied to other types of ships, mainly tankers and LPG/LNG carriers.

Collision analysis models consist of three elements:

- an external ship dynamics sub-model;
- an internal sub-model of structural mechanics for the struck and striking ships; and
- the simulation approach that couples the internal and external sub-models.

Existing models use different sub-models and simulation or coupling approaches. These are discussed in the following sections.

2.1 EXTERNAL SHIP DYNAMICS

The external sub-model calculates the ship dynamics in collision. Different models have been developed from different assumptions and for different purposes. The simplest is the one-dimensional approach (striking ship surge, struck ship sway) proposed by Minorsky [8]. MIT's collision analysis software, DAMAGE [15], adds an additional degree of freedom (struck ship yaw) and is more suitable for strikes away from the center of gravity of the struck ship. More sophisticated models consider three degrees of freedom (surge, sway and yaw), as in Crake [5, 7], Hutchison [16] and Zhang [17].

2.1.1 Minorsky Method [8]

Collision analysis models were first developed for analyzing the design of ships transporting nuclear materials. The crashworthiness of these ships under the worse case conditions was the primary concern. The totally inelastic right angle collision with the struck ship at rest was considered the "worse case". Hence, the majority of currently available models considers only right angle collisions, and assumes that the kinetic energy parallel to the struck ship's centerline is negligible. The most popular of these approaches is the one proposed by Minorsky.

Minorsky's approach is based on the following assumptions:

- The collision is totally inelastic.
- The system kinetic energy along the struck ship's longitudinal direction is negligible.
- The rotations of the struck and striking ships are small and can be neglected.

The first two assumptions define the so-called "worse case". The third is based on the observation of only small rotations in actual collisions during the damage event. Small rotations have also been observed in theoretical analysis.

With these assumptions, the system becomes one dimensional and the final velocities of both striking and struck ships can be derived as follows on the basis of conservation of momentum:

$$
\begin{aligned}
&(M_A + M_B + dm_A)v = M_B v_B \\
&v = \frac{M_B v_B}{M_A + M_B + dm_A}
\end{aligned}
\qquad [2.1]
$$

where

M_A	-	mass of struck ship;
M_B	-	mass of striking ship;
dm_A	-	added mass of struck ship in the sway direction;
v	-	final velocity in the Y direction, normal to the struck ship's centerline;
v_B	-	initial velocity of the striking ship in Y direction.

Hence, the total kinetic energy absorbed in the collision, ΔKE, is

$$\Delta KE = \frac{1}{2} M_B v_B^2 - \frac{1}{2}(M_A + M_B + dm_A)v^2 = \frac{M_B (M_A + dm_A)}{2(M_A + M_B + dm_A)} v_B^2$$

Minorsky estimated the added mass in sway, dm_A, to be $0.4M_A$. The collision angle, ϕ, is introduced to calculate the velocity of the striking ship in the sway direction of the struck ship. The absorbed kinetic energy in the struck ship transverse direction is:

$$\Delta KE = \frac{M_A M_B}{2M_A + 1.43M_B}(V_B \sin\phi)^2 \qquad [2.2]$$

where V_B is the initial velocity of the striking ship.

It is important to note that a right angle collision may not be the "worse case". Equations [2.1] and [2.2] may underestimate the kinetic energy lost in collisions at oblique angles (by the bow) and/or when the struck ship has forward speed. Side structure may also offer more resistance when it is struck at right angle than oblique angles. This will be investigated in later sections.

2.1.2 DAMAGE [15]

In DAMAGE, a second degree of freedom, yaw, is allowed for the struck ship, but the struck ship is still assumed to have zero initial forward speed and the collision angle is assumed to be a right angle. It is also assumed that the striking ship remains on its course during the collision, which means the striking ship only has one-degree of freedom, surge. Using conservation of linear and angular momentum, the final velocity of both struck ship and striking ship are derived as follows:

$$\begin{aligned}
&M_{1y}v_1^a + M_{2x}v_2^a = M_{2x}v_2 \\
&I_{1z}\omega_1^a + M_{2x}x_1v_2^a = M_{2x}x_1v_2 \\
&v_2^a = v_1^a + x_1\omega_1^a \\
&v_1^a = v_2\frac{1}{1 + M_{1y}x_1^2/I_{1z} + M_{1y}/M_{2x}} \\
&\omega_1^a = v_2\frac{M_{1y}x_1/I_{1z}}{1 + M_{1y}x_1^2/I_{1z} + M_{1y}/M_{2x}}
\end{aligned} \qquad [2.3]$$

where

M_{1y} - virtual mass of the struck ship including added mass in the sway direction;

M_{2x} - virtual mass of the striking ship including added mass in the surge direction;

I_{1z} - virtual moment of inertia in yaw of the struck ship including yaw added mass (moment of inertia);

$v_1{}^a$ - final velocity of struck ship in the sway direction;

$\omega_1{}^a$ - final angular velocity of struck ship;

v_2 - initial velocity of striking ship;

$v_2{}^a$ - final velocity of striking ship in the sway direction of the struck ship; and

x_1 - impact point to the midship point of struck ship.

The kinetic energy lost in collision is:

$$\Delta KE = \frac{1}{2} M_{1y} v_1^{a^2} + \frac{1}{2} M_{2x} v_2^{a^2} + \frac{1}{2} I_{1z} \omega_1^{a^2} - \frac{1}{2} M_{2x} v_2{}^2 \qquad [2.4]$$

DAMAGE cannot correctly analyze collisions with an oblique striking angle or an initial striking ship velocity.

2.1.3 Approaches with Three Degrees of Freedom

2.1.3.1 Hutchison Model [16]

In Hutchison's study for barges carrying radioactive cargo, a global coordinate system with three degrees of freedom is used. The virtual masses of both struck and striking ships are developed in matrix form, including the added mass terms. The kinetic energy and momentum of the ship is determined from the velocity vector and virtual mass matrix. The same model is used in Crake's research [5, 7].

It is necessary to calculate the final velocities of both struck and striking ships in order to determine the lost kinetic energy. In Hutchison's study, this is accomplished using conservation of momentum with the following assumptions:

- Changes in the global orientation angles, or rotation angles of the ships during the collision are small and can be neglected in certain parts of the analysis.

- There is no change in the distribution of mass after the initial contact.

- After the "inelastic" collision, the striking ship is attached to the struck ship and both ships move together as a single body.

Similar three degree of freedom dynamics are used in the SIMCOL model, and are described in detail in Section 3.2. In SIMCOL, external dynamics are calculated simultaneously with internal mechanics in a time-stepping solution.

2.1.3.2 Zhang's Model [17]

Instead of considering the collision in a global system as in Hutchison's study, Zhang applies three local coordinate systems to the striking ship, the struck ship and the impact point separately (Figure 2.1). By analyzing the motions and impulses around the impact point, the kinetic energy lost in collision is derived. Implicit assumptions in this analysis include: 1) small rotation during the collision (the angles α and β in Figure 2.1 are considered constant); and 2) a constant ratio of absorbed plastic deformation energy is assumed in the transverse and longitudinal directions. The absorbed energy is calculated uncoupled from the internal mechanics problem.

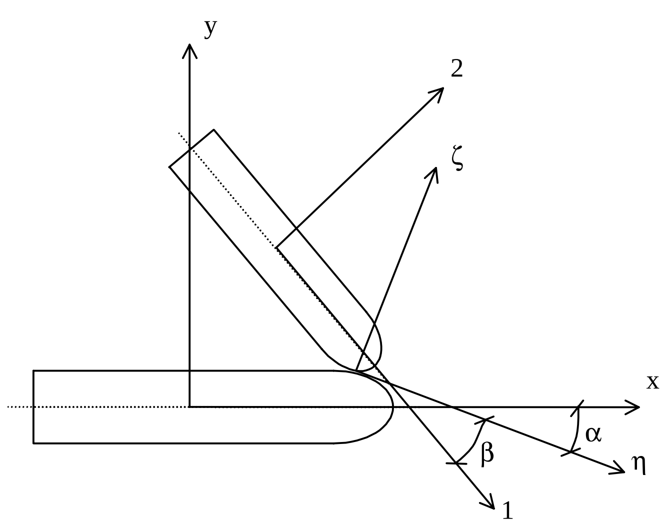

Figure 2.1 DTU Ship Dynamics Model

This approach is used in the Technical University of Denmark (DTU) collision simulation model.

2.2 INTERNAL MECHANICS

Currently available methods for analyzing internal collision mechanics may be categorized as:

- Correlation of actual collision data;
- Direct calculations;
- Finite element analysis; and
- Model experiments.

2.2.1 Correlation Of Actual Collision Data

2.2.1.1 Minorsky Method

The Minorsky method [8] is representative of empirical formulae derived from data of actual accidents. Based on an investigation of 26 ship-ship collisions, Minorsky relates the volume of damaged structural steel to the energy absorbed during the collision.

The straight-line correlation between the damaged volume of ship structure and absorbed energy was found to be (Figure 2.2):

$$E_T = 414.5 R_T + 121{,}900 \qquad [2.5]$$

where

E_T - energy absorbed in collision (ltons-knots^2); and
R_T - resistance factor or damaged volume of structural steel (ft^2 in).

Later, Reardon and Sprung [9] revalidated Minorsky's approach by further investigation of 16 collisions and proposed the following correlation in metric units:

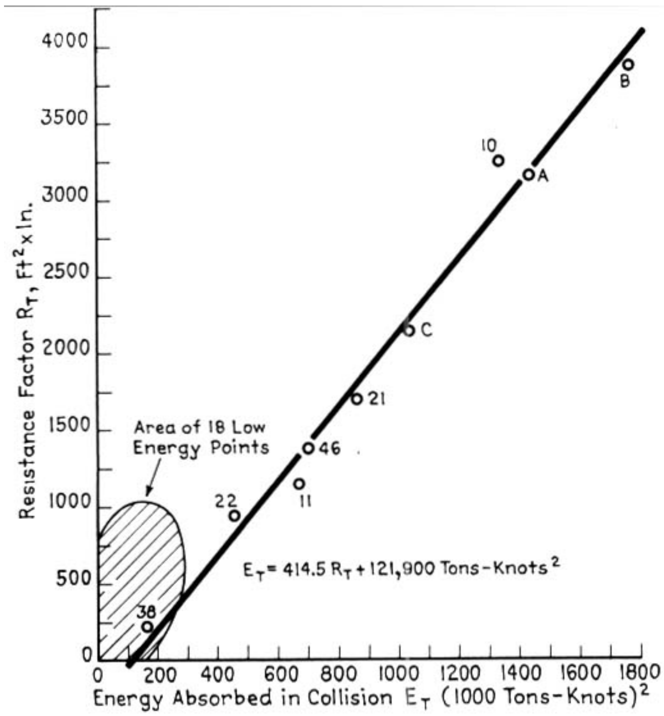

Figure 2.2 Minorsky's Correlation

$$\Delta KE = (47.1 \pm 8.8)R_T + 28.4 \qquad [2.6]$$

where

ΔKE - lost kinetic energy in MJ; and

R_T - resistance factor in m^3.

By solving Equations [2.2] and [2.6], a closed form solution of damage volume, and consequently the penetration, can be made.

The major problem with the Minorsky method is with low energy collisions that do not cause the rupture of side shell. As Reardon and Sprung stated, the intercept term of Minorsky's correlation, 121,900 ltons-knots^2 in the original Minorsky's formula and 28.4 MJ in Reardon and Sprung's revalidated one, is the energy expended puncturing and tearing through the shell of the struck ship. This single value approach is not accurate in low-energy collisions without rupture of the side shell.

2.2.1.2 Extensions of Minorsky Method

To correct the limitation of Minorsky's method at the low energy end, several approaches have been developed.

A simplified procedure introduced by Jones [10] extended the Minorsky correlation by modeling the ship's side shell as a clamped beam subjected to a concentrated load at mid-span (Figure 2.3). It is also assumed that membrane behavior occurs from the beginning of deformation. This results in the following equations for predicting the low energy structural response:

$$E_T = 0.030288\sigma_y\left(\frac{w}{L}\right)^2 R_T \qquad R_T = \frac{2LB_e t}{144} \tag{2.7}$$

where

σ_y	-	yielding strength of the beam (psi);
w	-	deformation of the beam at mid-span (in);
L	-	one half of unsupported span of the beam (in);
B_e	-	breadth of the beam (in); and
t	-	thickness of the beam (in).

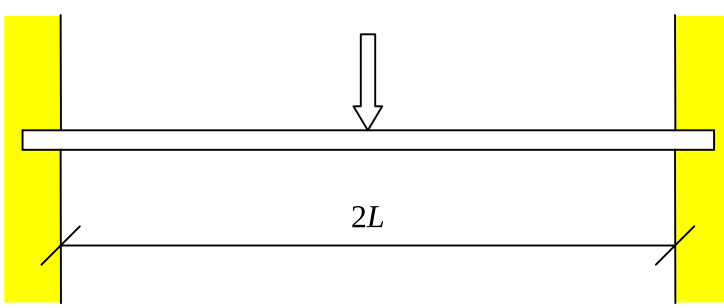

Figure 2.3 Jones' Beam Model

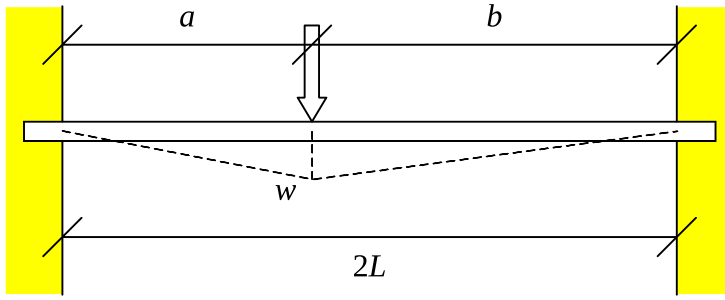

Figure 2.4 Van Mater's Beam Model

Based on a study by McDermott, Van Mater extended Jones' analysis to off-center striking (Figure 2.4) and derived the maximum deflection of the side panel based on a rupture strain of 0.1 [10]:

$$E_{(a,b)} = E_{CL}\frac{a}{b}$$
$$w_m = 0.453a \qquad [2.8]$$

where

$E_{(a,b)}$ - absorbed energy when striking point is away from mid-span (lton-knots^2);

E_{CL} - absorbed energy derived by Jones (lton-knots^2);

a - distance from striking point to the close support (in);

b - distance from striking point to the far support (in); and

w_m - maximum deformation of the side panel (in).

On the basis of measurements of lengthening of the broken side shell to membrane stress in German GKSS tests, Woisin also proposed an alternative to the intercept term in Minorsky's correlation [18]. He suggested the energy absorbed by the ruptured shell be calculated as follows:

$$b = 0.5\sum H\, t_s^2 \qquad [2.9]$$

where

b - absorbed energy by ruptured side shell and longitudinal bulkheads (MJ);

H - height of broken or heavily deformed side shell and bulkheads (m); and

t_s - thickness of side shell and longitudinal bulkheads (cm).

With these improvements, the Minorsky method is a very effective way to estimate damage extents of ships in collision in the past, and is still a powerful tool today. A major limitation in these improvements is that they do not consider many important side shell design parameters, and cannot properly be applied to new and unique designs including double hulls.

2.2.2 Direct Calculations

Collision research continues to develop new methods to predict the structural response of ships in collision from the first principles of engineering. There are several analysis schemes available today. The basic principle behind these methods is similar. They decompose the struck ship into simple substructures or components, such as plates, stiffeners, web frames and panels, etc. The energy absorbed in each substructure during the collision process is calculated separately. The total absorbed energy up to rupture of the cargo boundary is obtained by summing up the absorbed energy for all components.

A number of these methods are based on plastic membrane tension analysis. These include methods proposed by McDermott [11], the Rosenblatt study [12] and Reckling [19]. These schemes were developed primarily for minor ship collisions before rupture of cargo boundaries. Others are derived based on the energy absorbed during plastic deformation of basic structural elements such as angles, T-sections and cruciforms. MIT's DAMAGE and the DTU model are examples of energy-based methods.

2.2.2.1 Rosenblatt Study

The methods used in the Rosenblatt study [12] were developed and summarized by McDermott et al [11]. They were developed for analyzing minor collisions, which are defined as collisions without rupture of cargo boundaries. Their purpose is to calculate the maximum kinetic energy that can be absorbed in the tanker side structure without rupture so that the structure can be optimized for crashworthiness in the design stage. They assume that the bow of the striking ship is infinitely stiff and that only the striking ship absorbs plastic energy. Thus, the collision procedure can be decomposed into a series of deformation mechanisms, including bending of the stiffened hull plating, membrane stretching, web frame failures, and deck folding, until rupture of the cargo boundary. Figure 2.5 shows the assumed idealized collision imprint into the struck ship. Possible side structure plastic deformation mechanism options for a single hull ship are depicted in Figure 2.6. Deformation mechanisms considered for double hull ships are

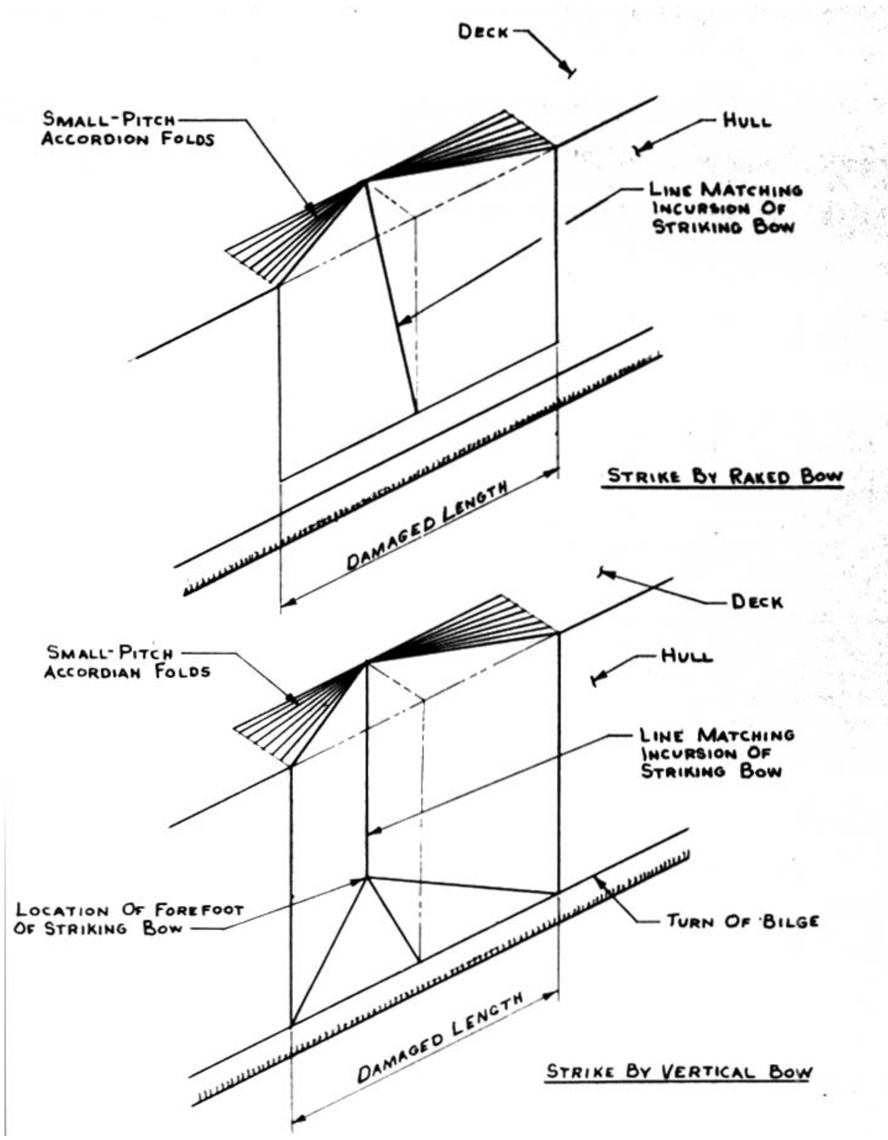

Figure 2.5 Assumptions for Collision Imprint in Struck Ship [12]

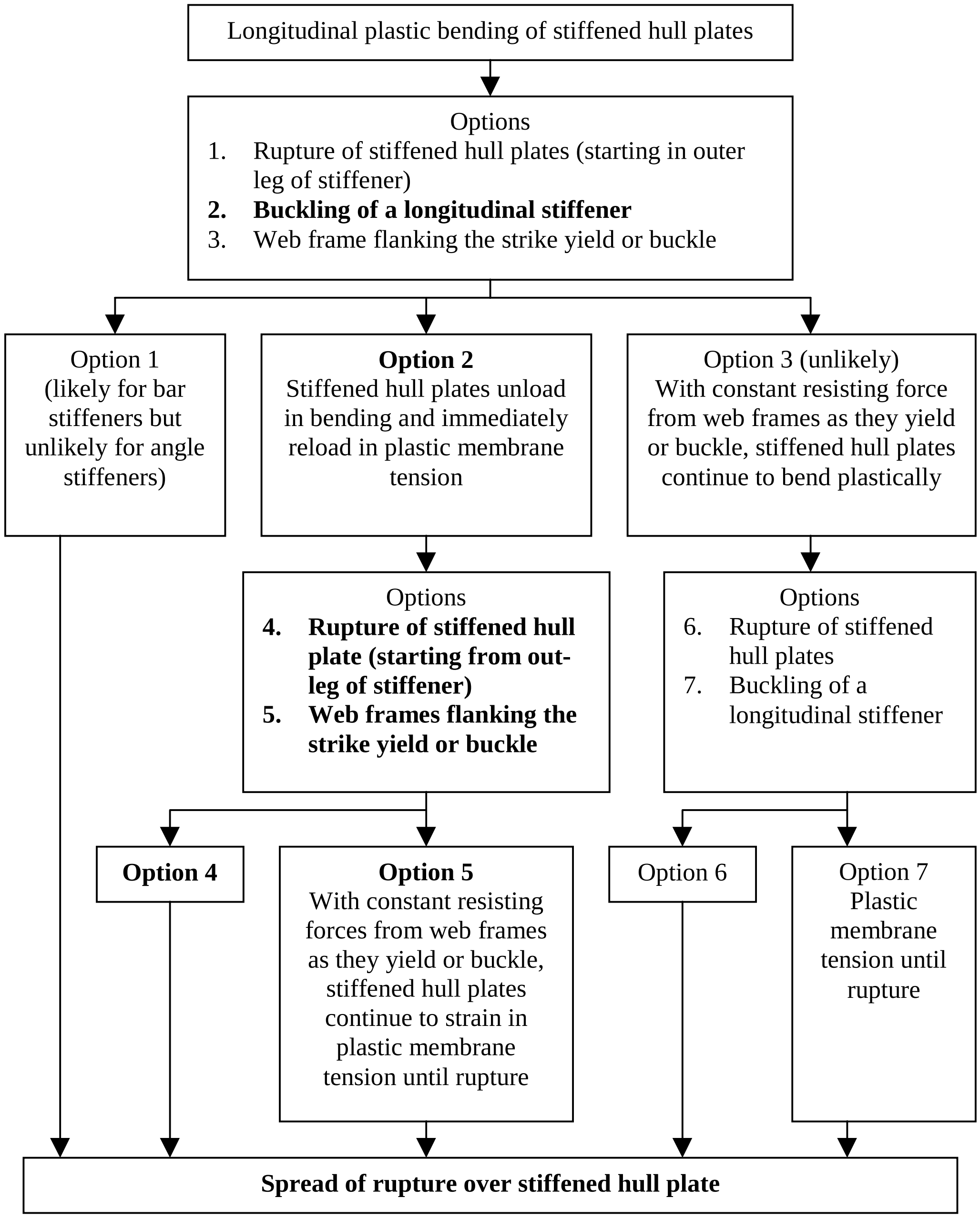

Firgure 2.6 Flow Diagram for Deformation Analysis of Single Hull or Outer Shell [12]

shown in Figure 2.7. The analysis procedure follows the consequence of these deformation mechanisms.

In the Rosenblatt study, the rupture of plates under membrane tension is determined by the following criteria:

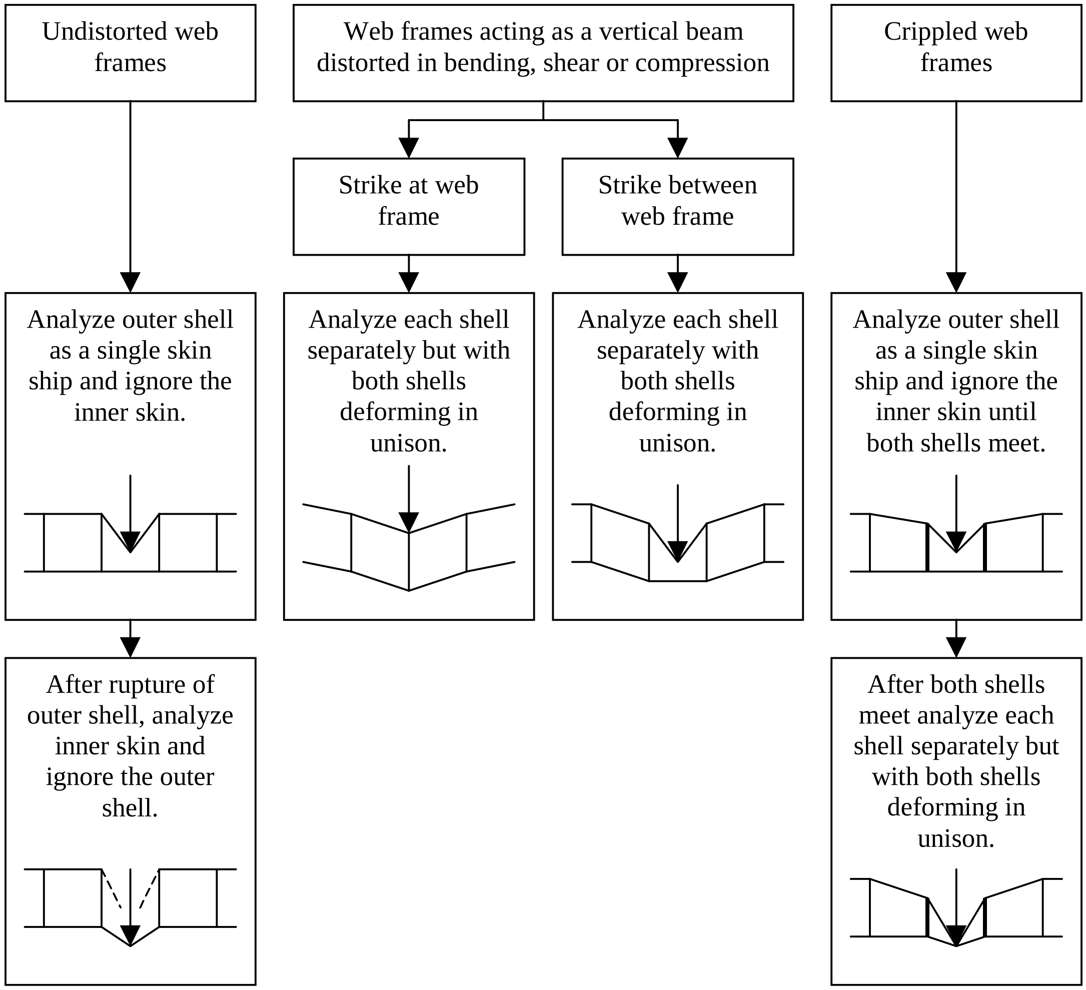

Figure 2.7 Flow Diagram for Collision Energy Analysis of a Double Hull Ship [12]

- The strain in the plate reaches the rupture strain, ϵ_r, which is typically taken as 10% level ABS steel; or

- The bending angle at a support reaches the critical value as defined in the following formula:

$$\varepsilon_m = \frac{4}{3}\frac{\sigma_m}{\sigma_u - \sigma_m \cos\theta_c}\sin\theta_c \tan\theta_c = 1.5D \qquad [2.10]$$

where

ϵ_m - maximum bending and membrane-tension strain at hull rupture;

σ_m - in-plate stress under membrane-tension (MPa);

σ_u - ultimate stress of the plate (MPa);

θ_c - critical bending angle; and

D - tension test ductility in a 2-in gage length, 32% for ABS steel.

The in-plate stress during the membrane-tension phase, σ_m, is assumed to be:

$$\sigma_m = \frac{1}{2}(\sigma_u + \sigma_y) \quad [2.11]$$

SIMCOL uses the mechanisms in Rosenblatt study starting with Version 1.1. Details are given in Chapter 3.

2.2.2.2 Reckling's Model [19, 20]

Reckling's model is actually an extension of the Rosenblatt methods. In this model, the striking bow is no longer treated as a rigid wedge, and can deform. Therefore, the collision force exerted by the deformed striking bow is not treated as a concentrated force, but a distributed one over a certain length. To determine the resistant force and deformation of the striking bow, Reckling introduced detailed calculations of crushing loads of different shapes of plates under different loads. Deformations of both striking and struck ships are determined by comparing their collision resistant forces. Reckling also suggested a 5% rupture strain instead of the 10% strain used in the Rosenblatt method.

2.2.2.3 Super-Element Methods

Both DAMAGE and the DTU model calculate the absorbed energy for direct contact deformation of struck ship super-elements by the striking ship bow. This is not a finite element method. Deformation away from the actual striking ship penetration is not considered.

The DTU model is based on Pederson's study of bow collisions [13], where Amdahl's method [21] and Yang and Caldwell's model [22] are investigated and compared. Both

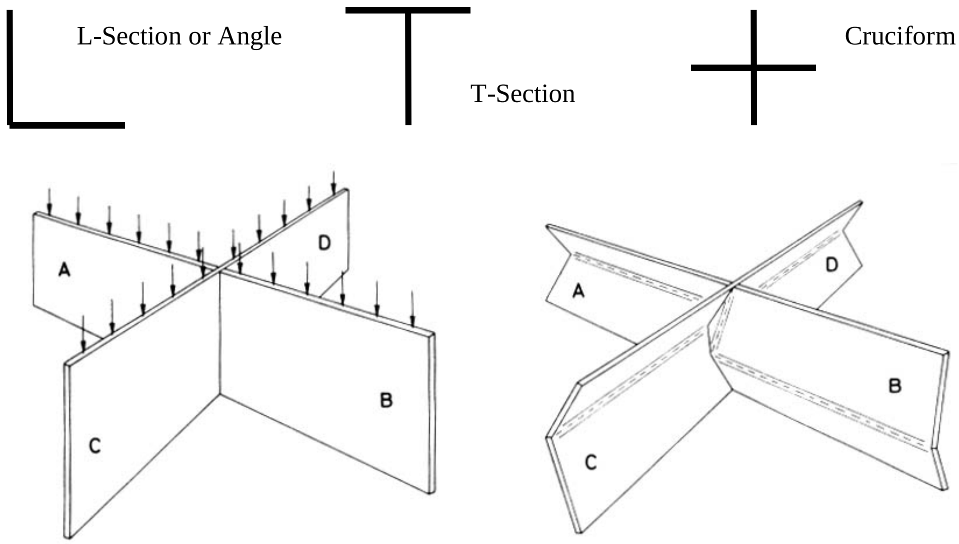

Crushing Mechanism of cruciformed structural element

Figure 2.8 Basic Structural Elements and Crushing Mechanism [23]

methods are based on the deformation and energy evaluation procedure and folding mechanisms proposed by Wierzbicki [23]. By summing the deformation energy absorbed by various sections and intersections during the folding process, i.e. angles, T-sections and cruciforms, the membrane tension energy absorbed in the shell plate and the total crushing force is obtained (Figure 2.8). These sections and intersections are called Super-Elements.

DAMAGE [15] is developed based on the same methodology and mechanics.

2.2.3 Finite Element Analysis

With the assistance of computers, many structural problems can be solved by the finite element method. The finite element method is also used widely as a tool to simulate and recreate model tests and actual accidents.

Because of the size and complexity of the ship structure, a finite element analysis usually takes hundreds of hours to create and solve. This is a significant disadvantage and much effort has been applied to simplifying these models.

In the 1980s, Ito, et al. [24, 25, 26] carried out a series of theoretical and experimental studies to develop a simplified method. Since most deformation in collisions is local, instead of modeling the whole struck ship or a whole segment of it, Ito only modeled a piece of the side panel with coarse triangular elements. The principle of stationary potential energy was applied to analyze the deformation and energy at the point of rupture.

Another simplified method, the Idealized Structural Unit Method (ISUM), was developed by Paik [27, 28]. ISUM is an idealized non-linear stress-strain method. A coarse mesh method is used to model a segment of the struck ship with elements the size of whole panels supported by web frames and stringers. These are also super-elements, but solved in a finite element matrix vice by direct contact. ISUM considers the coupling between local and global deformation and failure modes inside model. Based on ISUM, Paik developed the collision simulation software, ALPS/SCOL.

With these simplifications, the computing time is reduced dramatically, and in the case of Paik's model, the time is reduced to a fraction of hour to run a single collision case.

2.2.4 Model Experiments

Because of the complexity of the ship structure and collision mechanisms, and the lack of accurate and detailed data of actual collisions, it is necessary to conduct experiments to understand the internal mechanics behind collisions. An important example is the German GKSS experiments [18]. Based on these experiments, Woisin developed an extension to Minorsky's correlation and proposed methods to improve the crashworthiness of several types of ships.

To adequately simulate the structural response of ships in collisions, it is necessary to use full scale or at least large-scale models so that the structural behavior of the model represents that of a real ship. These experiments are extremely expensive. Therefore, experiments are more often used as a tool to verify the theoretical results derived from other methods rather than as a direct simulation approach.

Experiments conducted at US Steel Research Laboratory were used extensively in the Rosenblatt study [11]. On the basis of the results of a series model tests, Ito et al. generated and verified their simplified method to analyze the response of double hull structures in minor collisions [24]. Recently, Paik has also completed an experimental study of internal collision mechanics to demonstrate the accuracy of his ISUM model [27]. These experiments have also uncovered unexpected collision mechanisms.

2.3 COUPLING INTERNAL AND EXTERNAL MODELS

Most of the previous and current work in collision analysis, including the Minorsky method [8], DAMAGE [15], the DTU model and Paik's ALPS/SCOL, determine the lost kinetic energy in an uncoupled solution of the external problem, then calculate the deformation energy of the colliding structures with increasing penetration, and finally find the maximum penetration by matching the deformation energy to the lost kinetic energy. This approach relies on the solution of final velocities of struck and striking ships by an external model. This uncoupled solution requires significant simplifying assumptions, and/or restricting degrees of freedom of the system.

The analysis can also be done in the time domain with a fully coupled time-stepping solution similar to Hutchison [16] and Crake [7]. Starting with the initial external condition, impact forces are calculated based on internal structural mechanics at each time step and applied to the struck and striking ships in the external model until the forces go to zero. This is the method used in the continued evolution of SIMCOL presented in Chapter 3.

CHAPTER 3 EVOLUTION OF THE SIMCOL MODEL

As discussed in Chapter 2, collision analysis models consist of three elements: 1) the external dynamics sub-model; 2) the internal mechanics sub-model; and 3) the simulation model that connects internal and external sub-models. SIMCOL includes these three elements.

3.1 SIMULATION MODEL

The selection of internal and external models depends to a large extent on the method chosen to simulate the collision process.

Since this study provides a collision model for probabilistic analysis considering all likely collision scenarios, a full three-degree of freedom model is selected so that the effect of different collision scenarios is best captured. Most collision research has focused on penetration. In order to obtain an uncoupled solution of the external problem of ship dynamics, the degrees of freedom, especially yaw, are frequently restricted in these studies. Although convenient, this is a questionable simplification that may not yield conservative results.

The simulation model used in SIMCOL is depicted in Figure 3.1. The simulation is stopped under the following conditions:

- The impact point moves beyond the cargo block. This is because this study is restricted to cargo block structures.
- The relative motion of struck and striking ship at the impact location is small.
- The reaction forces calculated from the internal collision mechanisms are small.
- There is only small or zero loss of kinetic energy during the time step.

An important consideration in a time domain simulation is the time step. As in Crake's model, the time step is calculated by the method proposed by Hutchison [16].

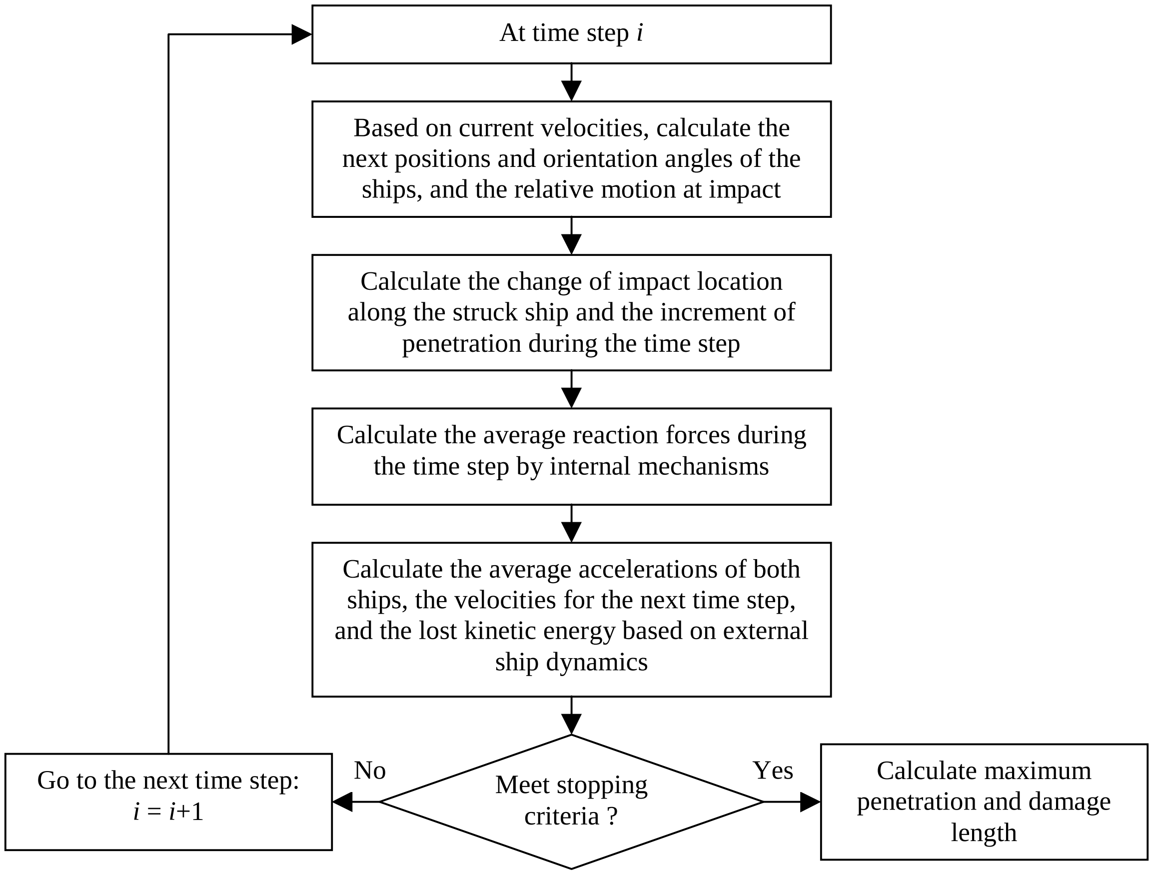

Figure 3.1 Simulation Process

In Hutchison, the maximum penetration and collision duration when a rigid bow strikes the center of gravity of the struck ship at a right angle are derived based on Minorsky's method. The duration formula is rearranged using metric units as follows:

$$
\begin{aligned}
T &= \frac{\pi}{2}\sqrt{\frac{1}{2\times 47.1\times 10^{6}}\cdot\frac{1}{t\cdot\tan\alpha}\cdot\frac{M_{V1}\cdot M_{V2}}{M_{V1}+M_{V2}}} \\
&= 1.6184\times 10^{-4}\sqrt{\frac{1}{t\cdot\tan\alpha}\cdot\frac{M_{V1}\cdot M_{V2}}{M_{V1}+M_{V2}}}
\end{aligned}
\qquad [3.1]
$$

where

T - duration time of collision (seconds);

t - aggregated thickness of deck plating and bottom shell (m);

α - half entrance angle of the striking bow;

M_{V1} - virtual mass of the struck ship in sway direction (kg); and

M_{V2} - virtual mass of the striking ship in surge direction (kg).

In this analysis, a fraction of this duration, calculated by Equation [3.1], is used as the time step of the simulation. The time step, τ, is:

$$\tau = c_T T \qquad [3.2]$$

SIMCOL Version 2.0 uses c_T equal to 1/200. The analysis results of Version 1.0 indicate that, with the above time step, the accuracy of the simulation converged very well and there is only a 0.3% difference from direct calculation with Minorsky's mechanism when the striking ship hits the midship point of the stuck ship at a right angle. However, it is found that, with the above c_T value and a high striking speed, the relative movement of striking bow into the struck ship during one time step is large once the side shell is ruptured. The membrane tension energy absorbed during this time step cannot be calculated accurately. Since the membrane tension effect is important in collision resistance, c_T is reduced to 1/2000 in Version 2.1 in order to capture the subtlety of structural response.

3.2 EXTERNAL PROBLEM

The next model element is the external ship dynamics problem. Important components of the external problem are the coordinate system and resulting equations of motion.

3.2.1 Coordinate System

To simulate the collision scenario by the time domain method, i.e. to determine the locations and speeds of the striking and struck ships at each time step, requires careful selection of the coordinate systems.

The external collision geometry is defined as shown in Figure 3.2, where ϕ is the collision angle, θ_1 and θ_2 are, respectively, the longitudinal directions of the struck and striking ships, and l is the longitudinal location of the impact point measured from

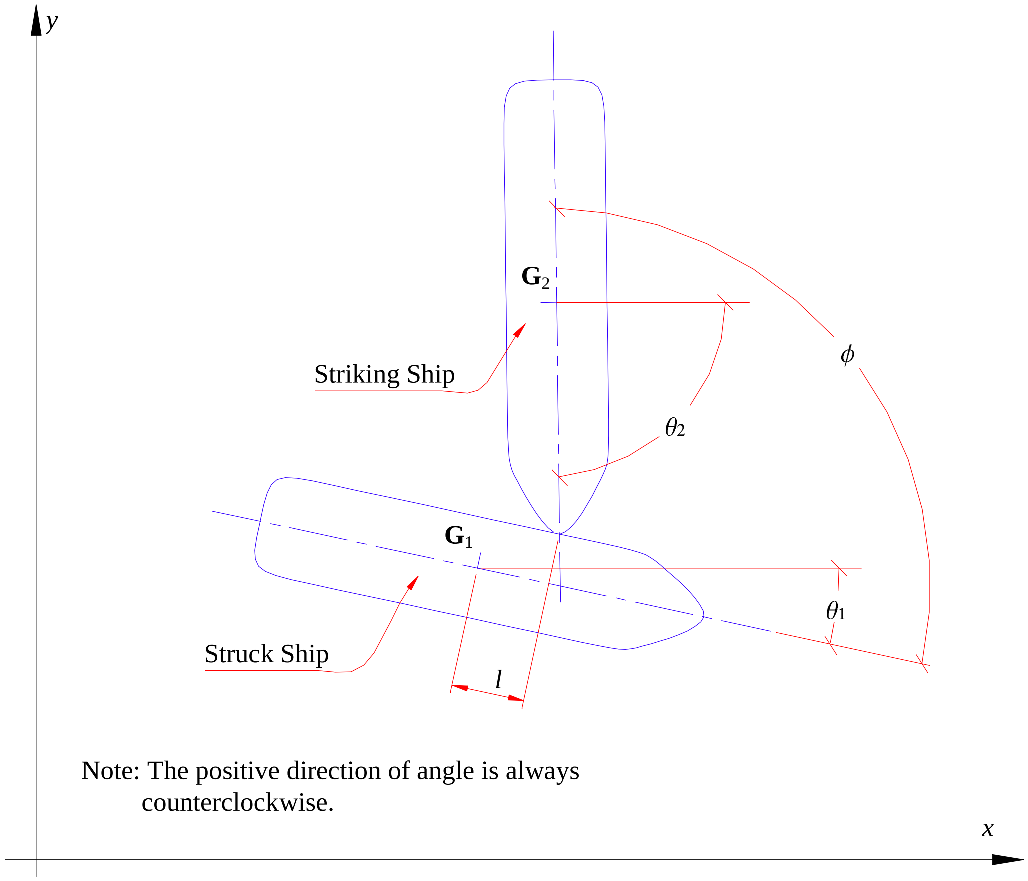

Figure 3.2 Collision Scenario Definitions and Global Coordinate System

midship in the struck ship towards the stern. The global coordinate system is established in terms of these variables. Its origin is set at the location of the center of gravity of the struck ship with the x-axis towards the bow of the struck ship.

The initial locations and orientations of the struck and striking ships in the global coordinate system are:

$$
\begin{aligned}
&x_{1,0} = 0 \qquad y_{1,0} = 0 \qquad \theta_{1,0} = 0 \\
&x_{2,0} = -l_0 + \frac{L_{BP2}}{2}\cos\phi_0 \\
&y_{2,0} = \frac{B_1}{2} + \frac{L_{BP2}}{2}\sin\phi_0 \\
&\theta_{2,0} = \phi_0 - \pi
\end{aligned}
\qquad [3.3]
$$

where

x_1, y_1 - center of gravity of the struck ship (m), which is assumed at midship;

θ_1 - angle of the longitudinal direction of the struck ship;

x_2, y_2 - center of gravity of the striking ship (m), which is assumed at midship;

θ_2 - angle of the longitudinal direction of the striking ship;

L_{BP2} - length between perpendiculars of the striking ship (m);

B_1 - breadth of the struck ship (m); and

ϕ - collision angle.

In order to calculate relative movement and collision forces, a local coordinate system, ξ-η system as shown in Figure 3.3, is introduced on the struck ship, where d is the depth of penetration. The origin of this system is set at midship point on the shell plate of the damaged side of the struck ship. Axes ξ and η are pointing aft and inboard relative to the struck ship.

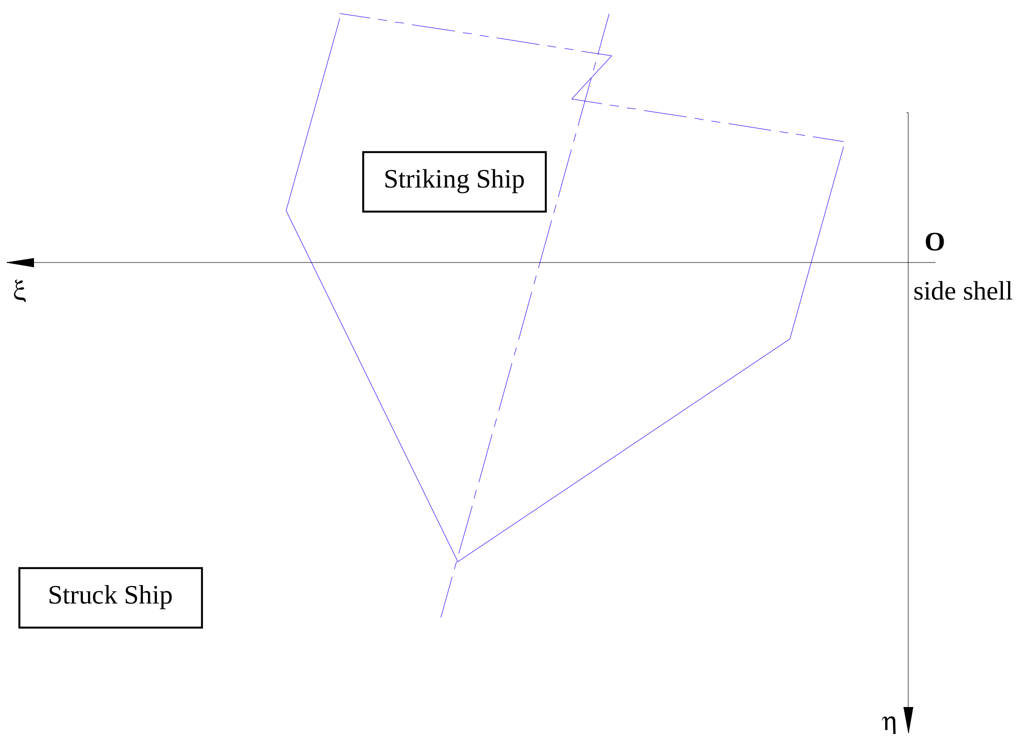

Figure 3.3 Local coordinate System, ξ-η

By applying the following relations, forces and moments in the local ξ-η system can be transformed to the global x-y system.

$$\begin{aligned}
&\left|\mathbf{F}_{xy}\right| = \left|\mathbf{F}_{\xi\eta}\right| \\
&\zeta_{xy} = \zeta_{\xi\eta} + \theta_1 - \pi \\
&M_{\mathbf{G}} = -\mathbf{F}_{\xi\eta} \cdot \mathbf{r}_{\mathbf{G}} + M_{\mathbf{O}}
\end{aligned} \qquad [3.4]$$

where

F - force vector in relative coordinate system;

ζ - force direction angle in relative coordinate system

M - moment about relative location, **O** or $\mathbf{G}_i$; and

$\mathbf{r_G}$ - vector $\overrightarrow{\mathbf{OG}_i}$ in ξ-η system that can be found from Figures 3.2 and 3.3.

3.2.2 Ship Dynamics in Collision

To simulate the movements of both struck and striking ships in three degrees of freedom, the ship dynamics, including hydrodynamic added mass, kinetic energy and equations of motion are defined based on Hutchison [16].

The hydrodynamic added mass for each ship is a tensor in the form:

$$\mathbf{A} = \begin{bmatrix} a_{11} & a_{12} & a_{13} \\ a_{21} & a_{22} & a_{23} \\ a_{31} & a_{32} & a_{33} \end{bmatrix}$$

in a system with three degrees of freedom, where

a_{ij} - added mass or inertia in direction i due to the motion in direction j; and

i, j - axes of the coordinate system.

To simplify the added mass tensor for each ship, we define each ship's local coordinate system such that its origin and axes are coincident with its midship point and its principal axes.

Considering the approximate symmetry of the ship, and with the center of gravity of the ships assumed to be at the midship point, the off-diagonal terms of the added mass tensor in each ship coordinate system are zeros:

$$\mathbf{A}_s = \begin{bmatrix} a_{11} & 0 & 0 \\ 0 & a_{22} & 0 \\ 0 & 0 & a_{33} \end{bmatrix} \qquad [3.5]$$

where

a_{11} - added mass in surge direction (kg);
a_{22} - added mass in sway direction (kg); and
a_{33} - added mass in yaw direction (kg-m^2).

Similarly, the actual mass of the ship can be represented by a tensor in the following form:

$$\mathbf{M}_{ship} = \begin{bmatrix} m_s & 0 & 0 \\ 0 & m_s & 0 \\ 0 & 0 & I_{s33} \end{bmatrix} \qquad [3.6]$$

where

m_s - mass of the ship (kg); and
I_{s33} - moment of inertia about yaw axes of the ship (kg-m^2).

Therefore, the virtual mass tensor becomes:

$$\mathbf{M}_V = \mathbf{M}_{ship} + \mathbf{A} \qquad [3.7]$$

Since it is preferred to have added mass tensors in the global coordinate system as shown in Figure 3.2, each ship added mass tensor is transformed in accordance with the orientation of the ship. The transformed tensor, $\mathbf{A}_\theta$, [16,17] is:

$$\mathbf{A}_\theta = \begin{bmatrix} a_{11}\cos^2\theta + a_{22}\sin^2\theta & (a_{11}-a_{22})\cos\theta\sin\theta & 0 \\ (a_{11}-a_{22})\cos\theta\sin\theta & a_{11}\sin^2\theta + a_{22}\cos^2\theta & 0 \\ 0 & 0 & a_{33} \end{bmatrix} \quad [3.8]$$

The added mass in surge is approximated by the displacement of a circumscribed circle of the same area as the ship's cross sectional area at midship [7]. Therefore, the added mass in surge, a_{11}, is:

$$a_{11} = \frac{4}{3}\rho\pi\left(\frac{BT}{\pi}\right)^{\frac{3}{2}} = 0.75225\rho(BT)^{\frac{3}{2}} \quad [3.9]$$

where

ρ - density of sea water, 1025 kg/m^3;
B - breadth of the ship (m); and
T - draft of the ship (m).

The added mass in sway is calculated using strip theory. An approximation is given in Crake's model where the cross sections of ship are assumed to be rectangular [7]. The added mass in sway, a_{22}, is then:

$$a_{22} = 1.189\rho T^2 L_{BP} \quad [3.10]$$

where

L_{BP} - length between perpendiculars of the ship (m).

Similarly, by assuming the waterplane is rectangular, the original moment of inertia, I_{33s}, and added mass in yaw, a_{33}, are [7]:

$$I_{s33} = \frac{m_s L_{BP}^{\ 2}}{12}$$
$$a_{33} = \frac{2.378\rho T^2 L_{BP}^{\ 3}}{24} = 0.0991\rho T^2 L_{BP}^{\ 3} \quad [3.11]$$

Given the added mass for the principal axes, we can obtain the virtual mass that includes the actual mass of ship and the added mass. The virtual mass, $\mathbf{M}_V$, for each ship is:

$$\mathbf{M}_{V\theta} = \mathbf{M}_{ship} + \mathbf{A}_{\theta} = \begin{bmatrix} m_{V11} & m_{V12} & 0 \\ m_{V21} & m_{V22} & 0 \\ 0 & 0 & I_{V33} \end{bmatrix}$$
$$= \begin{bmatrix} m_s + a_{11}\cos^2\theta + a_{22}\sin^2\theta & (a_{11} - a_{22})\cos\theta\sin\theta & 0 \\ (a_{11} - a_{22})\cos\theta\sin\theta & m_s + a_{11}\sin^2\theta + a_{22}\cos^2\theta & 0 \\ 0 & 0 & I_{s33} + a_{33} \end{bmatrix} \quad [3.12]$$

The above matrix is symmetric, i.e. $m_{V12} = m_{V21}$.

Given the added mass and velocity of each ship, their kinetic energy is derived as follows:

$$KE = \frac{1}{2}(\mathbf{M}_{V\theta}\ \mathbf{V}_s) \cdot \mathbf{V}_s$$

where

KE	-	kinetic energy of the ship (J);
$\mathbf{V}_s$	-	velocity of the ship, and $\mathbf{V}_s = \{u, v, \omega\}^T$;
u	-	speed in the X direction of global coordinate system (m/s);
v	-	speed in the Y direction (m/s); and
ω	-	angular velocity of the ship in yaw (degree/s).

Therefore,

$$KE = \frac{1}{2}\begin{Bmatrix} m_{V11}u + m_{V12}v \\ m_{V21}u + m_{V22}v \\ I_{V33}\omega \end{Bmatrix} \cdot \begin{Bmatrix} u \\ v \\ \omega \end{Bmatrix} = \frac{1}{2}(m_{V11}u^2 + 2m_{V12}uv + m_{V22}v^2 + I_{V33}\omega^2) \quad [3.13]$$

By applying the internal collision mechanisms, we can obtain the forces exerted on the struck and striking ships during collision. The equations of motion for the ships are then:

$$\mathbf{F} = \mathbf{M}_{V\theta}\ \mathbf{V}_s'$$

where

$\mathbf{F}$ - forces exerted on ship, and $\mathbf{F} = \{F_x, F_y, M\}^T$;

F_x - force on X direction of global coordinate system (N);

F_y - force on Y direction (N);

M - moment about the center of gravity of the ship in Z direction (N-m);

$\mathbf{V}_s'$ - accelerations of ship, and $\mathbf{V}_s' = \{u', v', \omega'\}^T$;

u' - acceleration in X direction of global coordinate system (m/s^2);

v' - acceleration in Y direction (m/s^2); and

ω' - angular acceleration of ship in yaw (degree/s^2).

Hence, the accelerations of the ships are derived as follows:

$$u' = \frac{F_x m_{V22} - F_y m_{V12}}{m_{V11} m_{V22} - m_{V12}^2}$$
$$v' = \frac{F_y m_{V11} - F_x m_{V12}}{m_{V11} m_{V22} - m_{V12}^2} \qquad [3.14]$$
$$\omega' = \frac{M}{I_{V33}}$$

We can derive the velocities of the ships after a small period of time as:

$$\mathbf{V}_{s,n+1} = \mathbf{V}_{s,n} + \mathbf{V}_s' \tau \qquad [3.15]$$

where

n - number of time periods; and

τ - length of the time period (second),

The location and orientation of the ships is then:

$$\mathbf{X}_{n+1} = \mathbf{X}_n + \mathbf{V}_s \tau \qquad [3.16]$$

where

X - coordinates of gravity center and orientation of the ship in the globe coordinate system, and $\mathbf{X} = \{x, y, \theta\}^T$.

3.3 INTERNAL PROBLEM

An important criterion in the selection of the internal model is speed. Thousands of runs must be made in the probabilistic analysis. Therefore, the first candidate for the analysis is the Minorsky model. The extreme simplicity and the relative accuracy in high-energy collisions make this method most attractive. However, as discussed in Chapter 2, the Minorsky method does not properly calculate the resistance of side structure and longitudinal bulkheads.

In order to address this shortcoming, direct calculation methods, first Van Mater's method and later the Rosenblatt methods, are added to the model. Although these approaches are based on a series of assumptions, they are relatively simple tools with reasonable accuracy. The internal problem is separated into the following two sub-models:

- Minorsky mechanism for horizontal structural members: decks, bottoms and stringers; and

- Van Mater or Rosenblatt method for vertical structural members: side structures and longitudinal bulkheads.

Also, in order to keep the model as simple as possible, SIMCOL Versions 0.0 to 2.0 assume that the striking bow is rigid and has a wedge shape defined by a half entrance angle with infinite vertical extents. SIMCOL Version 2.1 considers the upper and lower extents of the bow relative to the struck ship.

3.3.1 Horizontal Structural Members

The reacting forces of horizontal structural members are calculated using the Minorsky method. Based on the damaged volume of structural steel at each time step, the absorbed energy may be calculated by Equation [2.5] or [2.6]. Since the Minorsky method is only used for estimating the kinetic energy absorbed by damaging decks, bottoms and stringers of the struck ship, the intercept term of original Minorsky formula can be dropped and Equation [2.6] becomes:

$$\Delta KE = 47.1 \times 10^6 R_T \quad [3.17]$$

where we specify

ΔKE - kinetic energy absorbed by decks, bottoms and stringers (J); and

R_T - damaged volume of the above structural members (m^3).

And because there are few variations of structural details across the deck or bottom planes, the damaged volume is approximated as:

$$R_T = \sum A_i t_i \quad [3.18]$$

where

A_i - damaged area of the *i*-th decks or bottoms (m^2); and

t_i - thickness of the *i*-th decks or bottoms (m).

With assumptions that:

- the reacting force is in the direction opposite to the relative motion of the two ships, and,
- the work done by the collision force is equal to the absorbed energy for an inelastic collision,

the reacting force can be determined. This requires calculations for the damaged area of decks, bottoms and stringers, and the direction and magnitude of the relative movement between the two ships.

3.3.1.1 SIMCOL Baseline Version (Version 0.1)

Crake's model [7], SIMCOL Version 0.1, calculates the damaged area based on Reardon and Sprung's proposal [9]:

$$A = \frac{d^2 \tan\phi}{1 - \tan^2\phi / \tan^2\alpha} \qquad [3.19]$$

where

d - penetration of the striking bow (m); and

α - half entrance angle of the striking bow.

Assuming that the striking bow is vertical and has an infinite depth, t_i in Equation [3.17] can be lumped into a single value, t, the total thickness. The effect of longitudinal stiffeners and transverse web frames and floors is also considered by smearing them into t. Stringers are not counted in the damaged volume in this version.

In time step n, the kinetic energy absorbed in horizontal structures becomes:

$$\Delta KE_n = 4.7\times10^6 (R_{T\,n+1} - R_{T\,n}) = 4.7\times10^6 (A_{n+1} - A_n)t \qquad [3.20]$$

where A_n is calculated in accordance with Equation [3.18].

In this model, it is assumed that the collision force is acting on the striking ship bow tip in the direction opposite to its moving course relative to the struck ship.

In accordance with the coordinate systems and collision geometry shown in Figures 3.2, the velocities of both ships at the impact point are:

$$\begin{aligned} u_{c1} &= u_1 + (y_1 - y_c)\omega_1 \\ v_{c1} &= v_1 - (x_1 - x_c)\omega_1 \\ u_{c2} &= u_2 + (y_2 - y_c)\omega_2 \\ v_{c2} &= v_2 - (x_2 - x_c)\omega_2 \\ x_c &= x_2 + \frac{L_{BP2}}{2}\cos\theta_2 \end{aligned} \qquad [3.21]$$

$$y_c = y_2 + \frac{L_{BP2}}{2}\sin\theta_2$$

where

u_1, v_1	-	velocities of the struck ship in X and Y directions (m/s);
ω_1	-	angular velocity of the struck ship (1/s);
u_2, v_2	-	velocities of the striking ship in X and Y directions (m/s);
ω_2	-	angular velocity of the striking ship (1/s);
u_{c1}, v_{c1}	-	velocities of the struck ship at impact point (m/s);
u_{c2}, v_{c2}	-	velocities of the striking ship at impact point (m/s); and
x_c, y_c	-	location of impact point in global system (m).

The relative movement of the striking bow into the struck ship in the time step, s, and its direction angle in the global system, ζ, is:

$$s = \tau\sqrt{(u_{c1} - u_{c2})^2 + (v_{c1} - v_{c2})^2}$$
$$\zeta = \arctan\frac{v_{c1} - v_{c2}}{u_{c1} - u_{c2}} \quad (+\pi) \qquad [3.22]$$

Hence, during time step n, the impact location in the ξ-η system (Figure 3.3) is:

$$l_{n+1} = l_n - s_n \cos(\theta_{1n} - \zeta_n)$$
$$d_{n+1} = d_n + s_n \sin(\theta_{1n} - \zeta_n) \qquad [3.23]$$

The magnitude of the average reacting force is:

$$F_n = \frac{\Delta KE_n}{s_n} \qquad [3.24]$$

3.3.1.2 Improved SIMCOL Versions (Version 1.0 and later)

The geometry used in Version 0.1 is not descriptive of the actual damage volume when:

- the striking bow moves along the longitudinal axis of the struck ship; or

- there is relative rotation between the striking and struck ships.

The damaged geometry is changed in later versions to solve these problems.

With the assumption of a wedge-shaped rigid striking bow, the intrusion portion of the bow is described with five nodes, as shown in Figure 3.4. The shaded area in Figure 3.4 is exactly the damaged area of decks and/or bottoms during the time step.

Coordinates of the five nodes in the ξ-η system at each time step are derived from the penetration and location of the impact, the collision angle, ϕ, and the half entrance angle, α, of the striking bow. $\mathbf{P}_3$ is always found as follows:

$$\mathbf{P}_3 = \{\xi_3, \eta_3\} = \{l, d\} \qquad [3.25]$$
$$\phi' = \pi - \phi$$

If the parallel body of the striking ship has not penetrated into the struck ship:

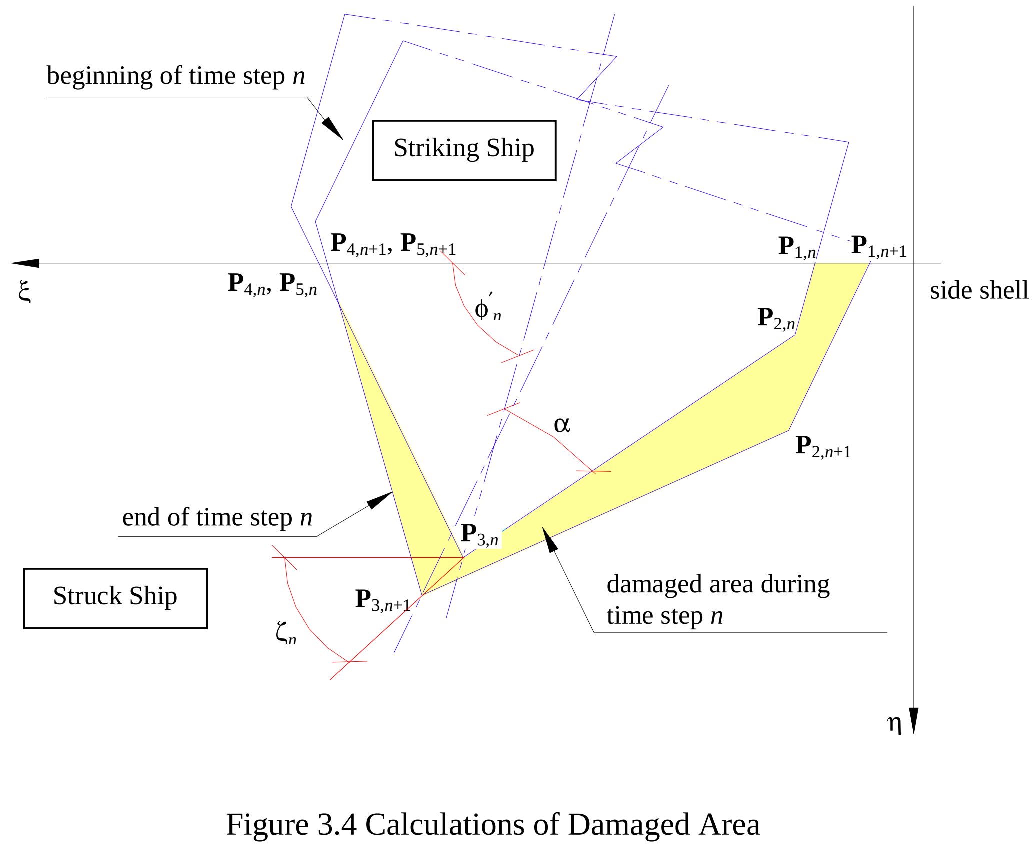

Figure 3.4 Calculations of Damaged Area

$$\overline{\mathbf{P}_2\mathbf{P}_3} \le \frac{B_2}{2\sin\alpha} \text{ or } \overline{\mathbf{P}_3\mathbf{P}_4} \le \frac{B_2}{2\sin\alpha}\text{, then}$$

$$\begin{aligned}
\mathbf{P}_2 &= \{\xi_2, \eta_2\} = \left\{\xi_3 - \frac{\eta_3}{\tan(-\alpha+\phi')}, 0\right\} \\
\mathbf{P}_1 &= \{\xi_1, \eta_1\} = \mathbf{P}_2 \\
\mathbf{P}_4 &= \{\xi_4, \eta_4\} = \left\{\xi_3 - \frac{\eta_3}{\tan(\alpha+\phi')}, 0\right\} \\
\mathbf{P}_5 &= \{\xi_5, \eta_5\} = \mathbf{P}_4
\end{aligned} \quad [3.26]$$

If the parallel body of the striking ship has penetrated into the struck ship:

$$\overline{\mathbf{P}_2\mathbf{P}_3} > \frac{B_2}{2\sin\alpha} \text{ or } \overline{\mathbf{P}_3\mathbf{P}_4} > \frac{B_2}{2\sin\alpha}\text{, then}$$

$$\begin{aligned}
\mathbf{P}_2 &= \{\xi_2, \eta_2\} = \left\{\xi_3 - \frac{B_2}{2\sin\alpha}\cos(-\alpha+\phi'), \eta_3 - \frac{B_2}{2\sin\alpha}\sin(-\alpha+\phi')\right\} \\
\mathbf{P}_1 &= \{\xi_1, \eta_1\} = \left\{\xi_2 - \frac{\eta_2}{\tan\phi'}, 0\right\} \\
\mathbf{P}_4 &= \{\xi_4, \eta_4\} = \left\{\xi_3 - \frac{B_2}{2\sin\alpha}\cos(\alpha+\phi'), \eta_3 - \frac{B_2}{2\sin\alpha}\sin(\alpha+\phi')\right\} \\
\mathbf{P}_5 &= \{\xi_5, \eta_5\} = \left\{\xi_4 - \frac{\eta_4}{\tan\phi'}, 0\right\}
\end{aligned} \quad [3.27]$$

where

$\mathbf{P}_i$ - node of penetrated bow;

ξ_i, η_i - coordinates of node in ξ-η system (m); and

B_2 - breadth of the striking ship (m).

Once we have the coordinates of these nodes before and after the particular time step, the segment of the bow plan that has caused further damage during this time step and, consequently, the area swept by a specific segment can be determined. In the case of the segment $\mathbf{P}_1\mathbf{P}_2$ in Figure 3.4, the out-sweeping area, A_1, during time step n can be calculated as follows:

$$A_{1,n} = \frac{1}{2}\left(\begin{vmatrix} \xi_{2,n} & \xi_{1,n} \\ \eta_{2,n} & \eta_{1,n} \end{vmatrix} + \begin{vmatrix} \xi_{2,n+1} & \xi_{2,n} \\ \eta_{2,n+1} & \eta_{2,n} \end{vmatrix} + \begin{vmatrix} \xi_{1,n+1} & \xi_{2,n+1} \\ \eta_{1,n+1} & \eta_{2,n+1} \end{vmatrix} + \begin{vmatrix} \xi_{1,n} & \xi_{1,n+1} \\ \eta_{1,n} & \eta_{1,n+1} \end{vmatrix} \right) \quad [3.28]$$

Therefore, the kinetic energy absorbed through sweeping of segment $\mathbf{P}_1\mathbf{P}_2$ of the striking bow, ΔKE_1, is:

$$\Delta KE_{1,n} = 47.1\times10^6\, R_{T1,n} = 47.1\times10^6\, A_{1,n}\; t \quad [3.29]$$

The damage length of deck, L_D, can also be derived as follows:

$$L_D = \max(\xi_{i,j}) - \min(\xi_{i,j}) \qquad i = 1, \ldots, 5 \qquad j = 1, \ldots, m \quad [3.30]$$

where, m is the total iteration number

In SIMCOL Version 2.0 and later, the same approach is used for calculating the damaged area and absorbed energy of stringers or partial decks by excluding the sweeping area beyond their transverse extent. Version 2.1 introduces a striking bow with limited depth. Thereafter, the plating thickness t is the sum thickness of deck and/or bottom structures that are within the upper and lower extents of the striking bow.

The Minorsky force exerted on both striking and struck ships is calculated based on the following assumptions:

- The resistant force acting on each out-sweeping segment is in the opposite direction of the average movement of the segment. The force exerted on the struck ship is in the direction of this average movement.
- The work of the resistant force is done on the distance of this average movement.
- The total force on each segment is acting through the geometric center of the sweeping area.

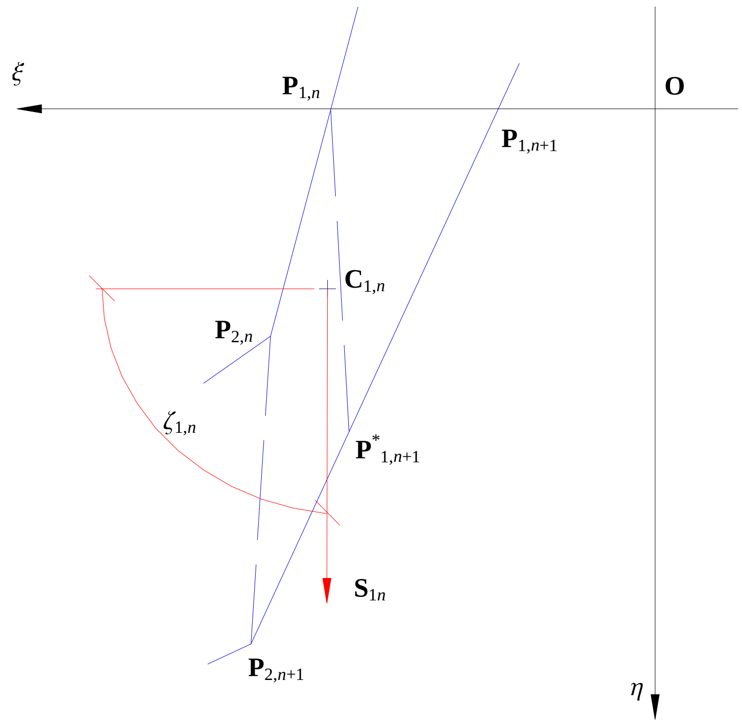

Figure 3.5 Details of Segment $\mathbf{P}_1\mathbf{P}_2$ in Figure 3.4

Using the segment $\mathbf{P}_1\mathbf{P}_2$ in Figure 3.4 as an example (see Figure 3.5), its average movement, $\mathbf{S}_1$, and the geometric center of the sweeping area, $\mathbf{C}_1$, in time step n can be approximated as follows:

Take $\mathbf{P}^*_{1,n+1}$ on $\mathbf{P}_{1,n+1}\mathbf{P}_{2,n+1}$, so that $\overline{\mathbf{P}^*_{1,n+1}\mathbf{P}_{2,n+1}} = \overline{\mathbf{P}_{1,n}\mathbf{P}_{2,n}}$

$$\begin{aligned} \mathbf{S}_{1,n} &= \frac{1}{2}(\overrightarrow{\mathbf{P}_{2,n}\mathbf{P}_{2,n+1}} + \overrightarrow{\mathbf{P}_{1,n}\mathbf{P}^*_{1,n+1}}) \\ &= \frac{1}{2}[\mathbf{P}_{2,n+1} - \mathbf{P}_{2,n} + (\mathbf{P}_{2,n+1} - \mathbf{P}_{1,n+1})\frac{\overline{\mathbf{P}_{1,n}\mathbf{P}_{2,n}}}{\overline{\mathbf{P}_{1,n+1}\mathbf{P}_{2,n+1}}} - \mathbf{P}_{1,n}] \\ \mathbf{C}_{1,n} &= \frac{1}{4}(\mathbf{P}_{1,n} + \mathbf{P}_{2,n} + \mathbf{P}_{1,n+1} + \mathbf{P}_{2,n+1}) \end{aligned} \qquad [3.31]$$

The force exerted through the segment $\mathbf{P}_1\mathbf{P}_2$ on the struck ship, $\mathbf{F}_{1,n}$, and the moment to the origin of the local coordinate system, $M_{1,n}$, are:

$$
\begin{aligned}
F_{1,n} &= \left|\mathbf{F}_{1,n}\right| = \frac{\Delta KE_{1,n}}{s_{1,n}} \\
\mathbf{F}_{1,n} &= \begin{pmatrix} F_{\xi 1,n} \\ F_{\eta 1,n} \end{pmatrix} = \begin{pmatrix} F_{1,n}\cos\zeta_{1,n} \\ F_{1,n}\sin\zeta_{1,n} \end{pmatrix} \\
M_{1,n} &= \overrightarrow{\mathbf{OC}_{1,n}} \times \mathbf{F}_{1,n}
\end{aligned}
\qquad [3.32]
$$

where $s_{1,n} = \left|\mathbf{S}_{1,n}\right|$ and $\zeta_{1,n}$ is the direction of $\mathbf{S}_{1,n}$.

Forces and moments acting on other segments are calculated similarly. The total exerted force, $\mathbf{F}_n$, is, therefore, the sum of the forces on each segment, which can be represented in a more general way as:

$$
\mathbf{F}_n = \sum_{i=1}^{4} \left\{F_{\xi i,n}, F_{\eta i,n}, M_{i,n}\right\} \qquad [3.33]
$$

Note that the forces and the moments here are calculated for the struck ship in the local coordinate system, i.e. the ξ-η system. They are converted to the global system using Equation [3.4]. The force and moment on the striking ship have the same magnitude and the opposite direction.

3.3.2 Vertical Structural Members

The reacting force from vertical structural members also results from the deformation of these members during collision. The plastic membrane tension on plates and stiffeners of side shell and longitudinal bulkheads is used in SIMCOL Versions 0.1, 1.0 and 1.1.

3.3.2.1 SIMCOL Baseline Model (Versions 0.1 and 1.0)

Similar to the study of horizontal members, the first model for vertical members used in this research is also from Crake. Crake uses the Jones method [10] discussed in Section 2.2.1.1.

Based on the assumption that web frames are rigid in both the longitudinal and transverse directions unless struck directly, this approach is applied to side structures and longitudinal bulkheads with some modifications for simulation in the time domain. In Version 0.1, the Jones method is improved by adding Van Mater's extension [10] for off-center striking. The absorbed energy in time step n is then:

$$\Delta KE_n = \frac{2\sigma_y \, t \, B_e}{L_d} \frac{a}{L_d - a} (w_{n+1}^2 - w_n^2) \qquad [3.34]$$

where

- ΔKE_n - kinetic energy absorbed by side shell or longitudinal bulkhead (J);
- σ_y - yielding stress of side shell or bulkhead (Pa);
- t - smeared thickness of side shell or bulkhead (m);
- B_e - effective breadth of side shell or bulkhead (m);
- L_d - damage length, or distance between adjacent webs ($2L$ in Figure 2.4), (m);
- a - distance from impact point to the nearest webs (m); and
- w_n - deflection of side shell or bulkhead at time step n (m).

As with deck structures, the plate thickness t is smeared to include longitudinal stiffeners.

Since the striking bow is considered to have infinite depth, the effective plate breadth B_e is simply taken as the depth of the struck ship.

As indicated in Equation [2.8], the deflection of side shell or bulkhead, w_n, cannot exceed $0.453a$, otherwise the particular side shell or bulkhead is assumed to rupture. Once the side shell or bulkhead is ruptured, it is not considered in subsequent time steps.

Version 1.0 considers strain hardening in plastic membrane tension by using σ_m as calculated in Equation [2.11] in place of σ_y.

It is assumed that the reacting force from the membrane effect is always perpendicular to the struck side shell or bulkhead. Therefore, the magnitude and direction angle of this reacting force in the ξ-η system are

$$F_n = \frac{\Delta KE_n}{w_{n+1} - w_n}$$
$$\zeta_n = \frac{\pi}{2} \qquad [3.35]$$

3.3.2.2 Improved SIMCOL Model (Version 1.1 and later)

As discussed in Section 2.2.1.2, Van Mater's extension [10] is actually a simplified model from the Rosenblatt study. The Rosenblatt method uses different membrane tension mechanisms for right angle collision and oblique angle collision and considers the deformation of flanking web frames. Van Mater's approach is limited to right angle collision. Therefore, it is a natural step to improve SIMCOL by incorporating the methods used in the Rosenblatt study.

Deformation mechanism options considered in the Rosenblatt study are discussed in Section 2.2.2.1 and shown in Figures 2.6 and 2.7 for single hull (or double hull outer shell) and double hull ships. Referring to Figure 2.6, only bolded options are considered in SIMCOL, and the following steps or options are not considered:

- Longitudinal Plastic Bending

  As other studies have indicated, the contribution of plastic bending in the transverse deformation of longitudinally stiffened hull plates is negligible. The sample calculation sheets in the Rosenblatt report support this argument. In the six test cases, the energy absorbed in plastic bending never exceeds 0.55% of the total absorbed energy when the cargo boundary is ruptured. It is a good assumption that the plastic membrane tension phase starts from the beginning of collision penetration.

- Rupture of stiffened hull plates starting in stiffener - Option 1 in Figure 2.6

  As indicated in McDermott's paper, this mechanism is unlikely for most structures, except flat-bar stiffened plates. It is a normal practice to use angles instead of flat bar for longitudinal stiffeners of side shell and longitudinal bulkheads, therefore, this option is not considered in SIMCOL.

- Web frames yield or buckle before plates load in membrane tension - Options 3, 6 and 7 in Figure 2.6

  McDermott demonstrates that Option 3 and subsequent Options 6 and 7 are unlikely and do not contribute significantly to absorbed energy in any case. This is because Option 3 requires very weak web frames that would not be sufficient to satisfy normal sea and operational loads as required by ABS.

SIMCOL Version 1.1 assumes that flanking web frames are rigid, which means only the left side options of Figure 2.7 are considered. Version 2.0 and subsequent versions consider the deformation of flanking webs.

Similar assumptions are made for double hull ships with additional mechanism options considered that are unique to the double hull configuration as shown in Figure 2.7:

1) Fully rigid undistorted web frames (Version 1.1)

In the right angle collision case, the following equation gives the total plastic energy absorbed in membrane tension at the beginning of time step *n*, E_n, with the assumption that the plate is not ruptured (Figure 3.6):

$$E_n = T_m \; e_{tn}$$
$$T_m = \sigma_m \, t \, B_e \qquad [3.36]$$

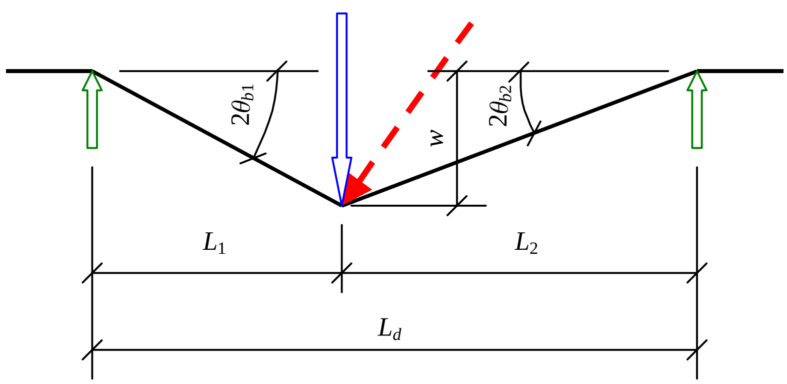

Figure 3.6 Collisions with Rigid Web Frames

where e_{tn} is the total elongation of shell or bulkhead structure within the damaged web spacing, and σ_m, t and B_e are same as those defined in Section 3.3.2.1. There is another term in the original formula from McDermott's paper [11] that represents the elongation in the web spacing beyond the flanking web frames. In SIMCOL, this term is dropped because the flanking web frames are assumed rigid in longitudinal direction and there is no elongation of shell plate if the flanking web frames have not deformed laterally.

The elongation is estimated by the first two terms of a binomial series [11]:

$$
\begin{aligned}
e_i &= \sqrt{L_i^2 + w^2} - L_i \cong \frac{w^2}{2L_i} \\
e_t &= e_1 + e_2 = \frac{L_d}{2L_1 L_2} w^2
\end{aligned}
\qquad [3.37]
$$

where e_1 and e_2 are the elongation of legs L_1 and L_2 respectively. There is another term in McDermott's formulation, which is related to compression in the side shell caused by longitudinal bending of ship hull girder. Since this term is relative small [11] and its calculation requires more structural information and more complicated formulation, it is dropped to give a simpler formula and a more conservative result.

In order to derive the maximum allowable deflection of side shell or bulkhead plate, the criteria of rupture as stated in Section 2.2.2.1 is applied:

$$
\begin{aligned}
\varepsilon_i &= \frac{e_i}{L_i} \le \varepsilon_r \\
\theta_{bi} &= \frac{1}{2} \arctan \frac{w}{L_i} \cong \frac{w}{2L_i} \le \theta_c
\end{aligned}
\qquad [3.38]
$$

where

ϵ_i - strain in leg i; and

θ_{bi} - bending angle at flanking web frames of leg i.

Since the striking bow normally has a generous radius, the bending angle at the impact location is not considered in the rupture criteria. From the equations, it can be seen that only the strain and bending angle in the shorter leg need be considered for right angle collisions. Based on material properties of ABS steel, the resulting critical bending angle θ_c from Equation [2.10] is 19.896, 17.318 or 16.812 degrees for MS, H32 or H36 grades respectively. Once either of the rupture criteria is reached, the side shell or longitudinal bulkhead is considered ruptured and does not continue to contribute to the reacting force, while the absorbed energy is considered to reach the maximum.

For collisions at an oblique angle, the membrane tension is only fully developed in the leg behind the strike, L_2 in the case of Figure 3.6. This is demonstrated in the force diagram shown in Figure 3.7 [11], where T_1 is much smaller than T_2. It is also assumed that all the strain developed from membrane tension is behind the striking point. Therefore, the first rupture criterion in Equation [3.38] becomes:

$$\varepsilon_b = \frac{e_t}{L_b} \leq \varepsilon_r \qquad [3.39]$$

where ϵ_b and L_b represent the strain and length of the leg behind striking, and in the case of Figure 3.6, they are ϵ_2 and L_2. Equations [3.36] and [3.37] are also still applicable.

Given the total energy absorbed through membrane tension at the beginning and end of the time step, the energy absorbed within the time step is:

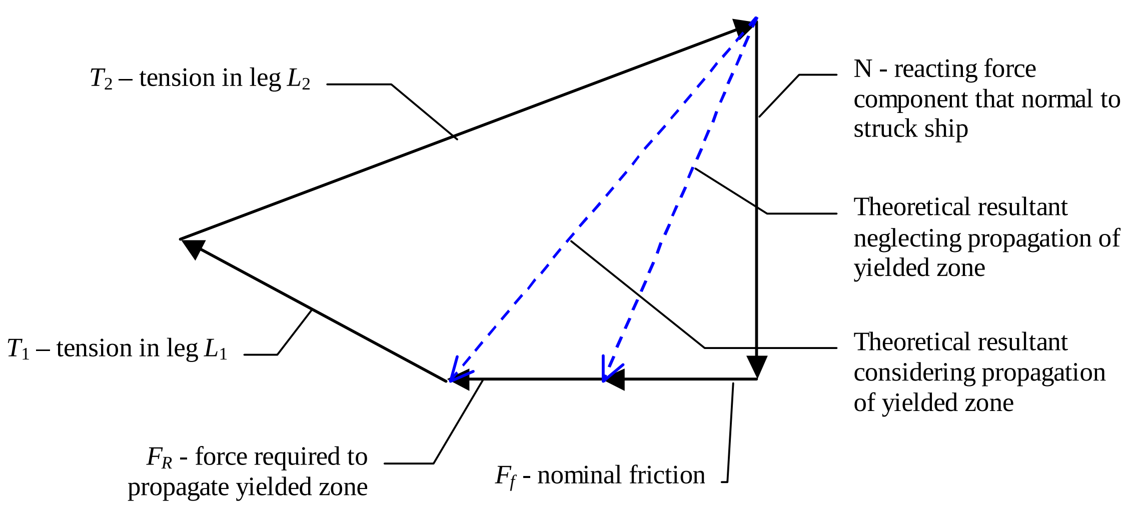

Figure 3.7 Force Diagram of Oblique Angle Collision for Structure in Figure 4.6

$$\Delta KE_n = E_{n+1} - E_n \qquad [3.40]$$

To distinguish right angle and oblique angle collisions, a one-degree threshold is selected. If the direction angle of relative movement, ζ, calculated by Equation [3.22] is between 89 and 91 degrees, collision is considered at right angle, otherwise, it is treated as oblique angle collision.

If the longitudinal component of the reacting force from membrane tension is ignored, particularly for collisions at oblique angle, Equation [3.35] is still valid.

2) Web frames with transverse deformation – bending, shear, compression (Version 2.0 and later)

In this deformation analysis option, the web frames are allowed transverse deformation while keeping their longitudinal locations. The transverse bulkheads are still considered to be fully rigid.

The resisting force is assumed constant at a distorted flanking web frame, and the lateral deformation of the web frame is uniform from top to bottom. The magnitude of this force is its maximum elastic capacity.

From Figure 3.6, the applied force on a rigid flanking web frame is [11]:

$$P_i = T_i \frac{w}{L_i} \qquad [3.41]$$

where P_i and T_i are referred to the particular leg L_i. If the applied force, P_i, is greater than the maximum elastic capacity of the flanking web, P_{wf}, the particular web frame is deformed as in Figure 3.8. The change of angle, γ_c, at the distorted web is [11]:

$$\gamma_{ci} \cong \frac{P_{wf}}{T_i} \qquad [3.42]$$

The Rosenblatt study [12] proposed an approach to determine whether P_i exceeds the capacity, P_{wf}, and to estimate the value of P_{wf}. First, the allowable bending moment and

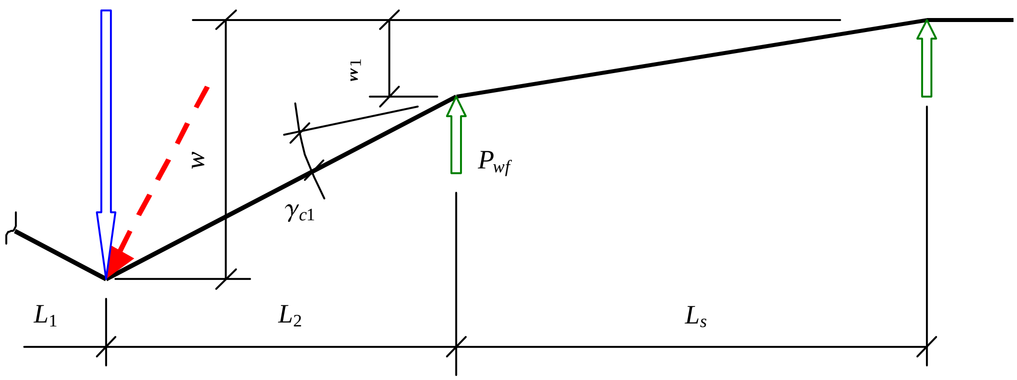

Figure 3.8 Collisions with Distortable Web Frames

shear force of the web frame at each support, the crushing load of the web, and the buckling force of supporting struts are calculated. Then, the load, P_i, is applied to the web frame, and the induced moments, shear forces and compression of the web frame and struts are calculated, considering the web frame as a beam with clamped ends. The ratios of the induced loads to the allowable loads are determined accordingly. If the maximum ratio, R_m, is greater than unity, the load, P, exceeds the capacity, and the web frame deforms. R_m is also used to estimate the number of distorted web frames. The capacity of the web is:

$$P_{wf} = \frac{P}{R_m} \qquad [3.43]$$

Using Equation [3.42], the deflection at the outermost distorted web frame is [12]:

$$w_n = \frac{L_s}{L_i + nL_s}\{w - \gamma_{c2}[nL_i + \frac{1}{2}(n-1)nL_s]\} \qquad [3.44]$$

where

n - total number of deformed web frames at L_i side; and

L_s - web frame spacing (m).

A positive w_n also verifies the estimate of n from R_m. The deflection at other deformed web frames is:

$$w_j = (n - j + 1)w_n + \frac{1}{2}(n - j)(n - j + 1)\gamma_{c2} L_s \qquad [3.45]$$

where j is the number of web frames counted from the striking point. The elongation in the web frame spacing is:

$$e_j = \sqrt{(w_j - w_{j+1})^2 + L_s^2} - L_s \qquad [3.46]$$

and the elongation in the striking span is:

$$e_{0i} = \sqrt{(w - w_1)^2 + L_i^2} - L_i \qquad [3.47]$$

The approximation in Equation [3.37] is not used here, because it is only appropriate for a small (w_j- w_{j+1}) to L_s ratio, which may not be valid in this case.

With these elongation and deformation results, the rupture criteria given in Equations [3.38] and [3.39] are applied to check the integrity of side and bulkhead structures. Also, the total elongation at the L_i side becomes:

$$e_{ti} = e_{0i} + \sum_{j=1}^{n} e_{ji} \qquad [3.48]$$

and energy absorbed in membrane tension and web deformation is:

$$E_i = T_i e_{ti} + P_{wf} \sum_{j=1}^{n} w_{ji} \qquad [3.49]$$

For right angle collisions, T_i always equals T_m as calculated in Equation [3.36]. In oblique angle collisions, T_i equals T_m if L_i is the side behind striking, otherwise, as suggested by Rosenblatt [12], ½ T_m is used to simplify the calculation.

For double hull ships, if the web frames are distorted because of bending, shearing and buckling of supporting struts, the deformed web frames push the inner skin into membrane tension, and the right angle collision mechanism is applied to the inner hull as shown in Figure 2.7. Its integrity is checked by Equation [3.38], and the energy absorbed in membrane tension is calculated using Equation [3.49].

The above analysis is based on an arbitrary deflection *w* of the side shell or longitudinal bulkhead at the impact point. In the simulation, the deflection at each time step is obtained, and the energy absorbed during the time step is:

$$\Delta KE_n = (E_{1,n+1} + E_{2,n+1}) - (E_{1n} + E_{2,n}) \qquad [3.50]$$

Considering the friction force, F_f, in Figure 3.7, and assuming the friction factor is a constant value of 0.15, the reacting force is:

$$\begin{aligned}
\Delta KE_n &= N_n (w_{n+1} - w_n) + F_{fn}\left| l_{n+1} - l_n \right| = N\left[(w_{n+1} - w_n) + 0.15\left| l_{n+1} - l_n \right|\right] \\
F_{\eta n} &= N_n = \frac{(E_{1,n+1} + E_{2,n+1}) - (E_{1n} + E_{2,n})}{(w_{n+1} - w_n) + 0.15\left| l_{n+1} - l_n \right|} \\
F_{\xi n} &= F_f \frac{(l_{n+1} - l_n)}{\left| l_{n+1} - l_n \right|} = 0.15 F_{\eta n} \frac{(l_{n+1} - l_n)}{\left| l_{n+1} - l_n \right|} \\
M_n &= -F_{\xi n} d_n + F_{\eta n} l_n
\end{aligned} \qquad [3.51]$$

In addition to the friction force, another longitudinal force, F_R, the force to propagate the yielding zone, is considered, as shown in Figure 3.7. McDermott provides an expression for this force [11]:

$$F_R = \frac{\sigma_y d'}{R}\left[d' t_w \left(1 - \frac{\sigma_y R}{d' E} \right)^2 + t_f (b - t_w) \left(\frac{d' - 0.5 t_f}{d'} - \frac{\sigma_y R}{d' E} \right) \right]$$

where

d'	-	depth of stiffener;
R	-	radius of striking bow;
t_w	-	thickness of web of stiffeners;
t_f	-	thickness of flange of stiffeners;
b	-	width of flange of stiffeners; and
E	-	modulus of elasticity.

The full implementation of this equation requires structural details that are not appropriate for a simplified analysis. In this study, a simplified formula is introduced:

$$c_F = \frac{F_R}{\sigma_y A_{stiff}}$$
$$c_A = \frac{A_{stiff}}{A_{total}} \qquad [3.52]$$
$$F_R = c_F c_A \sigma_y tB$$

where

c_F - force coefficient;
c_A - ratio of sectional areas;
A_{stiff} - sectional area of stiffeners themselves; and
A_{total} - total sectional area of stiffeners and their attached plate.

Both c_F and c_A should be derived from the typical design of ships. Based on the structural details of the baseline tanker design given in Chapter 4, $c_F \cdot c_A$ is assumed to have a constant value of 0.025 in this study.

Since F_R also contributes to membrane tension energy, Equation [3.51] becomes:

$$\Delta KE_n = F_{\eta n}\left[(w_{n+1} - w_n) + 0.15\left| l_{n+1} - l_n \right|\right] + F_R(l_{n+1} - l_n)$$
$$F_{\eta n} = \frac{(E_{1,n+1} + E_{2,n+1}) - (E_{1n} + E_{2,n}) - F_R(l_{n+1} - l_n)}{(w_{n+1} - w_n) + 0.15\left| l_{n+1} - l_n \right|} \qquad [3.53]$$
$$F_{\xi n} = (F_R + 0.15F_{\eta n})\frac{(l_{n+1} - l_n)}{\left| l_{n+1} - l_n \right|}$$
$$M_n = -F_{\xi n} d_n + F_{\eta n} l_n$$

3.3.2.3 Minorsky Mechanism in Side and Bulkhead Structures (Version 2.0 and later)

In the above analysis, the resistance from side structure and longitudinal bulkheads is ignored after rupture. However, there is still resistance due to the longitudinal crushing of the side structure and longitudinal bulkheads. Therefore, in Version 2.0, the Minorsky mechanism is applied to the longitudinal crushing of side structure and longitudinal bulkheads in a similar fashion as with the transverse crushing of decks, bottoms and stringers. This provides additional resistance to longitudinal extent of damage.

At a particular time step, the damaged volume of side structure or longitudinal bulkheads is:

$$R_{Tj} = t_j B_e \left| u_{\xi j} \right| \tau \qquad [3.54]$$

where

j - number of the structure counted from side shell; and

u_ξ - velocity of striking ship at the considering structure in ξ direction (m/s).

and the reacting force becomes

$$F_j = \frac{4.7 \times 10^6 R_j}{u_{\xi j} \tau} \qquad [3.55]$$

$$M_j = -F_j \eta_j$$

where η is the location of side or bulkhead structure in the ξ-η system.

3.3.2.4 Striking Bow with Limited Depth (Version 2.1)

Prior to SIMCOL Version 2.1, the striking bow is assumed to have infinite depth. This is not a good assumption even though it simplifies the problem dramatically. Therefore, a vertical striking bow with limited depth is introduced in Version 2.1.

It is assumed that the deflection of the side shell or longitudinal bulkhead is linear from the top and/or bottom of the striking bow to the next horizontal support that has not been struck. This is shown in Figure 3.9. It is also assumed that the lateral deformation of web frames is similar to the incursion of the striking bow as shown in Figure 3.9. The membrane tension energy is assumed to be proportional to deflection, and is also distributed linearly [11, 12]. Therefore, the effective breadth of the plates (actually depth) in Equation [3.36] becomes:

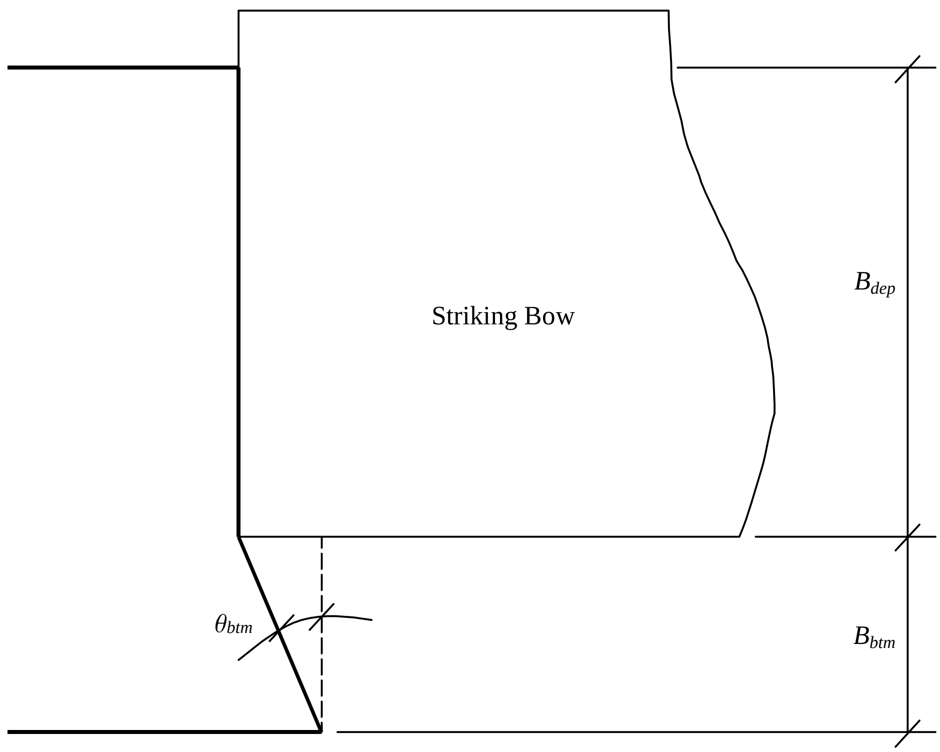

Figure 3.9 Striking Bow with Limited Depth

$$B_e = B_{dep} + \frac{1}{2} B_{btm} \qquad [3.56]$$

However, once the bending angle at the top or bottom of the striking bow, θ_{btm} in the case of Figure 3.9, is greater than the critical value from Equation [2.10], the relevant portion of the side shell or longitudinal bulkhead is considered ruptured, and the effective breadth for membrane tension is restricted to B_{dep} thereafter.

3.4 MODEL VERSION SUMMARY

The following sections summarize the evolution and highlight the differences in SIMCOL Version 0.1 through Version 2.1. Basic assumptions, necessary design and scenario descriptions are discussed. The complete FORTRAN code of SIMCOL Version 2.1 and input data structure is given in Appendix A.

3.4.1 Mechanisms and Basic Assumptions

A comparison of the mechanics adopted in the different SIMCOL versions is summarized in Table 3.1.

3.4.1.1 Version 0.1

With applying the mechanics listed in Table 3.1, Version 0.1 consists of the following basic assumptions:

Table 3.1 Version Summary of Mechanisms

<table>
<tr><td colspan="2">Version</td><td>0.1</td><td>1.0</td><td>1.1</td><td>2.0</td><td>2.1</td></tr>
<tr><td colspan="2">Simulation</td><td colspan="5">Simulation in time domain</td></tr>
<tr><td colspan="2">External Model</td><td colspan="5">Three degrees of freedom
(Hutchison and Crake)</td></tr>
<tr><td rowspan="5">Internal Model</td><td rowspan="2">Horizontal Members</td><td colspan="5">Minorsky mechanism as re-validated by Reardon and Sprung</td></tr>
<tr><td>Crake’s model</td><td colspan="4">Sweeping segment method to calculate damaged area and resulting forces and moments</td></tr>
<tr><td rowspan="2">Vertical Members w/o rupture of plate</td><td colspan="2">Jones and Van Mater</td><td colspan="3">McDermott / Rosenblatt Study methods</td></tr>
<tr><td>Crake’s model (Jones)</td><td>Van Mater’s extension of Jones</td><td>Does not consider deforma-tion of webs, friction force and the force to propagate yielding zone</td><td>Considers deforma-tion of webs, friction force and the force to propagate yielding zone</td><td>Striking bow with limited depth</td></tr>
<tr><td>Vertical Members w/ ruptured plate</td><td colspan="3">Neglected</td><td colspan="2">Minorsky method for calculating absorbed energy due to longitudinal motion</td></tr>
</table>

1. There is no significant effect of hydrodynamic damping on the ship dynamics due to the short duration of impact.

2. The center of gravity of the ship is assumed to be at midship and the ship's mass is distributed symmetrically about the center of gravity.

3. The collision is perfectly inelastic.

4. The striking ship bow is a rigid wedge with infinite depth.

5. In general, the various structural members react to the collision independently.

6. The force calculated from the Minorsky energy acts on the striking bow tip in the direction of motion.

7. There is no transverse deformation or longitudinal movement of web frames or transverse bulkheads unless hit directly. Therefore, the deformation of the inner skin is totally independent of the outer skin.

8. Both elastic and plastic bending phases of deformation of the stiffened side shell or bulkhead plates are negligible. Tension in the stiffened plate is constant during the plastic membrane phase.

9. The derivation of membrane force is based on a right angle collision at mid-span between the web frames. There is no difference in mechanics between right angle and oblique angle collisions.

10. There is no friction force in the longitudinal direction of the struck ship. Therefore, the reacting force from membrane tension is always perpendicular to the side of the struck ship.

11. There is no stiffness contribution from side shell and longitudinal bulkheads after rupture.

3.4.1.2 Version 1.0

SIMCOL Version 1.0 incorporates the following changes to the Version 0.1 assumptions:

1. The width of the striking wedge is limited to the beam of the striking ship.

2. With the introduction of the sweeping segment method, the force acting point and direction become the sweeping area center and average sweeping movement direction of each segment.

3. Cases of striking off-center between the webs are considered in calculating the energy absorbed in membrane tension although the results are still derived assuming right angle impact.

3.4.1.3 Version 1.1

The application of the Rosenblatt approach in Version 1.1 includes consideration of oblique angle collisions while the longitudinal force required to propagating the yielding zone is still ignored.

3.4.1.4 Version 2.0

The following changes are made to the assumptions of earlier versions:

1. The transverse deformation of web frames is considered, while web longitudinal movement is still prohibited. The transverse bulkheads are still considered rigid unless being hit directly.

2. After deformation, the support provided by web frames is a constant value equal to their elastic capacity (perfectly elastic/plastic). The lateral movement of web frames is uniform from top to bottom.

3. Both the friction force and the force to propagate the yielding zone are considered. A linear relationship is applied to the force to propagate yielding zone using total sectional area of side or bulkhead structure.

4. The Minorsky method is used to calculate the longitudinal resistance of ruptured side shell and bulkhead plating.

3.4.1.5 Version 2.1

In Version 2.1, the depth of striking bow is limited by the draft and bow height of the striking ship. To implement this limited depth bow, the following assumptions are added:

1. The deck or bottom that is not struck directly by the striking bow is considered intact and undistorted.

2. The deflection is linear from the top or bottom of the striking bow to the next intact horizontal support.

3. The lateral deformation of web frames assumes the similar shape as deflection at the impact location.

4. The membrane tension energy is proportional to deflection, and therefore, distributed linearly.

3.4.2 Ship Design Parameters in the Model

As the model becomes more complicated, it requires more design parameters to describe the struck and striking ships.

SIMCOL Versions 0.1 and 1.0 have almost identical requirements for design parameters including ship dimensions and structural data.

The following ship dimensions are required in SIMCOL Versions 0.1 and 1.0:

- Principal dimensions of both striking and struck ships, including length, breadth, depth, draft and displacement;

- half-entrance angle of the striking bow;

- longitudinal locations of transverse bulkheads in the struck ship; and
- transverse locations of longitudinal bulkheads in the struck ship.

The following structural parameters are also required:

- total smeared thickness of deck, bottom and inner bottom plates with stiffeners;
- smeared thickness of side and longitudinal bulkheads with stiffeners;
- yielding stress of side shell and longitudinal bulkheads and, in Version 1.0, the ultimate stress; and
- web frame spacing.

Version 1.1 requires the same data for ship dimensions and other structural data as the earlier versions, but requires the material grade of side shell and longitudinal bulkheads instead of stresses. Based on the standard material grade, the yielding and ultimate stresses and the critical bending angle are calculated in the program code.

In Version 2.0, the following additional structural parameters are required, most of which involve web frames:

- ship type: single hull or double hull;
- total smeared thickness of stringers on side and/or longitudinal bulkhead structure;
- width of stringers;
- number of struts supporting web frames;
- unsupported span of web frames;
- web depth;
- web thickness at supports;

- web material grade;
- section modulus of web frames at supports;
- spacing of stiffeners on the web;
- smeared thickness of stiffeners on the web;
- gyration radius of each stiffener with attached web plate;
- critical length of each strut;
- axial area of each strut;
- gyration radius of each strut; and
- material grade of each strut.

With the introduction of striking bow of limited depth in Version 2.1, the following ship dimension and structural parameters have become a part of the input data:

- bow height;
- double bottom height for double hull tankers;
- smeared thickness of individual decks and bottoms;
- smeared thickness of individual stringers;
- location of individual stringers measured from baseline; and
- effective heights of every support of web frames, including brackets of deck transverses, bottom floors and struts.

The sum of plate thickness for decks, bottom and stringers is no longer required.

3.4.3 Collision Scenario of the Model

Given the use of a three-degree of freedom system for all models, there are few restrictions on the collision scenario. All versions consider collisions with different striking locations and angles, with or without struck ship velocity. The collision scenario parameters include:

- initial velocity of the struck ship;
- initial velocity of the striking ship;
- impact location; and
- collision angle.

The only restriction in the model is on the collision angle, ϕ. Due to the algorithm, the acute angle between the struck and striking ship cannot be less than the half-entrance angle, α, of the striking bow. The practical range of the collision angle should be within the following range:

$$\alpha + 5° \leq \phi \leq 175° - \alpha \quad [3.57]$$

This range is generous enough since, if the collision angle is beyond this range, a glancing blow is most likely.

CHAPTER 4 TEST RESULTS AND COMPARISON

The consistency and accuracy of the collision model is verified in a series of test runs. The availability of actual collision validation data is very limited, and there is no data available for penetrating collisions with a double hull struck ship. In the absence of sufficient validating data, SIMCOL's performance is evaluated by comparison to the results of three other state-of-the-art collision models, and to actual damage in one actual collision case. Representative struck and striking ship designs are developed for this comparison.

4.1 STRUCK AND STRIKING SHIPS

4.1.1 Struck Ships

Since the intended application of SIMCOL is for probabilistic and parametric analysis of tanker oil outflow in collision, the basic tanker configurations provided in the Interim Guidelines [6] are excellent candidates for test ships. The Interim Guidelines provide four double hull tankers of different sizes and arrangements as reference designs. Among these reference tankers, the 150,000 dwt design is chosen as the baseline struck ship in this study. The struck ship in the model validation case from Kuroiwa's study [14] is a 100,000 dwt single hull tanker. The general arrangements of these tankers are shown in Figures 4.1(a) and (b). Their general dimensions are given in Table 4.1(a) and (b) respectively.

Based on this basic ship data, detail ship arrangements and midship structural details are developed for the selected tanker designs. HECSALV and SafeHull are used to develop these details consistent with IMO regulations and ABS Rules. The major structural data are presented in Table 4.2. The complete design data of these reference tankers are given in Appendix B.

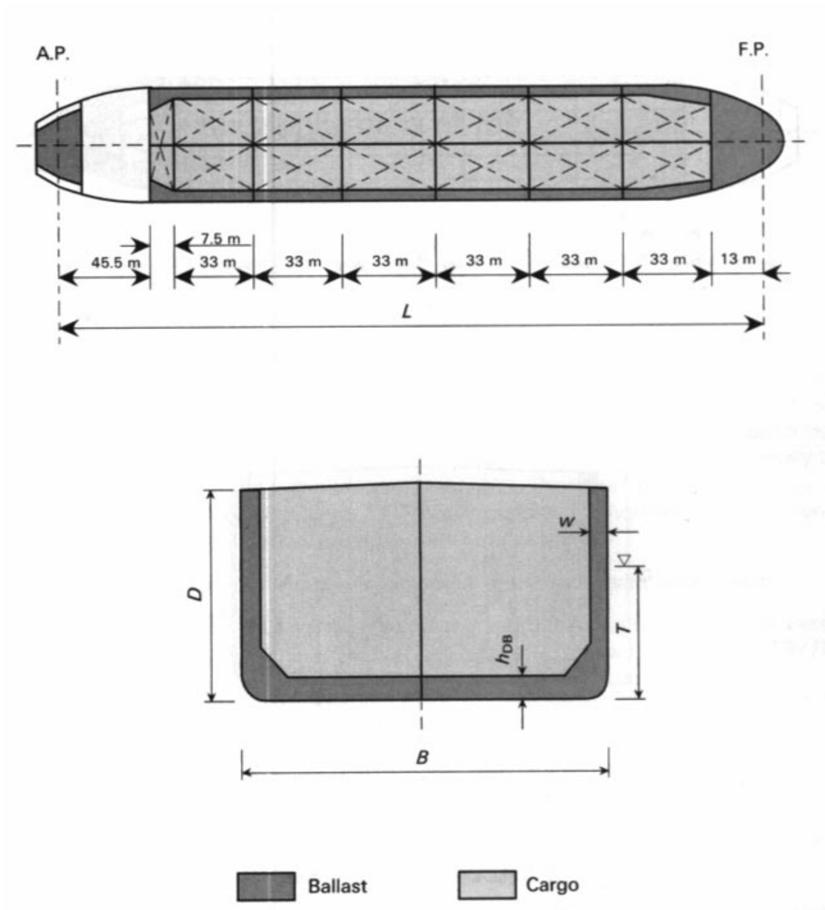

Figure 4.1(a) 150,000 dwt Reference Design

4.1.2 Striking Ships

The striking ship used in this study is a 150,000 dwt bulk carrier chosen from Pedersen's study of bow collisions [13]. Because of the similar size to the baseline struck ship, this bulk carrier is chosen over the other available bow designs. The striking ship in the validation case is a 23,000 dwt container ship [14]. The general dimensions of these striking ships are given in Table 4.3.

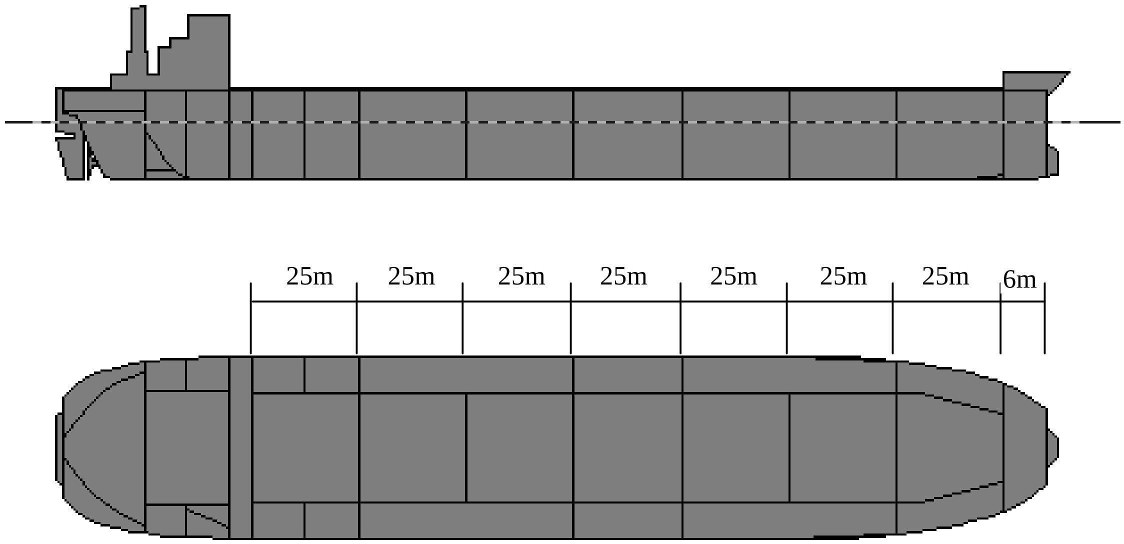

Figure 4.1(b) 100,000 dwt Single Hull Tanker

Table 4.1(a) General Dimensions of 150,000 dwt Reference Tankers

Deadweight, tonnes	150,000
Length *L*, m	264.00
Breadth *B*, m	48.00
Depth *D*, m	24.00
Draft *T*, m	16.80
Double Bottom Ht h_{DB}, m	2.32
Double Hull Width *W*, m	2.00
Displacement, tonnes	178,867

Table 4.1(b) General Dimensions of 100,000 dwt Tankers

Deadweight, tonnes		100,000
Length L, m		222.00
Breadth B, m		42.00
Depth D, m		20.30
Draft T, m	Full Load	13.35
	@ collision	6.97
Displacement, tonnes	Full Load	110,015
	@ collision	56,073

Table 4.2 Major Structural Data of the Struck Tankers

Ship		150,000 dwt double hull tanker	100,000 dwt single hull tanker
Web Frame Spacing L_s, m		3.30	5.00
Smeared Thickness t_h, mm	Deck	47.32	36.27
	Inner Bottom	26.92	--
	Bottom	28.29	44.20
	Stringers	3×15.34	--
Smeared Thickness t_v, mm	Side Shell	21.92	26.78
	Inner Skin	22.94	--
	Bulkhead	22.28	27.82
Web Thickness t_w, mm	Upper	12.00	15.00
	Lower	18.00	15.00

Table 4.3 General Dimensions of the Striking Ships

Ship Type	150,000 dwt bulk carrier	23,000 dwt container ship
Length *L*, m	274.00	220.90
Breadth *B*, m	47.00	26.01
Depth *D*, m	21.60	
Bow Height *H*, m	26.00	20.00
Draft *T*, m	15.96	9.68
Displacement, tonnes	174,850	37,076
Half Entrance Angle, α	49°	50°

4.2 RESULTS OF TEST AND VALIDATION CASES

In order to test the consistency and sensitivity of SIMCOL, a series of test cases were run. Three test matrices are completed using the 150,000 dwt double hull tanker as struck ship and 150,000 dwt bulk carrier as striking ship. The model validation case from Kuroiwa was also run. The relative locations between the struck and striking ships are given in Figure 4.2(a) and (b). Details are provided in the following sections.

4.2.1 Test Matrix 1

4.2.1.1 Collision Scenario

In the first testing matrix, the collision scenarios are defined as follows:

- Initial velocity of the struck ship: zero.
- Initial velocity of the striking ship: 3, 4, 5, 6 and 7 knots.

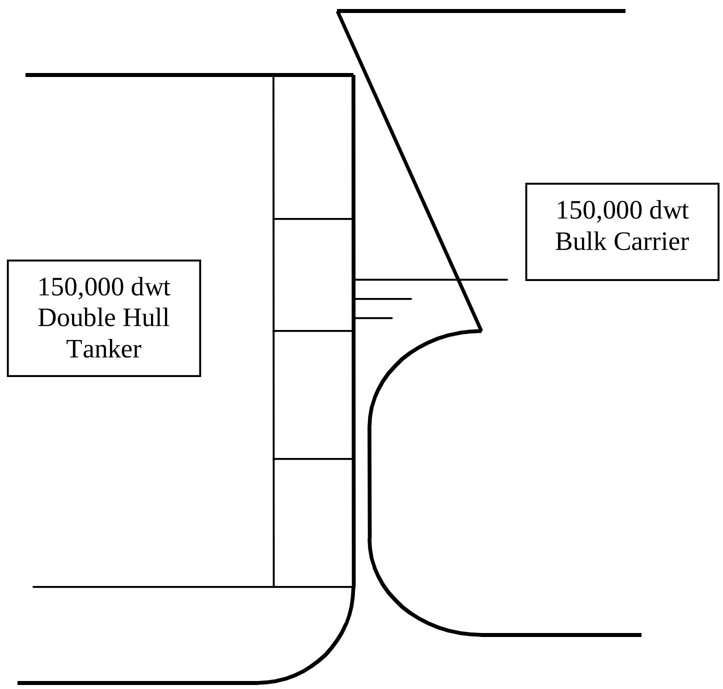

Figure 4.2(a) Collision Location of Test Matrices

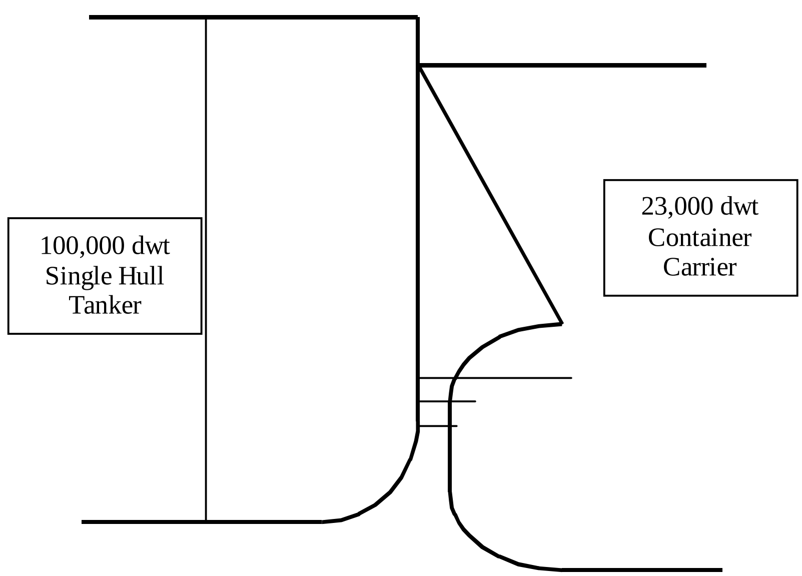

Figure 4.2(b) Collision Location of Validation Case

- Impact location: mid-point of each cargo oil tank, i.e. 62.5 and 29.5 meters aft and 3.5, 36.5, 69.5 and 102.5 meters forward of midship.

- Collision angle: 90 degrees.

This matrix tests the sensitivity of the striking ship speed and the impact location along the striking ship length.

4.2.1.2 Simulation Results and Comparisons

All versions of SIMCOL were tested with Matrix 1. The deepest penetration for SIMOCL Versions 0.1 to 2.1 as a function of striking location and speed are shown in Figures 4.3(a) to (e). Figures 4.3(d) and (e) also show penetration at the time of rupture of the inner and outer hulls. The damage length as a function of striking location and speed as calculated by SIMCOL Version 2.1 is given in Figure 4.3(f).

For every speed, comparisons of penetration versus impact location curves between SIMCOL versions are given in Figures 4.4(a) to (e). These figures have the following important characteristics:

- From the results, it can be seen that penetration depth and damage length always increases as striking velocity increases. The slope of these curves represents the resistance of the struck ship structure towards the striking bow. At high striking speeds, the curves are approximately straight parallel lines. This phenomenon is the result of the linear Minorsky correlation between absorbed energy and damaged volume.

- The penetration depths of Versions 2.0 and 2.1 are generally less than earlier versions, especially at high striking velocity. The earlier versions do not consider some important structural members or their effects. In Versions 0.1, 1.0 and 1.1, web frames are assumed to be rigid in the transverse direction. Therefore, the deformation of side or bulkhead structure is restricted to one or two frame bays. The crushing energy of web frames is not considered in these models, and absorbed energy is always underestimated since the web frames are struck directly in all Matrix 1 cases.

In addition to the web crushing energy, Versions 2.0 and 2.1 include the lateral deformation of web frames, which allows more transverse deformation of side or bulkhead structure, and postpones plate rupture. Versions 2.0 and 2.1 include damaged stringers in the damage volume for Minorsky correlation.

- Versions 0.1 through 1.1 have the same penetration versus location curve shape with a maximum at the midship location. Versions 2.0 and 2.1, and to a lesser extent Version 1.1 at 3 and 4 knots, have a different shape that looks like a "flying seagull". These curves have less penetration at the midship location. As the striking location moves away from midship, the penetration first increases, then decreases. The damage length versus location curves in Figure 4.3(f) shows similar "seagull" pattern.

  After examination of the detailed outputs for these cases, the "seagull" pattern is explained by two factors. One is the external ship dynamics with three degrees of freedom used in all SIMCOL versions. The other is the adoption of different membrane tension mechanisms for right angle and oblique angle collisions in Versions 1.1, 2.0 and 2.1. Currently, a one-degree threshold, i.e. 89 to 91 degrees, is used to identify right angle collision. Whenever the collision angle exceeds the threshold, the collision is considered in oblique angle. The three degrees of freedom system allows the struck and striking ships to rotate independently during the collision and the initial right collision angle becomes an oblique angle. The membrane mechanism for an oblique angle collision absorbs less membrane tension energy and causes the plate to rupture earlier than the right angle collision. As the impact point moves away from midship, the rotating angle of the struck ship becomes larger, and the oblique angle threshold is exceeded earlier, resulting in more penetration. This is why Version 1.1 also generates the "seagull" pattern at the low energy end where the penetration is governed by the membrane tension mechanism. In order to further demonstrate this phenomenon, the penetration depths, at the time of rupture of side shell or inner skin, are also shown in Figure 4.2(d) and (e). When the strike occurs even further away from midship, less kinetic energy is absorbed in the collision process because of the rotation of the struck ship, and therefore, less structural damage is caused. This effect exists for all models.

Penetration vs Striking Speed

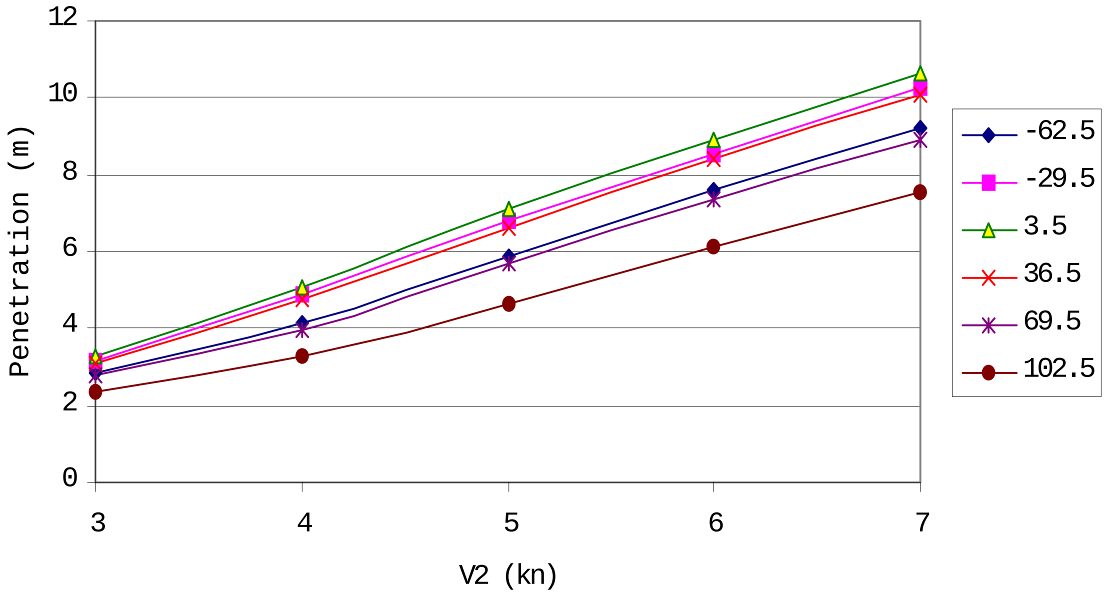

Penetration vs Location

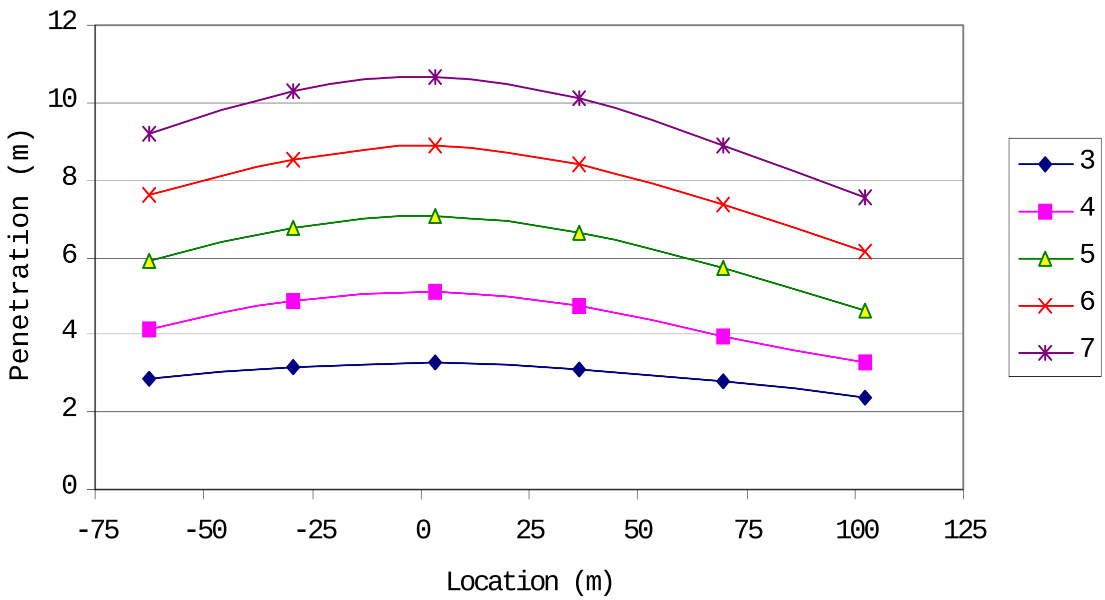

Figure 4.3(a) Penetration Results of Matrix 1 (Version 0.1)

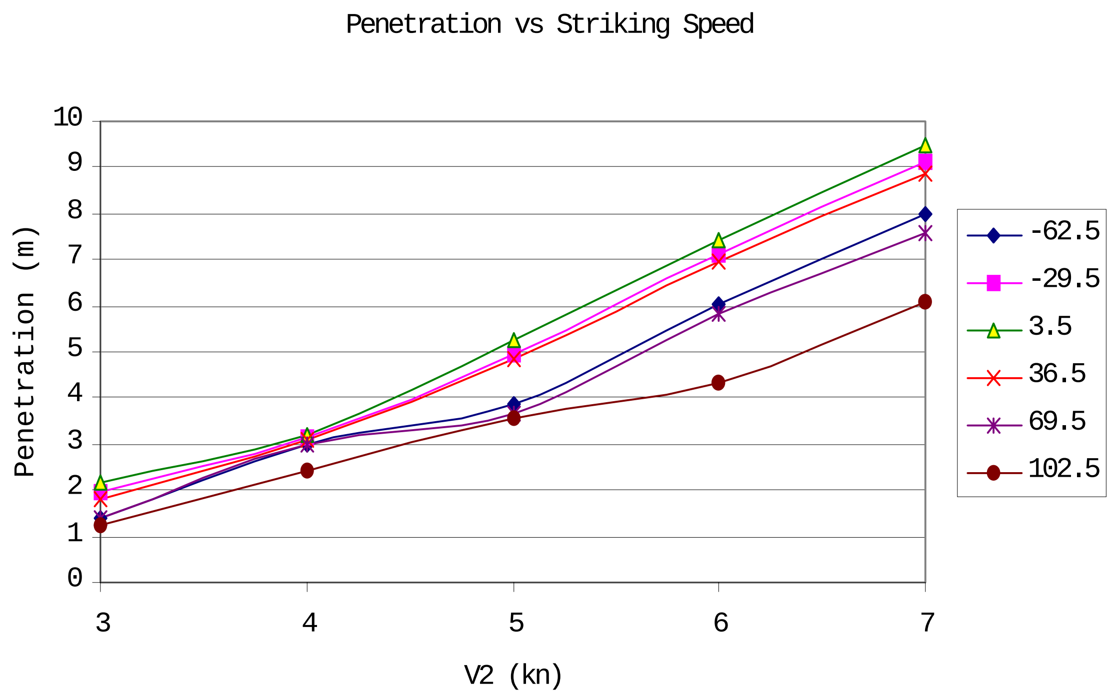

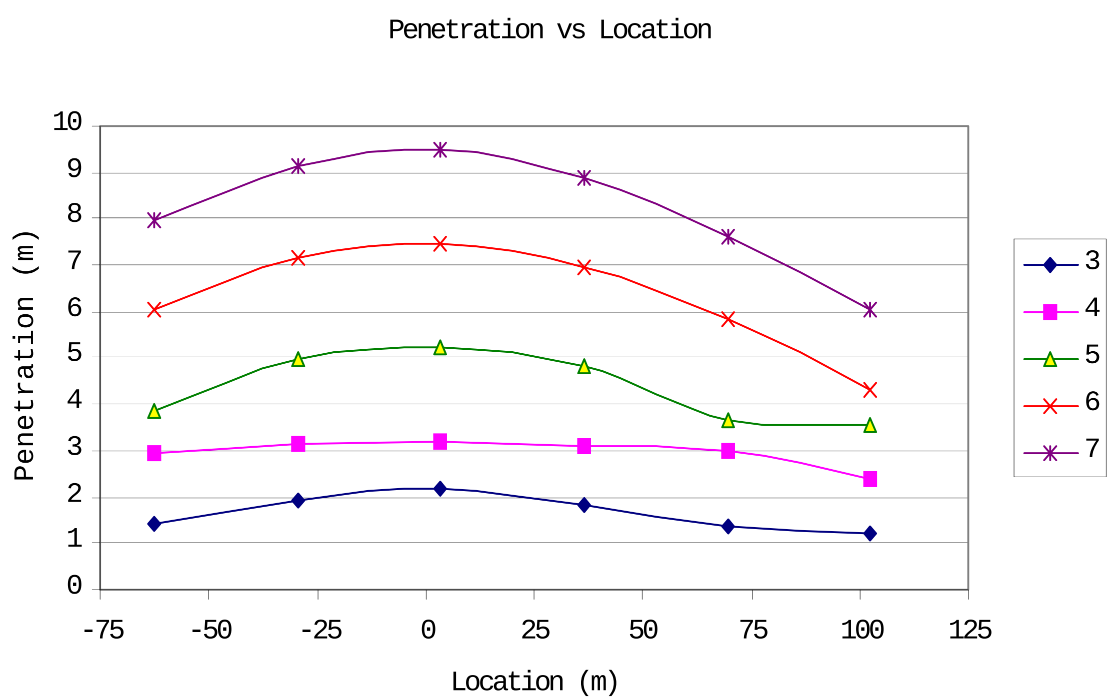

Figure 4.3(b) Penetration Results of Matrix 1 (Version 1.0)

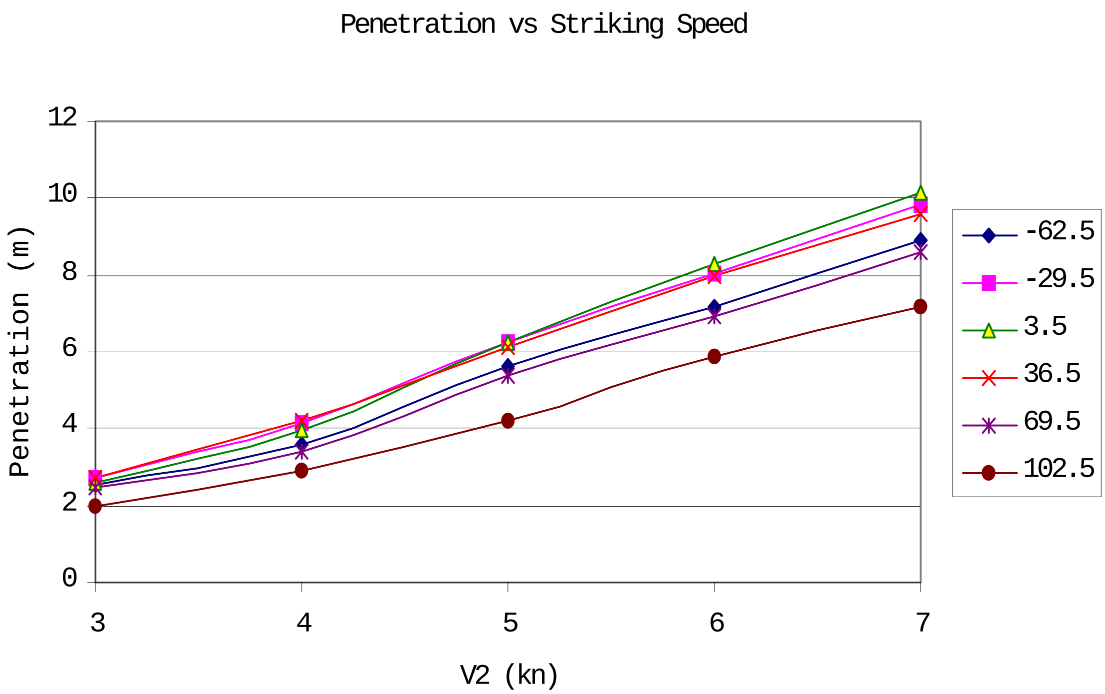

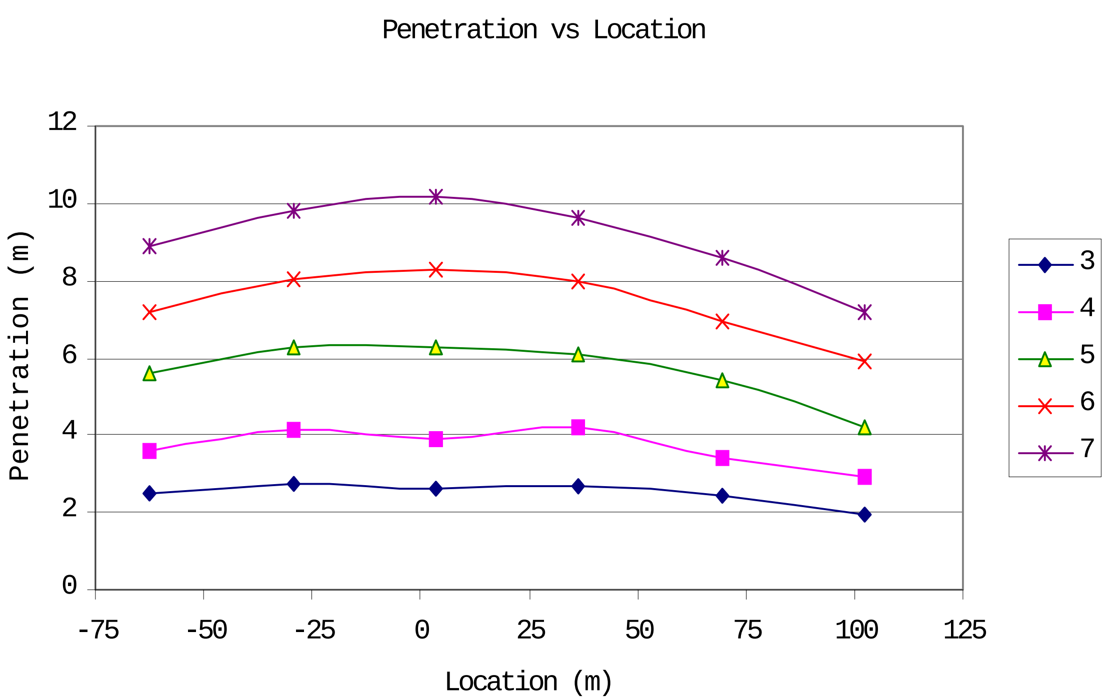

Figure 4.3(c) Penetration Results of Matrix 1 (Version 1.1)

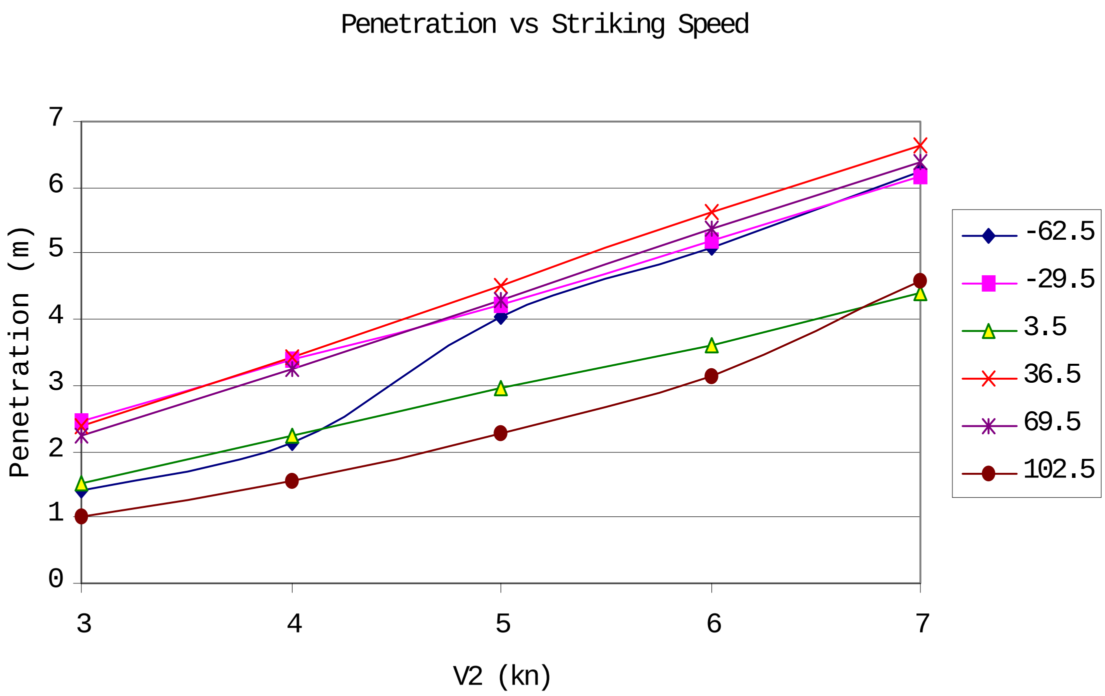

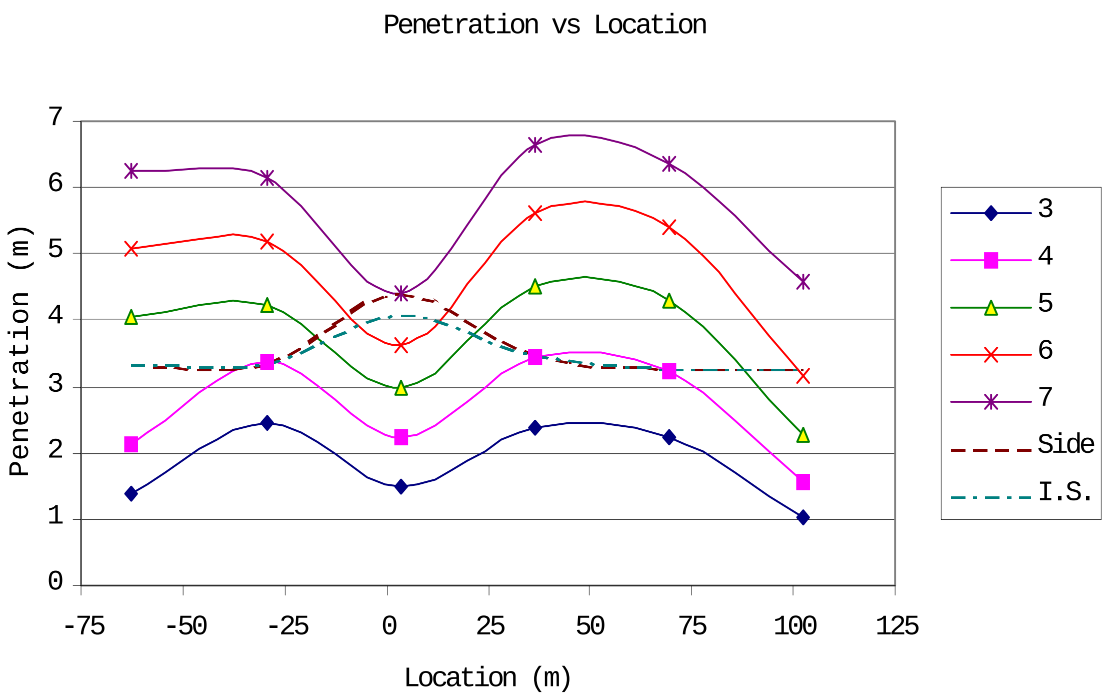

Figure 4.3(d) Penetration Results of Matrix 1 (Version 2.0)

Penetration vs Striking Speed

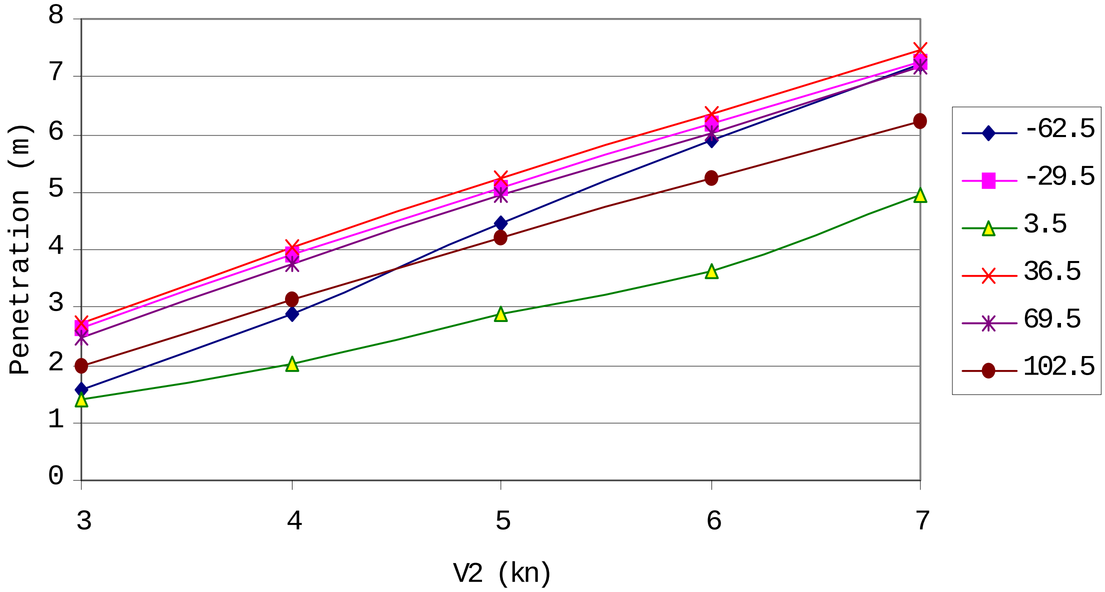

Penetration vs Location

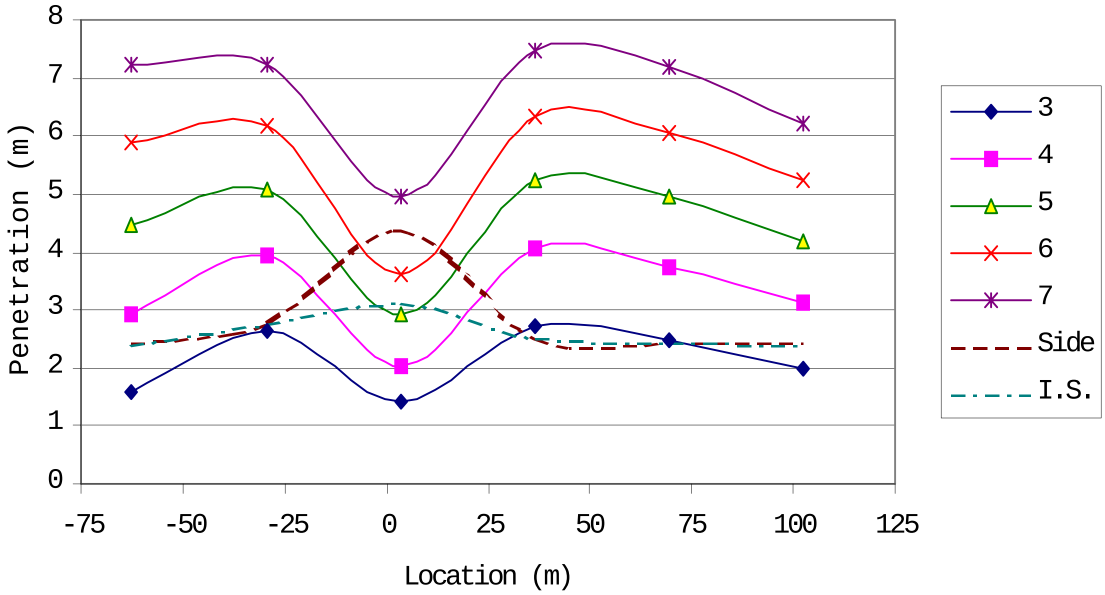

Figure 4.3(e) Penetration Results of Matrix 1 (Version 2.1)

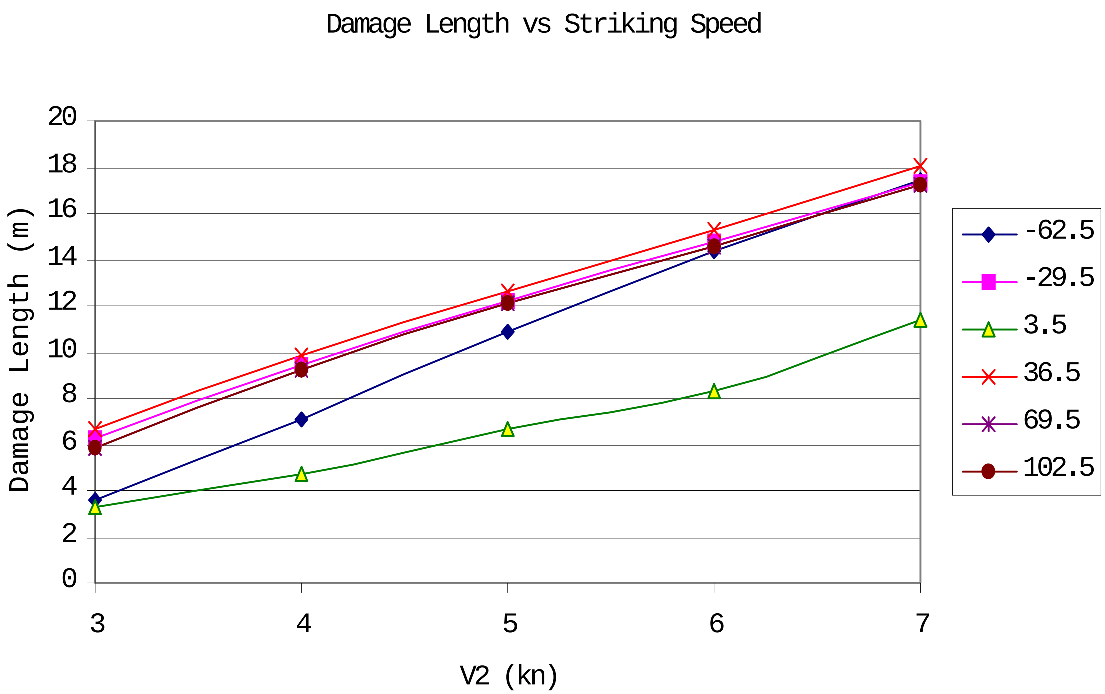

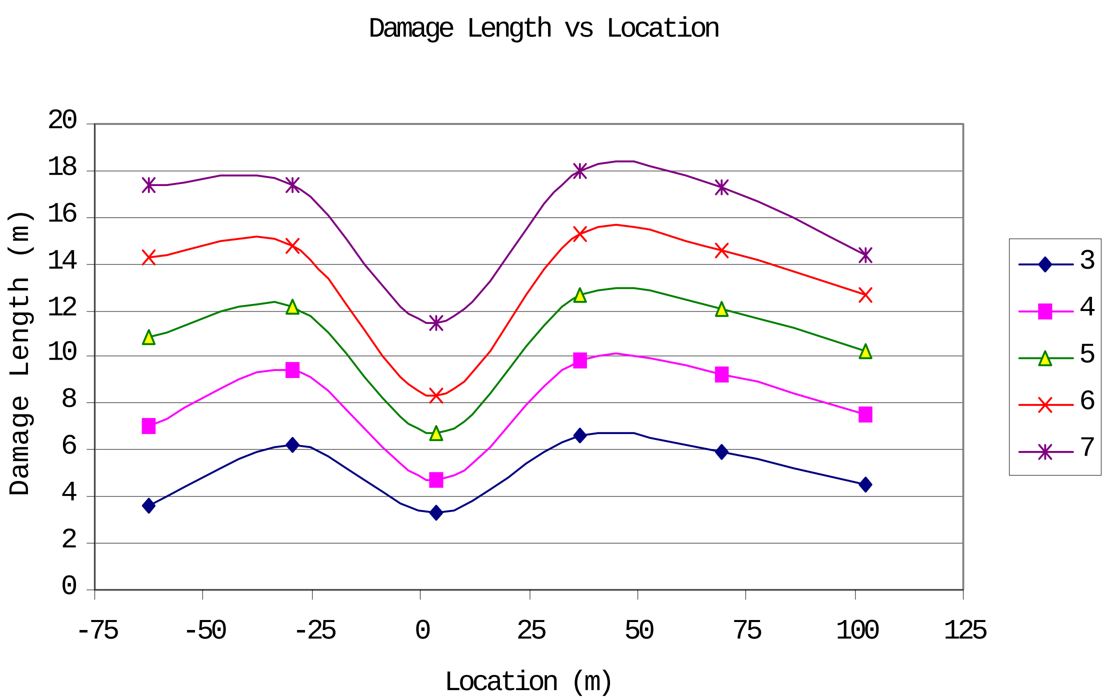

Figure 4.3(f) Damage Length Results of Matrix 1 (Version 2.1)

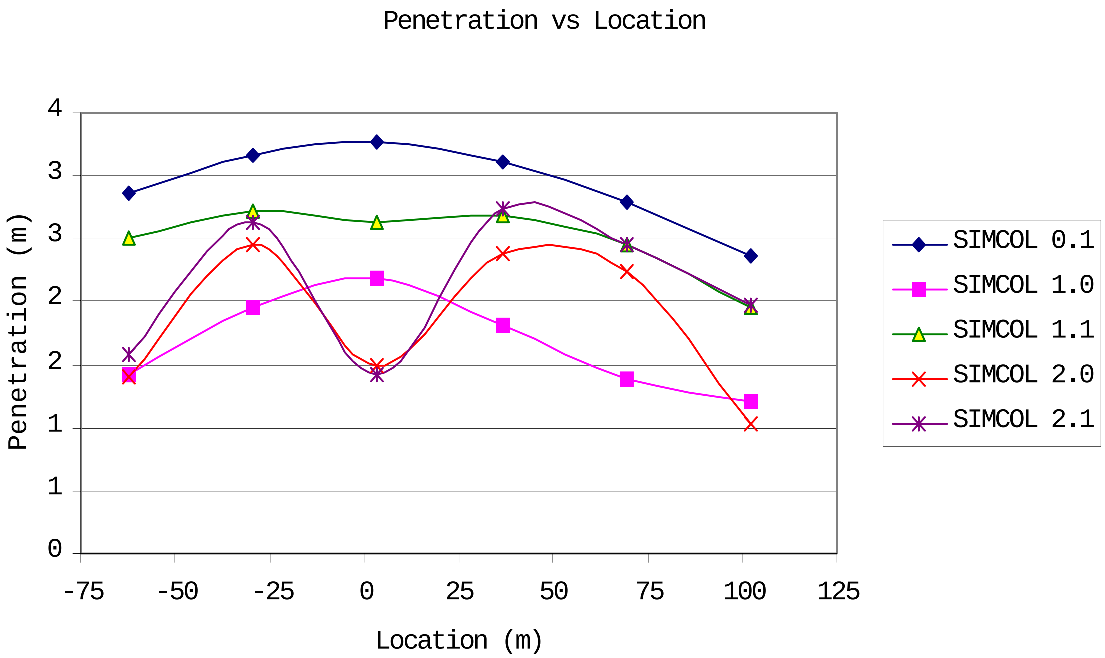

Figure 4.4(a) Penetration Results of Matrix 1 (3 knots)

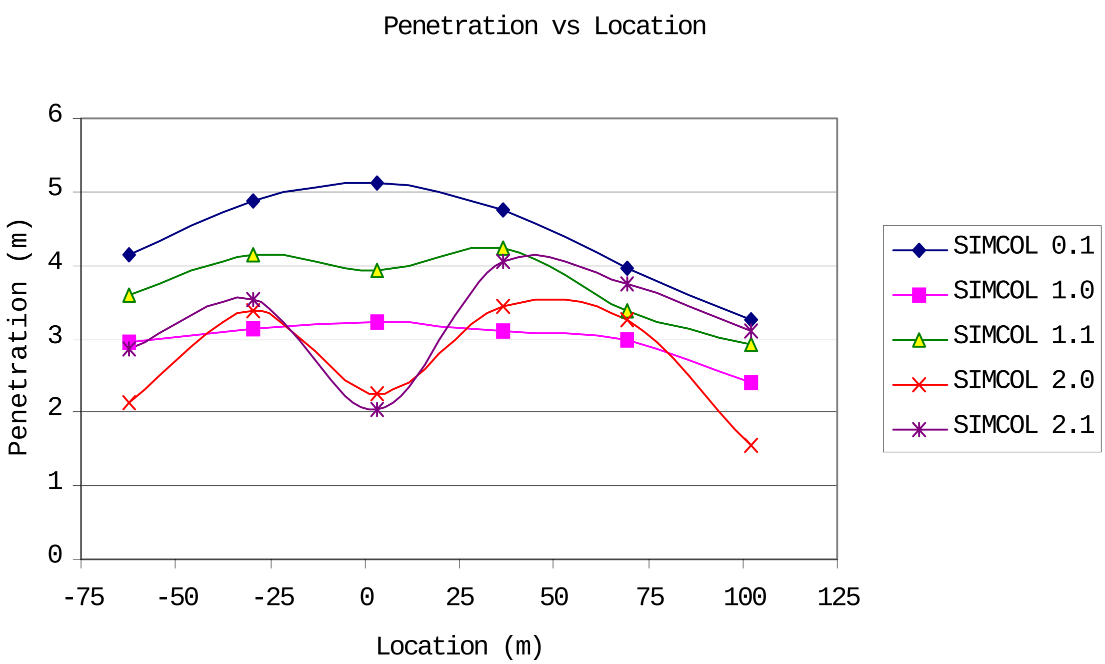

Figure 4.4(b) Penetration Results of Matrix 1 (4 knots)

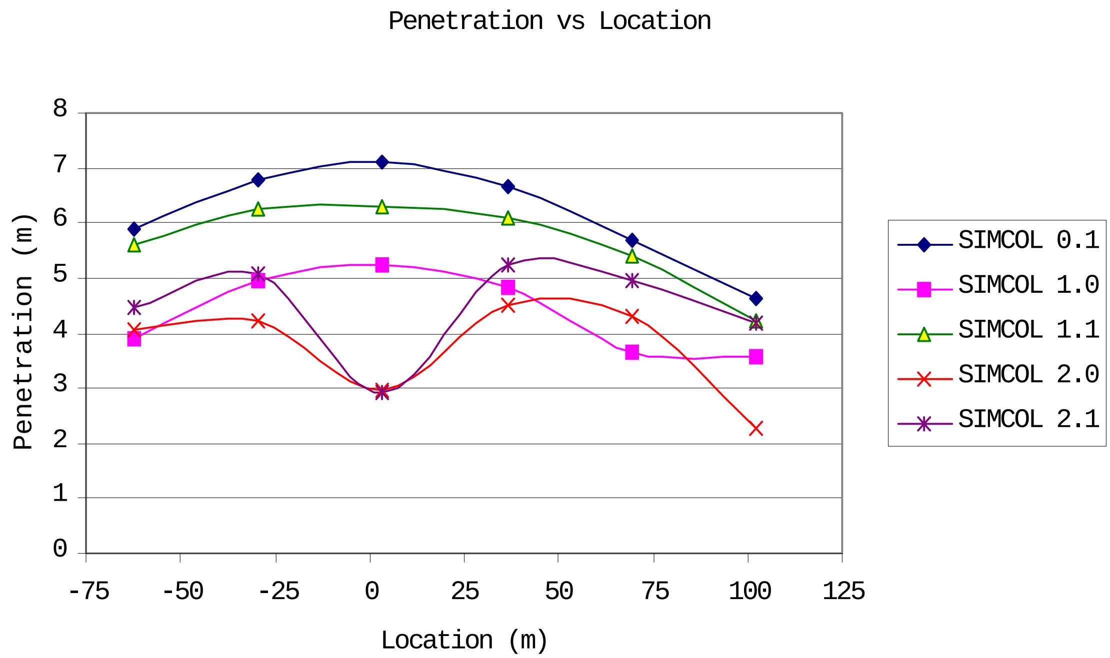

Figure 4.4(c) Penetration Results of Matrix 1 (5 knots)

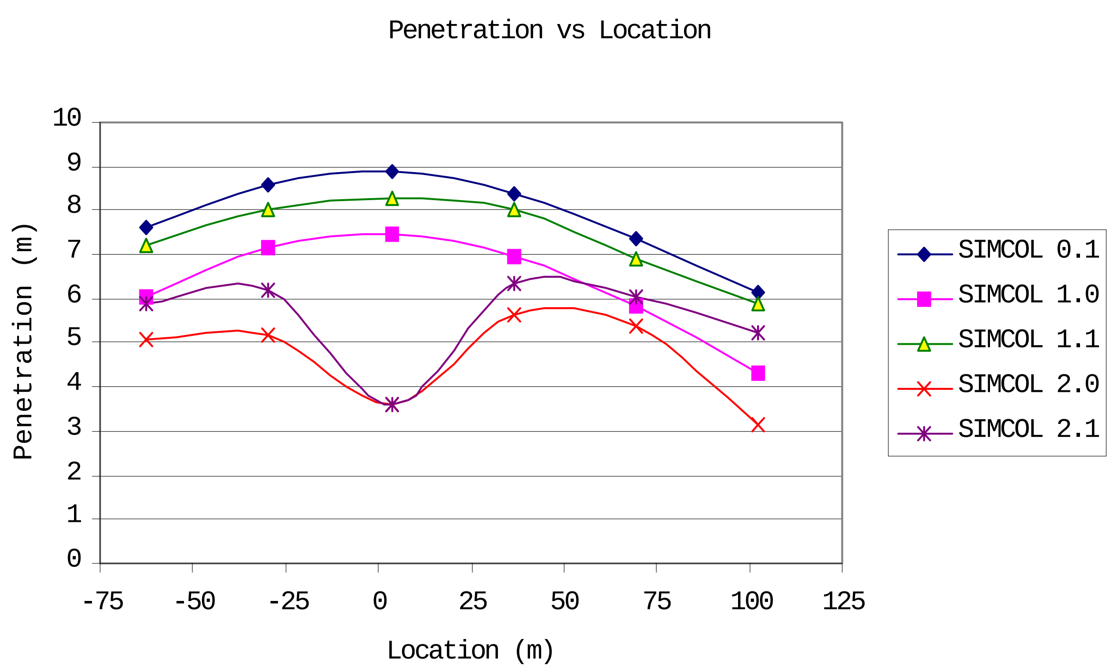

Figure 4.4(d) Penetration Results of Matrix 1 (6 knots)

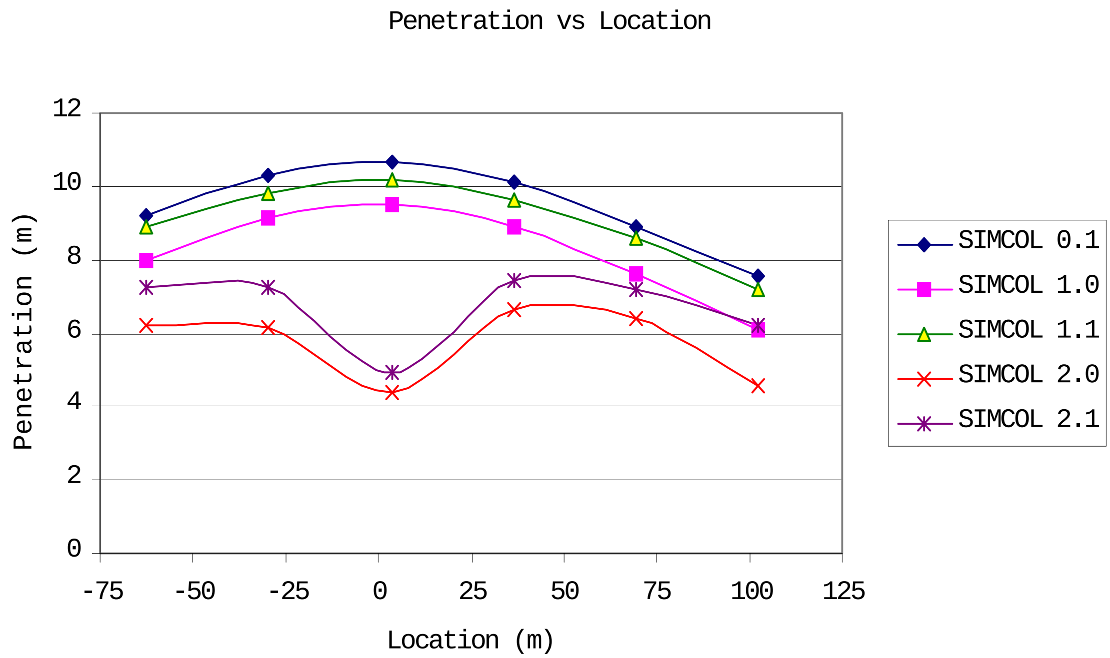

Figure 4.4(e) Penetration Results of Matrix 1 (7 knots)

- The penetration for Version 2.1 is normally larger than Version 2.0.

  In the Matrix 1 scenario, the limited depth bow in Version 2.1 does not cut the bottom shell, and therefore there is less damaged volume for a given penetration, and less Minorsky energy is absorbed. At same penetration, the transverse loads on the side web frames are also less than in Version 2.0. Less loads on web frames yields less web frame deformation, which makes web frames more rigid in terms of overall effect, and causes the side shell to rupture earlier (see Figure 4.3(d) and (e)).

- The rupture penetration curves, Figures 4.3(d) and (e), show that the inner hull is ruptured before the outer shell at the midship location.

  This is because the bending angle of the inner skin at the web frame, which is struck directly by the striking bow, exceeds the allowable value in Equation [3.38], while the bending radius of outer shell is still large because of the striking bow radius. The web, when struck directly, acts as a hard spot, and is driven through the inner hull.

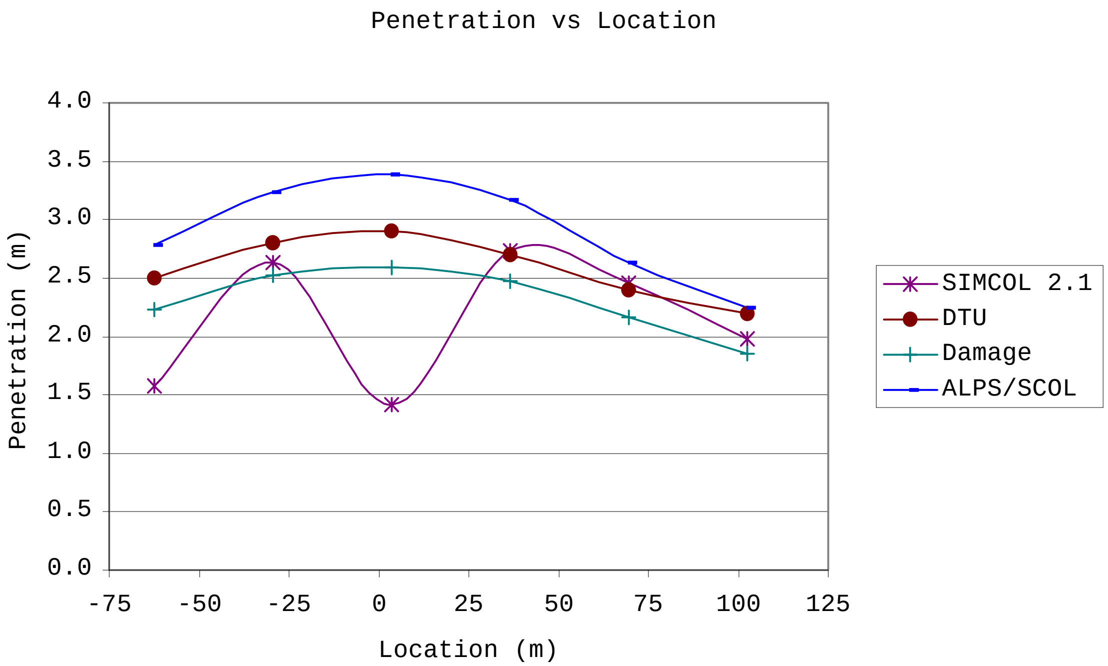

Figure 4.5(a) Comparison of Matrix 1 Results (3 knots)

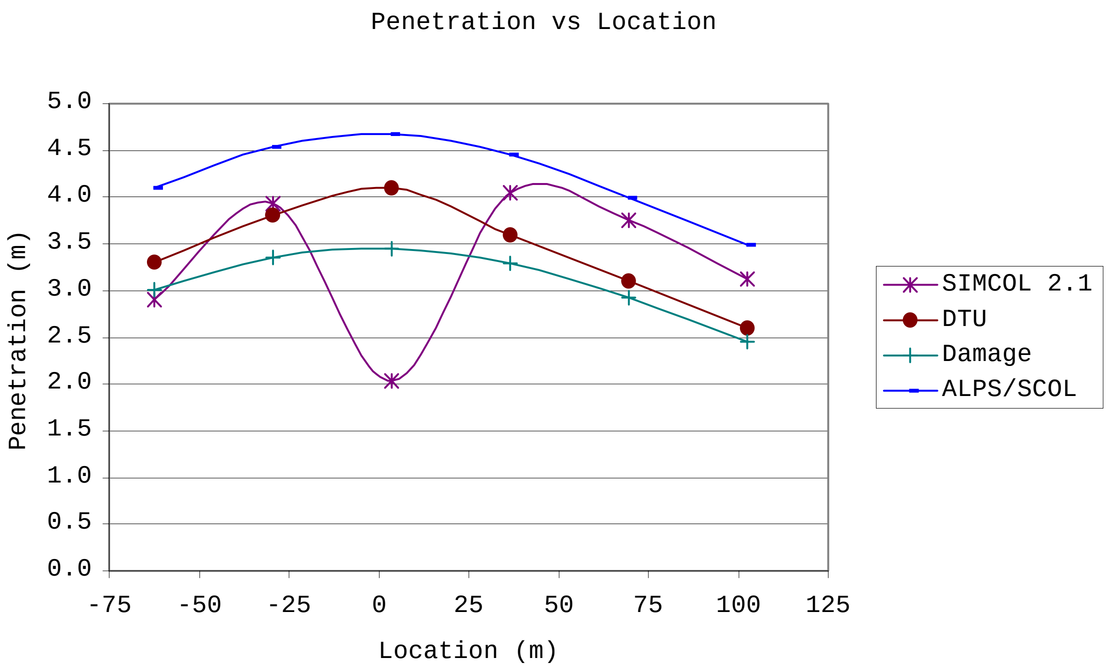

Figure 4.5(b) Comparison of Matrix 1 Results (4 knots)

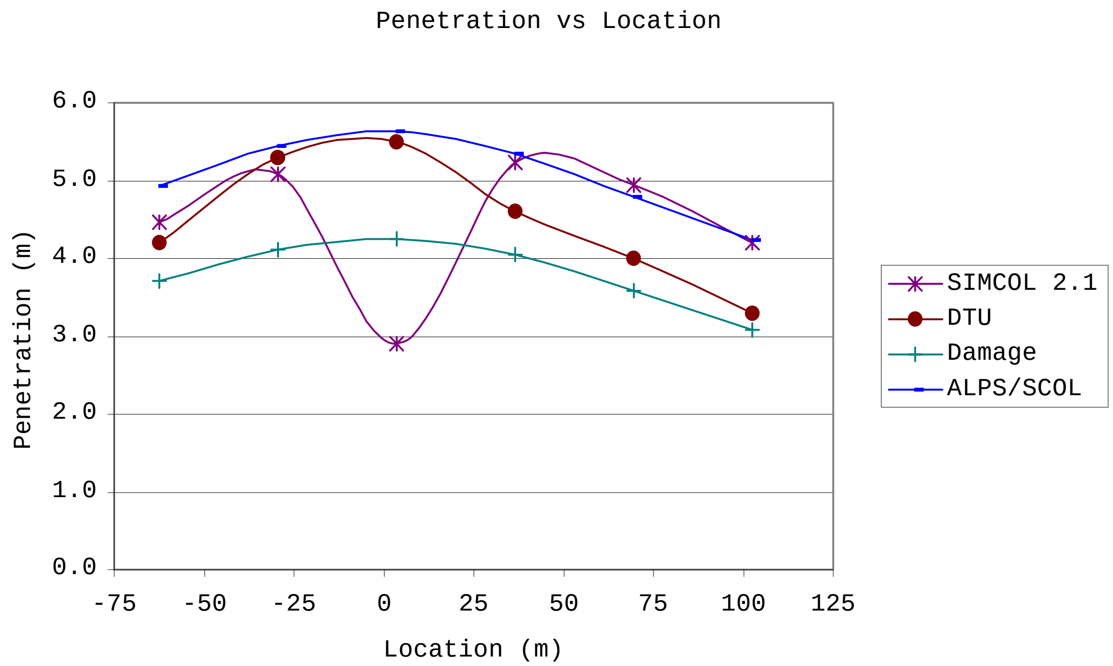

Figure 4.5(c) Comparison of Matrix 1 Results (5 knots)

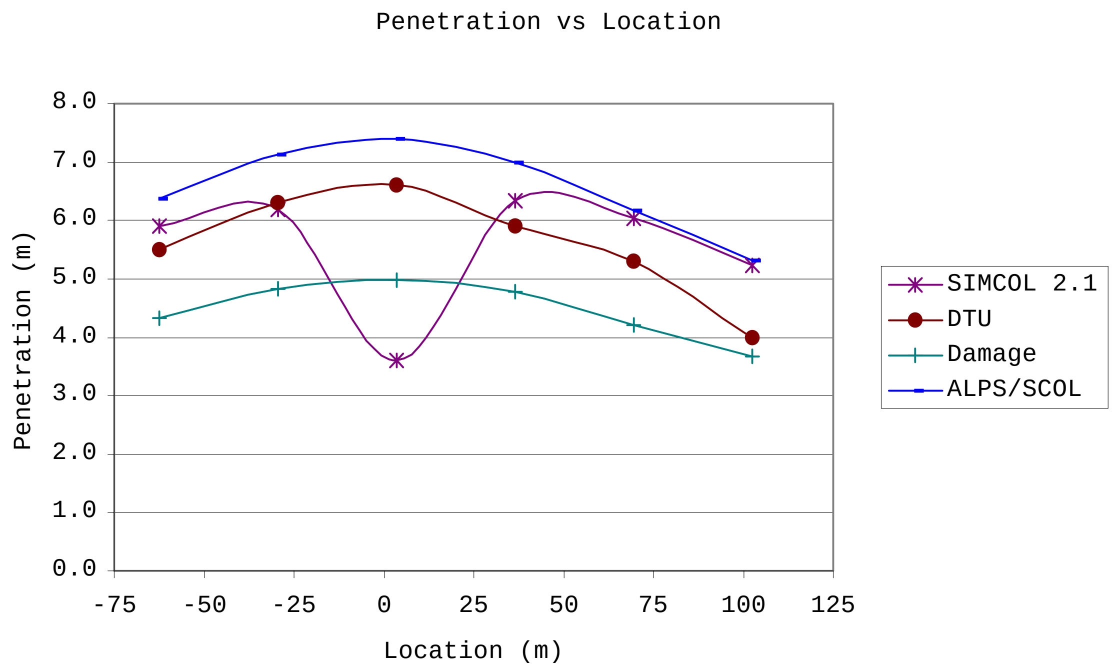

Figure 4.5(d) Comparison of Matrix 1 Results (6 knots)

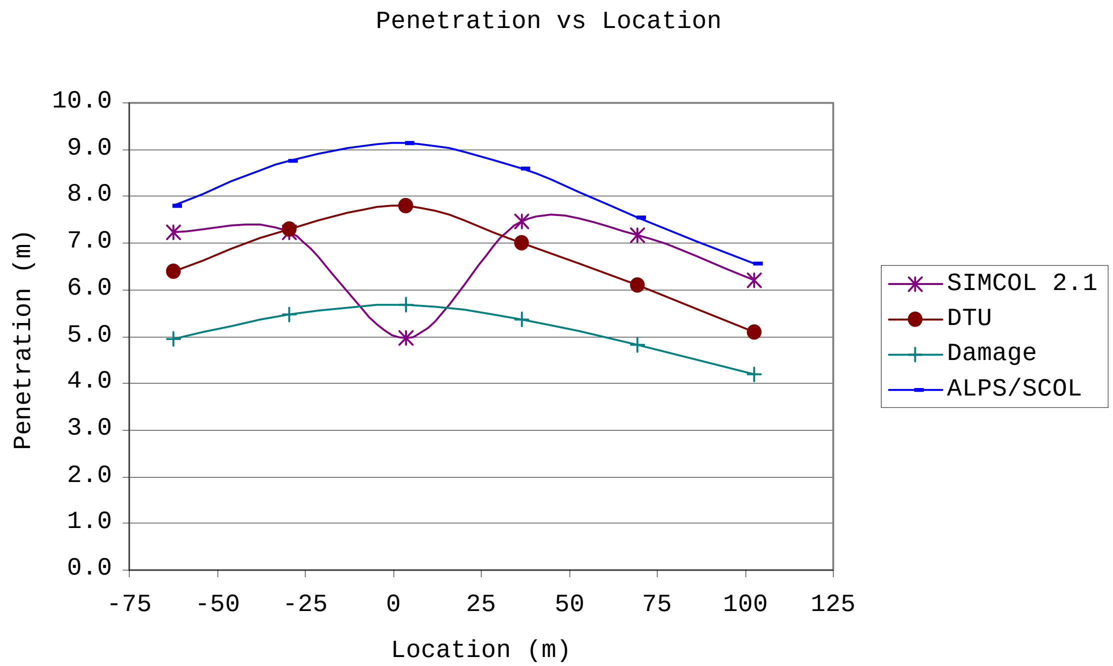

Figure 4.5(e) Comparison of Matrix 1 Results (7 knots)

In Figures 4.5(a) through (e), SIMCOL's performance is evaluated by comparison to the results of three other state-of-the-art collision models for the Matrix 1 scenarios. The results of the DTU model, DAMAGE, ALPS/SCOL and SIMCOL Version 2.1 are shown. The following observations are made:

- Penetration results of SIMCOL Version 2.1, the DTU model, DAMAGE and ALPS/SCOL have similar magnitude. DAMAGE generates the least penetration results except at midship location where SIMCOL's result is the least. ALPS/SCOL gives the most penetration. In addition to the different mechanism, the difference may also be caused by different assumption on added mass. In general, the more added mass in striking direction, the more kinetic energy will be lost during collision and the more penetration will be caused.

- Only SIMCOL predicts a reduction in penetration for the midship strikes, while DTU model, DAMAGE and ALPS/SCOL share same curve pattern. Only SIMCOL applies a true three degrees of freedom system and different internal mechanisms for right angle and oblique angle collisions respectively.

4.2.2 Test Matrix 2

4.2.2.1 Collision Scenario

In the second test matrix, the collision scenarios are defined as follows:

- Initial velocity of the struck ship: zero.
- Initial velocity of the striking ship: 3, 4, 5, 6 and 7 knots.
- Impact location: 1.85, 2.675, 3.5, 4.325 and 5.15 meters forward of midship which represent the mid-point, quarter point and on-web locations.
- Collision angle: 90 degrees.

This matrix tests the sensitivity of the impact location within one web frame spacing.

4.2.2.2 Simulation Results and Comparisons

Since Version 2.1 represents the most advanced SIMCOL model and compares well with DAMAGE and the DTU model results in Matrix 1, only Version 2.1 is used for sensitivity analysis with Matrix 2 and 3. The results are presented in Figure 4.6. SIMCOL, DAMAGE, the DTU model and ALPS/SCOL results are compared in Figures 4.7(a) though (e). The following observations are made:

- SIMCOL Version 2.1, the DTU model and DAMAGE presentation curves all have a “seagull” shape, while ALPS/SCOL gives an exactly opposite shape.

  From Equation [2.8], it can be seen that more energy is absorbed in membrane tension when the ship is struck at the web frame directly or at the mid-point of the web frame spacing. The opposite shape given by ALPS/SCOL implies a different internal mechanism.

- SIMCOL predicts less penetration than DAMAGE, DTU and ALPS/SCOL for all cases, particularly for lower energy collisions. This reflects Matrix 1 results at midship location.

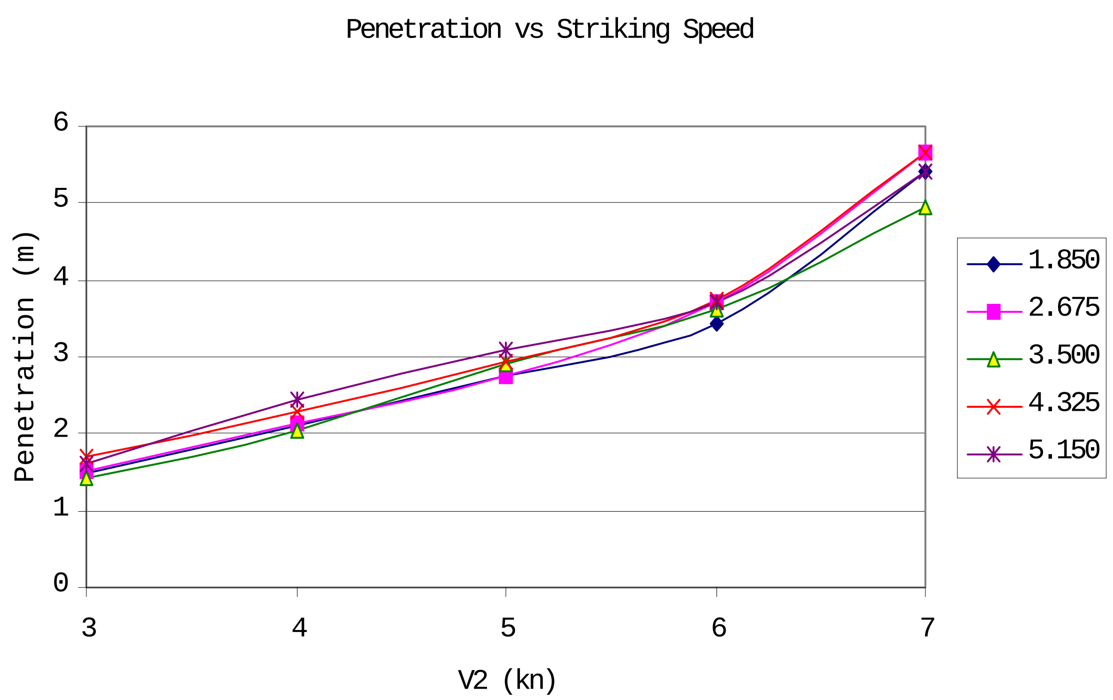

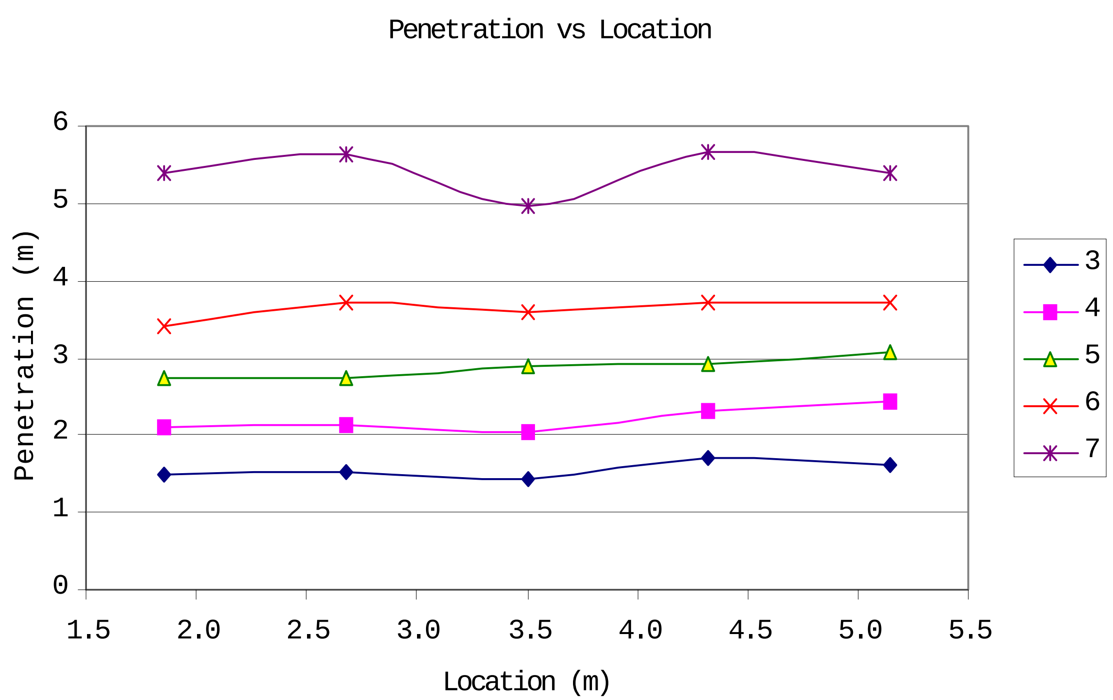

Figure 4.6 Penetration Results of Matrix 2 (Version 2.1)

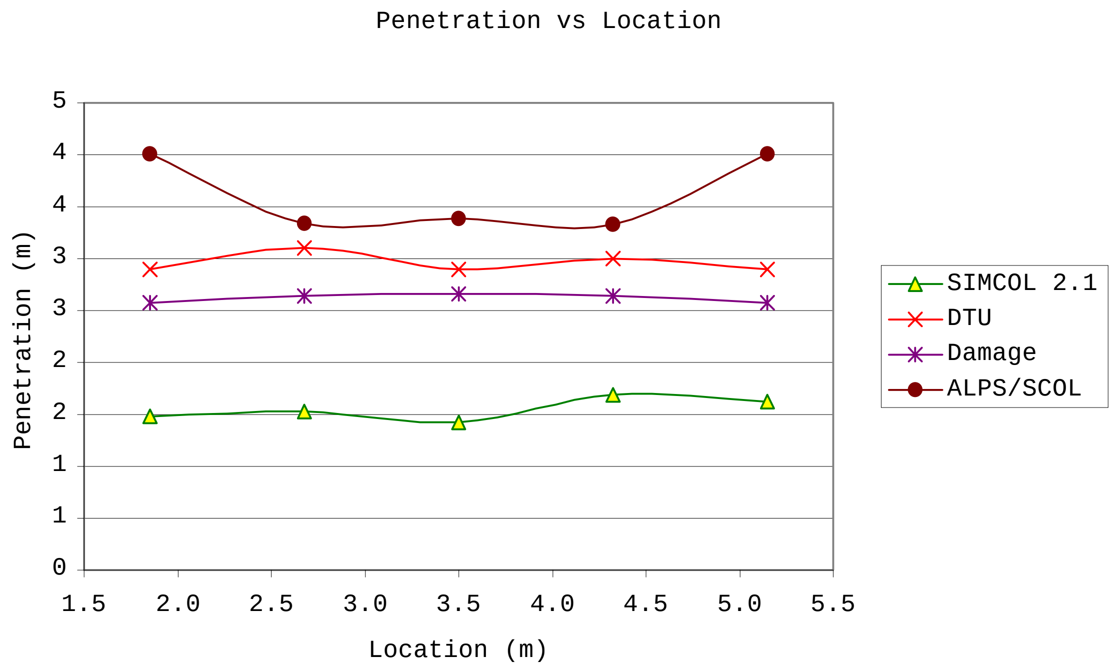

Figure 4.7(a) Comparison of Matrix 2 Results (3 knots)

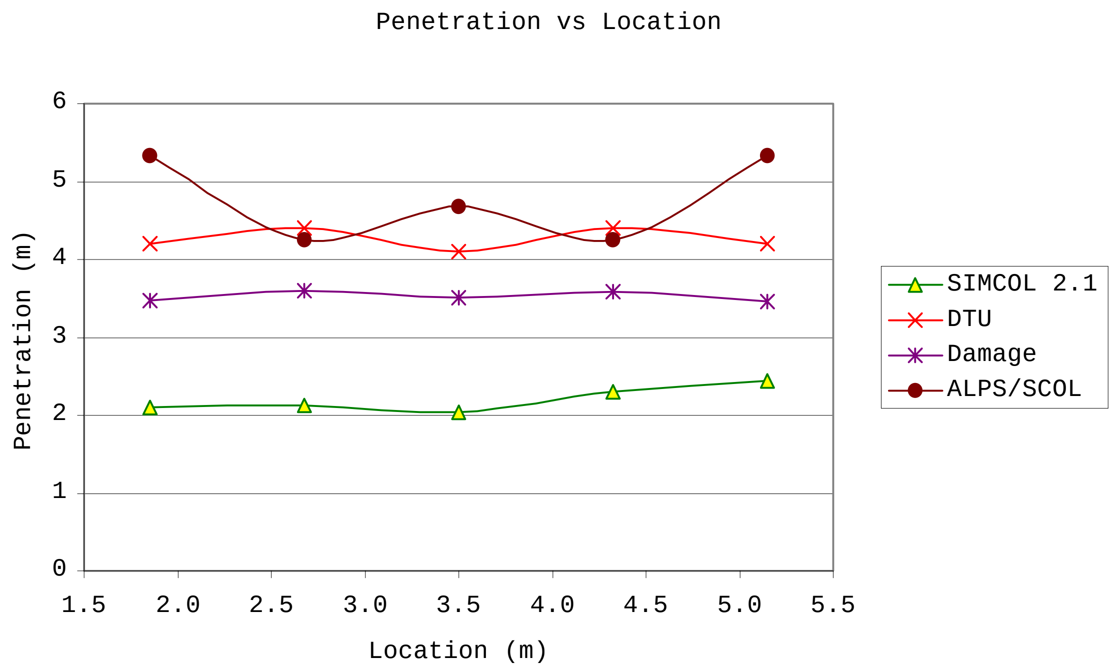

Figure 4.7(b) Comparison of Matrix 2 Results (4 knots)

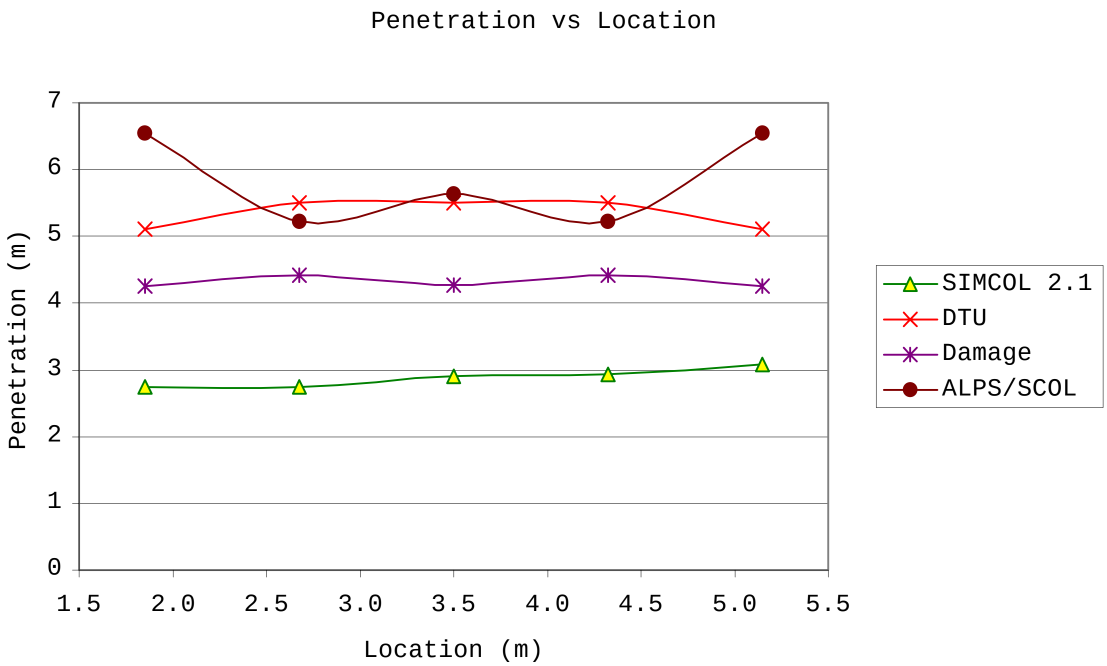

Figure 4.7(c) Comparison of Matrix 2 Results (5 knots)

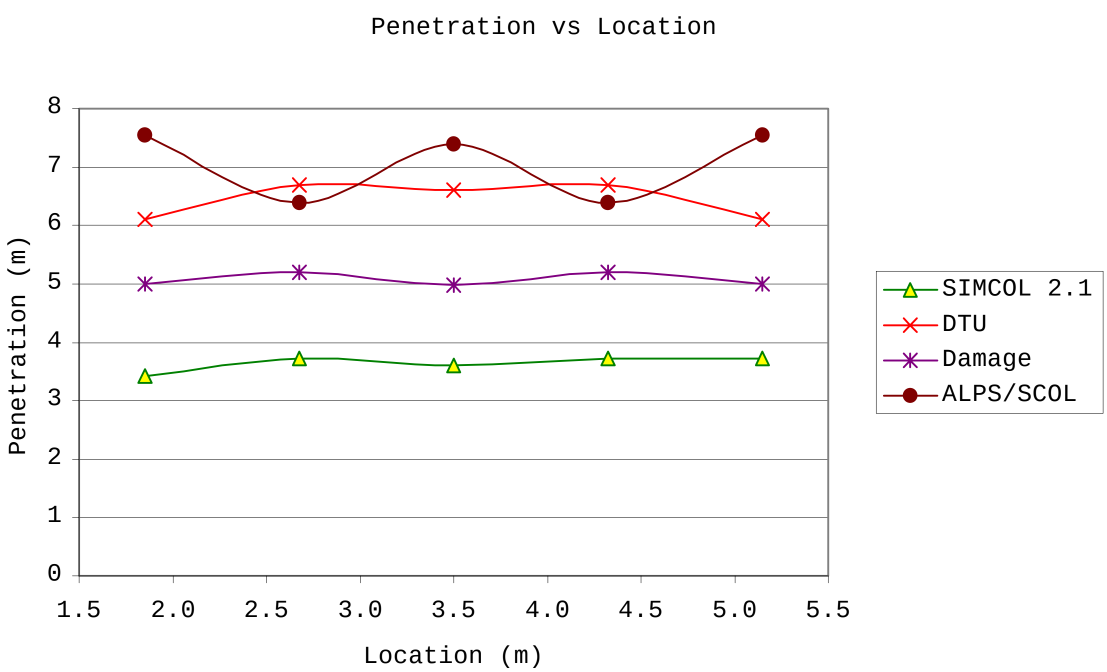

Figure 4.7(d) Comparison of Matrix 2 Results (6 knots)

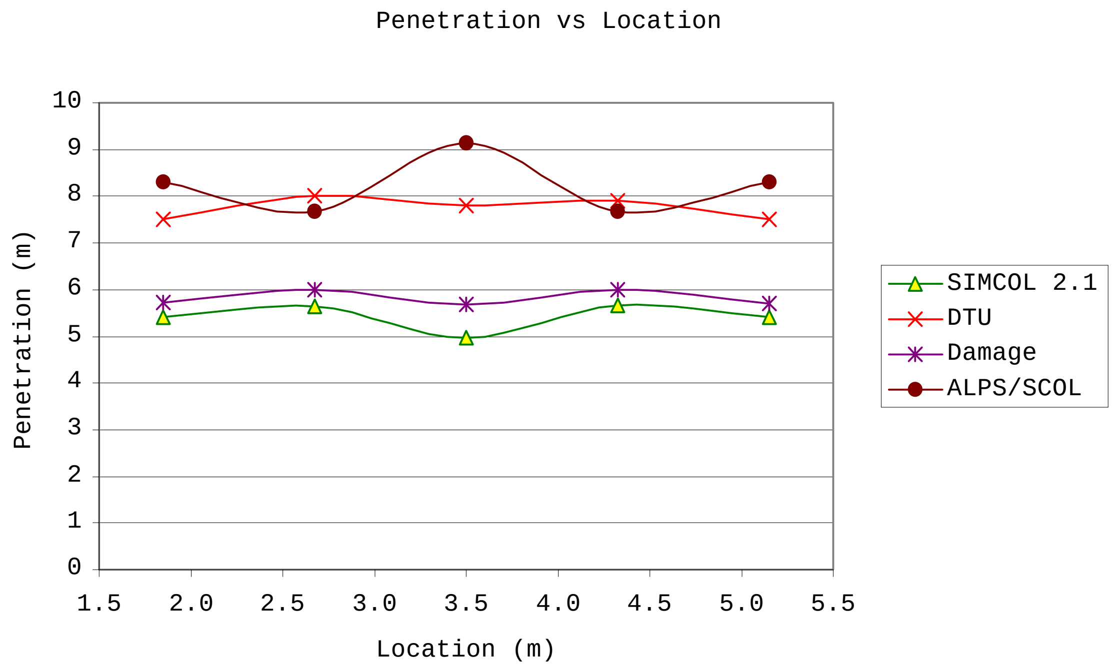

Figure 4.7(e) Comparison of Matrix 2 Results (7 knots)

4.2.3 Test Matrix 3

4.2.3.1 Collision Scenario

After looking at the penetration depth with regard to struck point, the next interesting issue would be the collision angle. In the third test matrix, the collision scenarios are defined as follows:

- Initial velocity of the struck ship: zero.
- Initial velocity of the striking ship: 3, 4, 5, 6 and 7 knots.
- Impact location: 3.5 meters forward of midship.
- Collision angle: 45, 60, 75, 90, 105, 120 and 135 degrees. However, because of the reason stated in Section 3.4.3, the collision angles of 54 and 126 degrees are chosen instead of 45 and 135 degrees for SIMCOL.

4.2.3.2 Simulation Results and Comparisons

The penetration depth and damage length results from Version 2.1 are presented in Figures 4.8(a) and (b). The comparison with the DTU model and ALPS/SCOL is given in Figures 4.9(a) though (e). Since DAMAGE cannot handle oblique angle collision, comparison with DAMAGE cannot be made for Matrix 3.

Again, the penetration versus striking angle curves from SIMCOL Version 2.1 are in "seagull" pattern. It again is the result of coupling of internal and external models. For a better understanding of the phenomenon, the penetration depths at rupture of side shell and inner skin are also given in Figure 4.8(a). From Figure 4.8(b), it can be found that the damage length increases as striking angle departs away from right angle, while penetration depth decreases except at right angle collision. This is because more energy is absorbed in longitudinal direction instead of lateral direction in oblique angle collisions.

The results from the DTU model and ALPS/SCOL are close in magnitude and have similar trend with SIMCOL results except at right angle.

4.2.4 Model Validation Case

4.2.4.1 Collision Scenario

The model validation case is an actual collision case as described by Kuroiwa [14]. The struck ship is a 100,000 dwt single hull tanker at ballast condition. The striking ship is a 23,000 dwt container ship. The collision scenario is defined as follows:

- Initial velocity of the struck ship: 12 knots.
- Initial velocity of the striking ship: 22 knots.
- Impact location: 30 meters aft of midship.
- Collision angle: 85 degrees

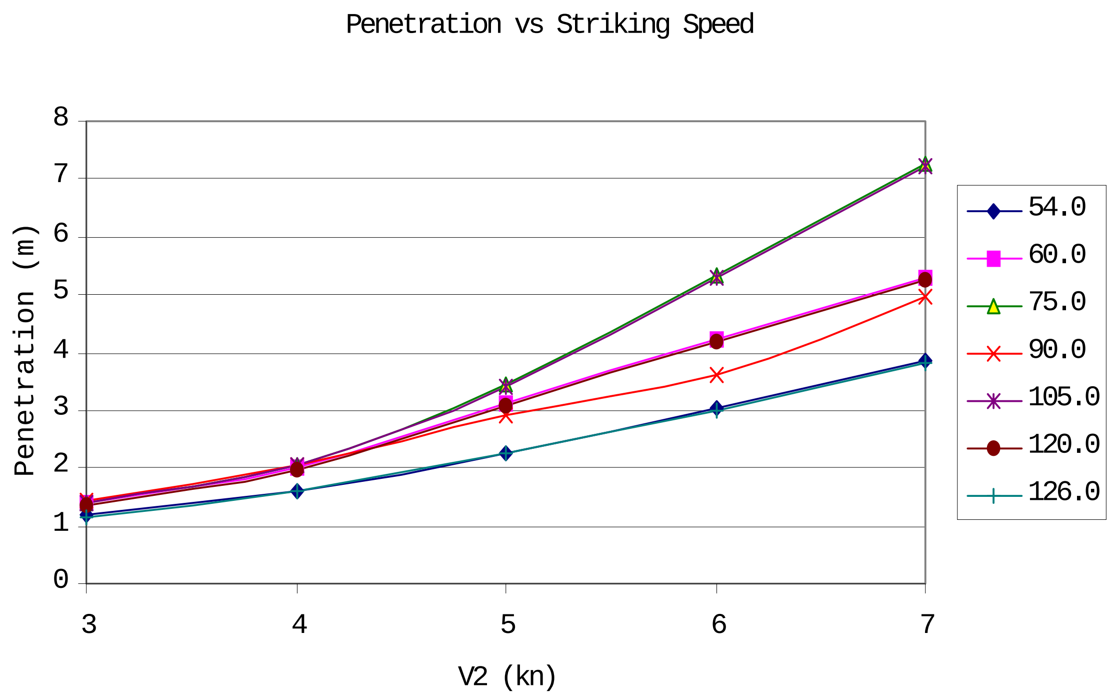

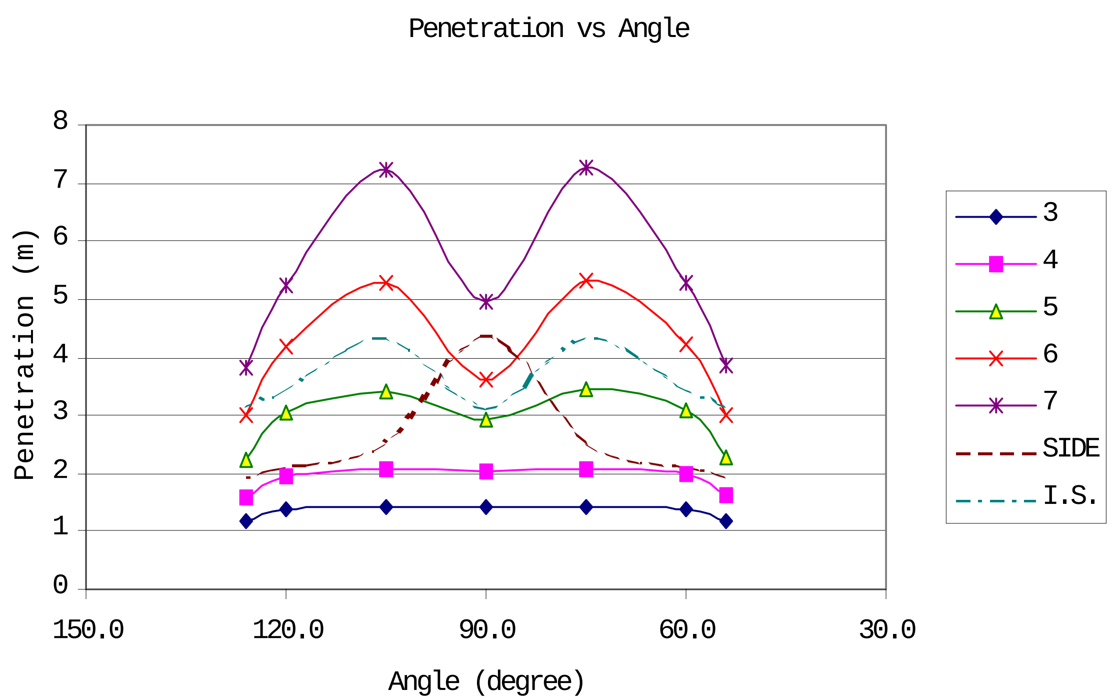

Figure 4.8(a) Penetration Results of Matrix 3 (Version 2.1)

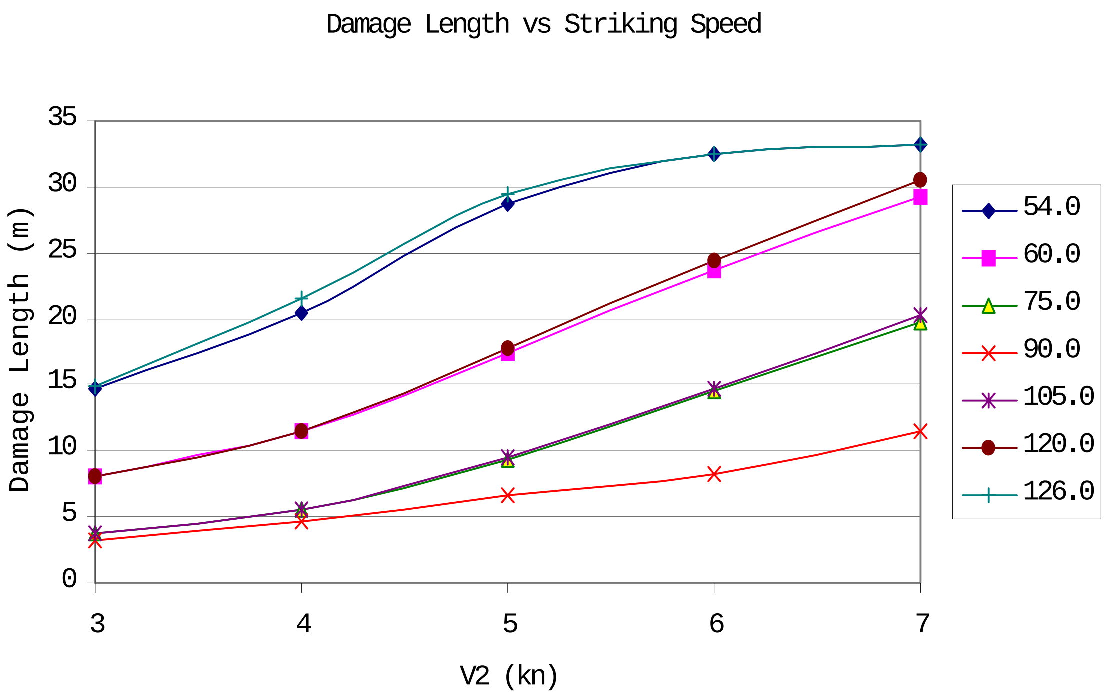

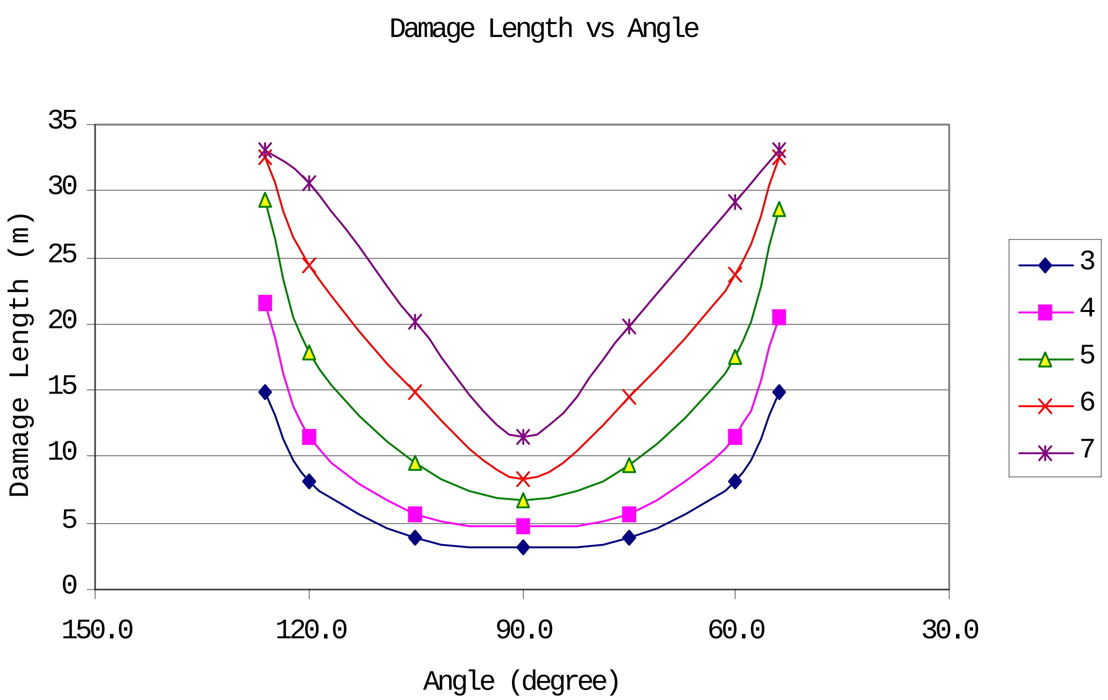

Figure 4.8(b) Damage Length Results of Matrix 3 (Version 2.1)

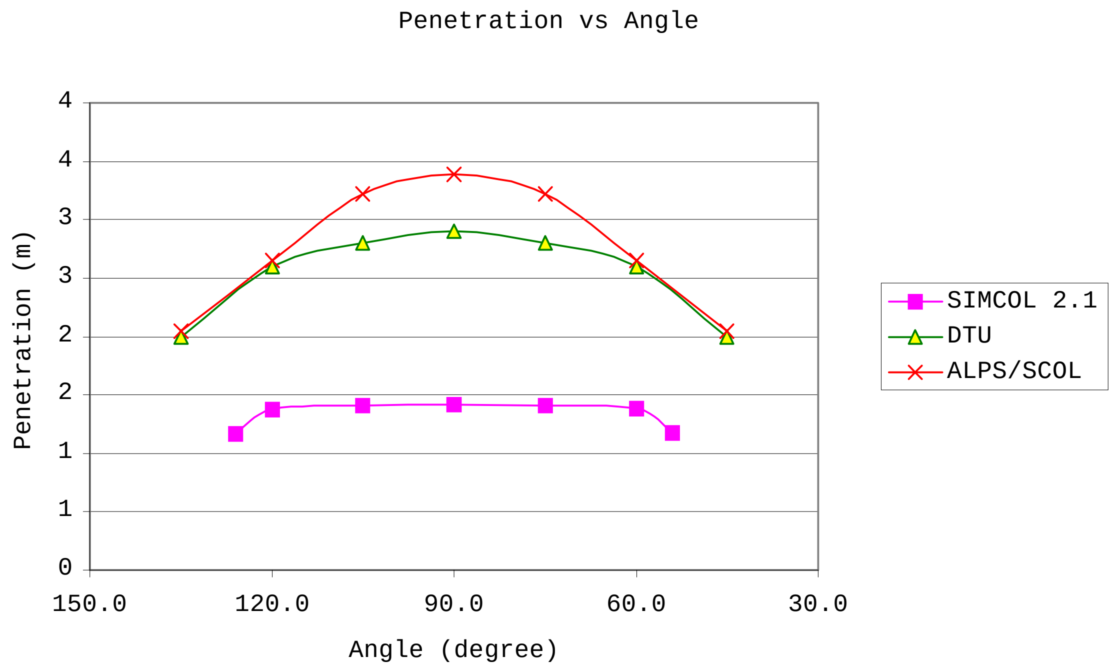

Figure 4.9(a) Comparison of Matrix 3 Results (3 knots)

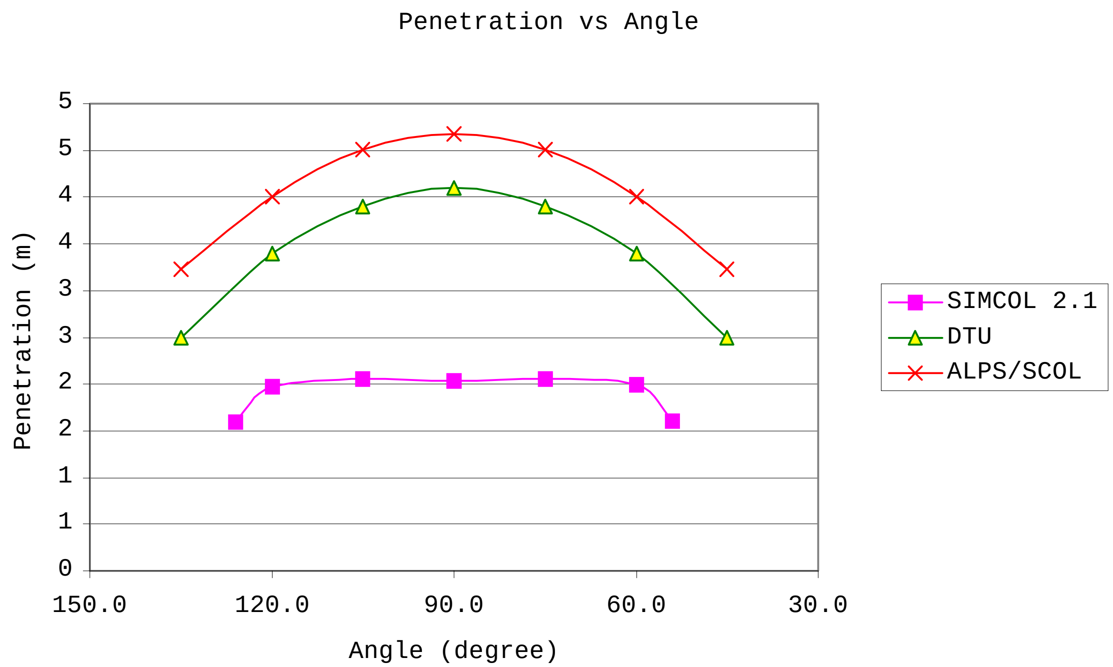

Figure 4.9(b) Comparison of Matrix 3 Results (4 knots)

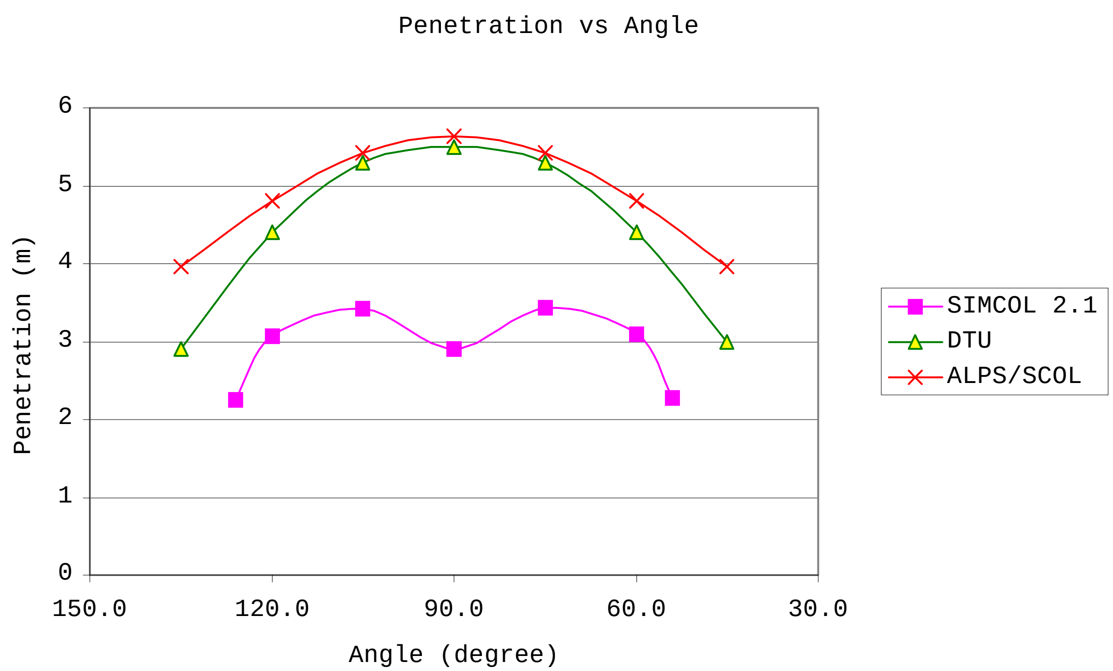

Figure 4.9(c) Comparison of Matrix 3 Results (5 knots)

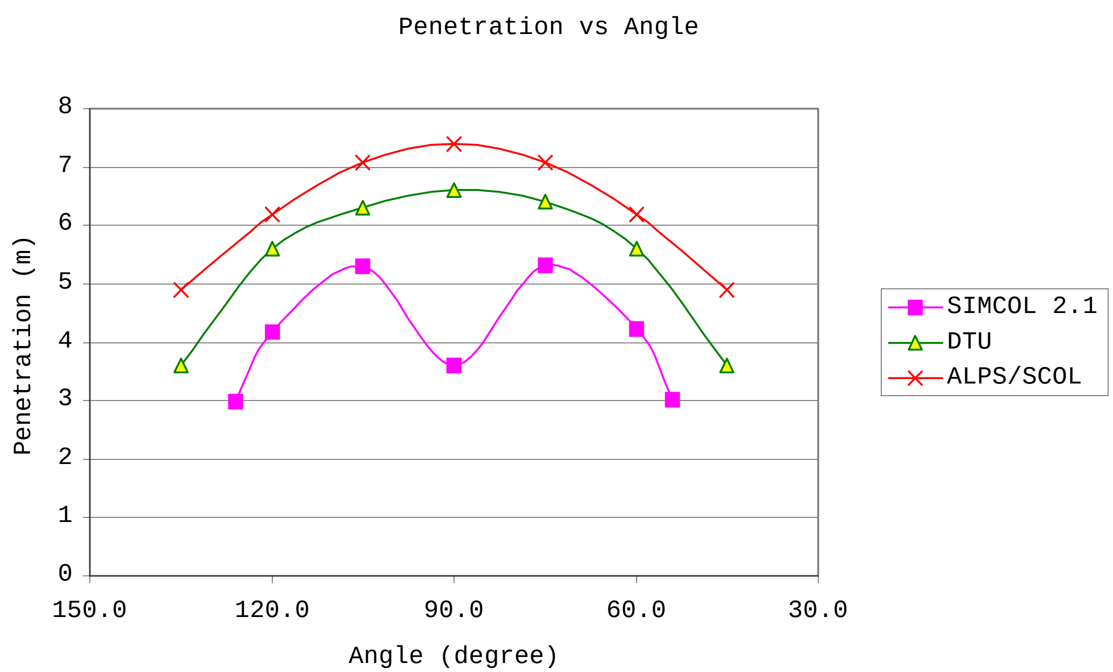

Figure 4.9(d) Comparison of Matrix 3 Results (6 knots)

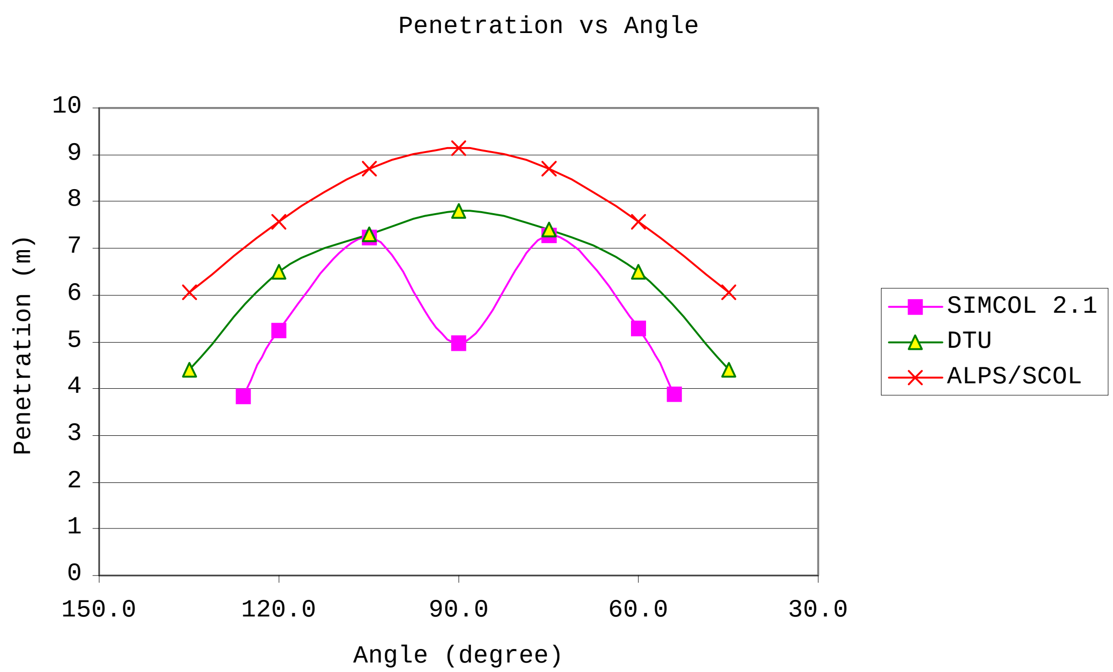

Figure 4.9(e) Comparison of Matrix 3 Results (7 knots)

4.2.4.2 Result and Comparison

The penetration result of SIMCOL Version 2.1 is 21.946 meters. The actual penetration is about 10 meters. The following may cause the difference:

- The transverse bulkhead between COT5 and COT6 has been struck directly. SIMCOL does not consider the resistance force from transverse bulkheads.

- The transverse bulkhead does not extend to the side. SIMCOL cannot model stepped transverse bulkheads.

Further improvements should be made to SIMCOL to consider transverse bulkheads.

CHAPTER 5 CONCLUSIONS AND FUTURE RESEARCH

5.1 CONCLUSIONS

Through this study, particularly the examination and comparison of the test matrix results and the validation case, the following conclusions are made:

1. The analysis approach selected for SIMCOL offers a consistent and reasonable result for ship collision analysis. Its result is comparable with other approaches. Even with a totally different deformation mechanism and external dynamic models, the results of SIMCOL Version 2.1 are comparable to those of the DTU model and DAMAGE. Although not a validation, this result increases confidence in these models.

2. The SIMCOL model yields more resistance from membrane tension because of distortable web frames, while DAMAGE and the DTU model offer more resistance from other supporting members. SIMCOL damage is more global.

3. The traditional "worst case" of right angle collision at midship may not be valid. As indicated in the results of Matrices 1 and 3, the actual worst case may be an oblique angle collision at a slightly forward or aft location.

4. Ignoring ship rotation in collision may not be a good assumption. In most analysis tools available today, the rotation is ignored so that the moving courses of struck and striking ships can be determined and the total kinetic energy absorbed in the process can be calculated uncoupled from the internal problem. The argument is based on the small rotation and short duration of the damage phase of collisions. However, even with a small rotation, the movement at impact point can still be significant. Indeed, take one case in Matrix 1 as an example, the rotating angle is about 1.4 degrees for the struck ship at maximum penetration and it is 0.09 degrees for the striking ship with the striking point at 102.9 meters forward and striking velocity of 7 knots. The induced motions at the impact point are in different direction and can reach 2.51 and 0.22 meters respectively, which can directly affect the maximum penetration. In this case, the collision angle is changed to 88.5 degrees, which exceeds the threshold set

for right angle collisions. With implementation of different mechanisms for right angle and oblique angle collisions, the difference caused by rotation may be even larger.

5. SIMCOL cannot predict resistance force and penetration properly when transverse bulkheads are directly involved in the collision. Improvement should be made.

5.2 FUTURE WORK

There are several areas where SIMCOL can be improved and also where more parametric study and validation is required. The following are suggestions for future research in their order of importance:

1. Currently, an arbitrary one-degree threshold is chosen to define the right angle collision. Therefore, a small change in collision angle may cause a dramatic difference in penetration and damage volume. It is suggested to refine the collision angles in Matrix 3, especially in the vicinity of 90 degrees, and study the results. Such study can help to find a more reasonable threshold. In order to prevent the abrupt transition in penetration curves as shown in Figure 4.8(a), it may be necessary to apply a mechanism that provides a smooth transition of energy absorbed in membrane tension between right angle and oblique angle collisions. An experiment similar to that conducted in the Rosenblatt study [11] could be very helpful in this regard.

2. The supporting capability of web frames is much larger in way of supports. Therefore, the uniform lateral movement assumption in Version 2.x may over-estimate the flexibility of web frames. A more realistic shape of the lateral movement of web frames would be a parabolic-like shape with less deformation at supports such as struts and stringers (see Figure 5.1). Struts and stringers also provide direct connections between inner and outer structure that may result in inner deformation before outer failure.

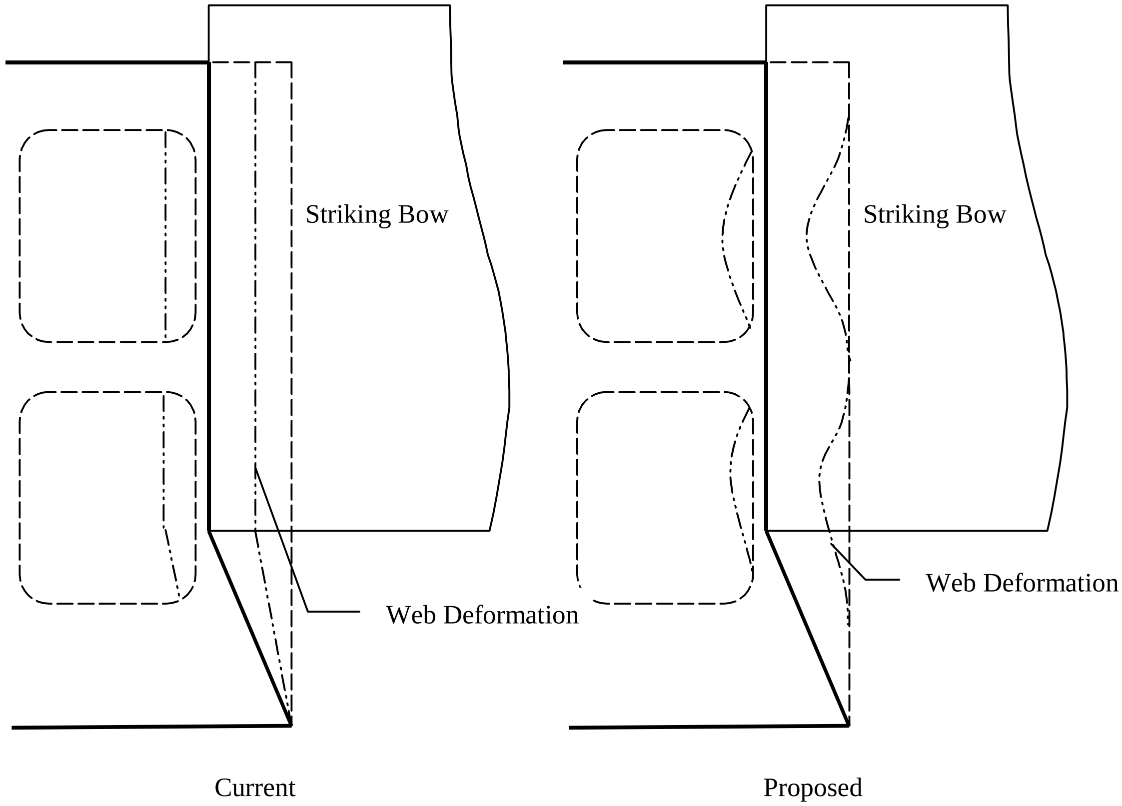

Figure 5.1 Deformation of Web Frames

3. Other structural members, especially the transverse bulkheads, should be included in the analysis as deformable structures. In addition to the direct contribution to the resistant force, transverse bulkheads may also be very important to containing the longitudinal extent of damage. Since there is no adequate study of the behavior of transverse bulkheads in collision, it is necessary to conduct finite element analysis or experimental studies before assumptions or models describing their behavior can be proposed.

4. SIMCOL does not properly consider the longitudinal resistance from web frames and transverse bulkheads. SIMCOL attempts to calculate damage length in collisions. The damage length of the ruptured cargo boundary is a key factor to determine the number of damaged cargo tanks and the amount of the oil outflow. But, at this stage, SIMCOL only considers local damage actually swept by the striking bow and does

not have any mechanism to properly consider longitudinal extent of ruptured cargo boundary as a separate phenomenon from penetration.

5. Evaluate the effect of eliminating the rigid bow assumption and including the deformation of the striking bow.

6. The vertical striking bow is not ideally representative of modern ship bows. Raked bow and bulbous bow models may be required for sufficient results. The ship bow can be modeled as two wedges: the upper bow as a raked wedge, and the lower bow as a vertical wedge. By keeping this wedge definition, the current code would require only small changes. With these modifications, the SIMCOL results can better be compared with DAMAGE or the DTU model. Alternatively, the half entrance angle could be made a changing parameter in the collision scenario.

7. Refine the external model further by considering the actual longitudinal location of the center of gravity. This extension is more important with coupling of internal and external models since it effects the relative movement of the ships.

8. Derive a new set of equations for added mass from a ship-shape model. Added mass plays an important role in ship collision model. It directly affects the total amount of kinetic energy absorbed in collision. The equations in Section 3.2.2 are derived for rectangular barges.

9. The calculation of the longitudinal force for propagating the yielding zone may be too rough. The selection of c_F and c_A could be refined.

REFFERENCES

[1] Brown, A.J., Congressional Testimony given to the US Coast Guard and Maritime Transportation Subcommittee, US Congress, Virginia Tech, June 29, 1999.

[2] Brown, A.J., Presentation to the National Research Council, Virginia Tech, June 29, 1999.

[3] Brown, A.J. and Amrozowicz, M., "Tanker Environmental Risk - Putting the Pieces Together", *SNAME/SNAJ International Conference on Designs and Methodologies for Collision and Grounding Protection of Ships*, August 1996.

[4] Sirkar, J., et al., "A Framework for Assessing the Environmental Performance of Tankers in Accidental Groundings and Collisions", *1997 SNAME Annual Meeting*, October 1997.

[5] Rawson, C., Crake, K. and Brown, A.J., "Assessing the Environmental Performance of Tankers in Accidental Grounding and Collision", *1998 SNAME Annual Meeting*, November 1998.

[6] IMO, "Interim Guidelines for Approval of Alternative Methods of Design and Construction of Oil Tankers under Regulation 13F(5) of Annex I of MARPOL 73/78", Resolution MEPC.66 (37), Adopted September 14, 1995.

[7] Crake, K., "Probabilistic Evaluations of Tanker Ship Damage in Grounding Events", Naval Engineer Thesis, MIT, 1995.

[8] Minorsky, V.U., "An Analysis of Ship Collisions with Reference to Protection of Nuclear Power Plants", *Journal of Ship Research*, Vol. 3, No. 1, pp. 1-4, 1959.

[9] Reardon, P. and Sprung, J.L., "Validation of Minorsky's Ship Collision Model and Use of the Model to Estimate the Probability of Damaging a Radioactive Material Transportation Cask During a Ship Collision", *Proceedings of the International*

Conference on Design and Methodologies for Collision and Grounding Protection of Ships, San Francisco, August 1996.

[10] Giannotti, J.G., Johns, N., Genalis, P. and Van Mater, P.R., "Critical Evaluations of Low-Energy ship Collision Vol. I - Damage theories and Design Methodologies", Ship Structure Committee Report No. SSC-284, 1979

[11] McDermott, J.F., et al, "Tanker Structural Analysis for Minor Collisions", *SNAME Transactions*, Vol. 82, pp. 382-414, 1974.

[12] Rosenblatt & Son, Inc, "Tanker Structural Analysis for Minor Collision", USCG Report, CG-D-72-76, 1975.

[13] Pedersen, P.T., et al, "Ship Impacts: Bow Collisions", *International Journal of Impact Engineering*, Vol. 13, No. 2, pp. 163-187, 1993.

[14] Kuroiwa, T., "Numerical Simulation of Actual Collision and Grounding Experiments", *Proceedings of the International Conference on Design and Methodologies for Collision and Grounding Protection of Ships*, San Francisco, August 1996.

[15] Simonsen, B.C., "Theory and Validation for the Collision Module", Joint MIT-Industry Program on Tanker Safety, Report No. 66, June 1999.

[16] Hutchison, B.L., "Barge Collisions, Rammings and Groundings - an Engineering Assessment of the Potential for Damage to Radioactive Material Transport Casks", Report No. SAND85-7165 TTC-05212, 1986.

[17] Zhang, S., "The Mechanics of Ship Collisions", Ph.D. Thesis, Department of Naval Architecture and Offshore Engineering, technical University of Denmark, Lyngby, 1999.

[18] Woisin, G., "Design Against Collision", *International Symposium on Advances in Marine Technology*, Trondheim, Norway, June 1979.

[19] Reckling, K.A., "Mechanics of Minor Ship Collisions", *International Journal of Impact Engineering*, Vol. 1, No. 3, pp. 281-299, 1983.

[20] Egge, E.D. and Bockenhauer, M., "Calculation of the Collision Resistance of Ships and its Assessment for Classification Purposes", *Marine Structures*, Vol. 4, pp. 35-56, 1991.

[21] Amdahl, J., “Energy Absorption in Ship-Platform Impacts”, Dr. Ing. Thesis, Report No. UR-83-84, The Norwegian Institute of Technology, Trondheim, 1983.

[22] Yang, P.D.C. and Caldwell, J.B., "Collision Energy Absorption in Ships Bow Structures", *International Journal of Impact Engineering*, Vol. 7, No. 2, 1988.

[23] Wierzbicki, T., "Crushing Behavior of Plate Intersections", *Structural Crashworthiness*, edited by A. Jones and T. Wierzbicki, Chapter 3, Butterworth and Co., London, 1983.

[24] Ito, H., et al, "A Simplified Method to Analyze the Strength of Double Hulled Structures in Collision", *Journal of Society of Naval Architects of Japan*, Vol. 156, pp. 283-295, 1984.

[25] Ito, H., et al, "A Simplified Method to Analyze the Strength of Double Hulled Structures in Collision, 2nd Report", *Journal of Society of Naval Architects of Japan*, Vol. 158, pp. 420-434, 1985.

[26] Ito, H., et al, "A Simplified Method to Analyze the Strength of Double Hulled Structures in Collision, 3rd Report", *Journal of Society of Naval Architects of Japan*, Vol. 160, pp. 401-409, 1986.

[27] Paik, J.K., et al, "On Rational Design of Double Hull Tanker Structures against Collision”, *1999 SNAME Annual Meeting*, 1999.

[28] Paik, J.K. and Pedersen, P.T., "Modeling of the Internal Mechanics in Ship Collisions", *Ocean Engineering*, Vol. 23, No. 2, pp. 107-142, 1996.